

**Structural and Functional Studies on the Ubiquitin-Specific
Protease Family**

Mark P.A. Vargas

ISBN: 978-90-8570-690-8

Cover artwork: Alessia Gasparini

Cover design: Jenny Daud (www.jennydaud.nl)

Printing: Wöhrmann Print Service

The research described in this thesis was performed in the Division of Biochemistry at the Netherlands Cancer Institute - Antoni van Leeuwenhoek Hospital (NKI-AVL), The Netherlands.

This research was financially supported by Rubicon Network of Excellence (EU), KWF (Koningin Wilhelmina Fonds) and NWO-CW (Nederlandse organisatie voor de wetenschappelijk onderzoek - chemische wetenschappen and CBG (Centre for Biomedical Genetics).

Copyright © by M.P.A. Luna-Vargas. All rights reserved. No part of this book may be reproduced, stored in a retrieval system, or transmitted in any form or by any means, without prior permission of the author.

Structural and Functional Studies on the Ubiquitin-Specific Protease Family

Structurele en functionele studies op de ubiquitine-specifieke
protease familie

Thesis

to obtain the degree of Doctor from the Erasmus University Rotterdam
by command of the rector magnificus

Prof.dr. H.G. Schmidt

and in accordance with the decision of the Doctorate Board

The public defence shall be held on
Wednesday 9 November 2011 at 09.30 o'clock

By

Mark Patrick Alexander Vargas

born in Amsterdam, The Netherlands



DOCTORAL COMMITTEE

Promotor:

Prof. dr. T.K. Sixma

Other members:

Prof. dr. J. Neefjes

Prof. dr. R. Kanaar

Prof. dr. C.P. Verrijzer

Table of contents

Chapter 1	General introduction	7
Chapter 2	A Genomic and functional inventory of deubiquitinating enzymes <i>(Cell, 2005)</i>	29
Chapter 3	Enabling high-throughput ligation-independent cloning and protein expression for the family of ubiquitin specific-proteases <i>(Journal of Structural Biology, 2011)</i>	51
Chapter 4	The differential modulation of USP activity by internal regulatory domains, interactors and ubiquitin-chain types <i>(submitted)</i>	65
Chapter 5	Ubiquitin-specific protease 4 is inhibited by its ubiquitin-like domain <i>(EMBO reports, 2011)</i>	89
Chapter 6	General discussion	111
Addendum	Summary	121
	Samenvatting	123
	List of abbreviations	127
	Curriculum vitae	131
	PhD portfolio	133
	List of publications	135
	Acknowledgements	137

General Introduction

1



Post-translational modification

When RNA translation has completed and the proteins have been properly folded, most proteins are subject to a diverse range of post-translational modifications that affect their function. It is an important cellular strategy that enables the cell to react dynamically to intracellular or environmental changes caused by exposure to stress factors, growth stimuli or differentiation signals. Proteins are modified by methylation, acetylation, hydroxylation, phosphorylation or conjugated to ubiquitin (Ub) and ubiquitin-like (Ubl) proteins. The post-translational modification with Ub of proteins has emerged to play an essential role in the regulation of virtually all aspects of cell biology ^{1,2}.

Ubiquitination pathway

Protein ubiquitination was discovered in the 1980s as a post-translational modification in which lysine residues of a target protein are modified with the addition of Ub. This small protein is a highly conserved 76 amino-acid polypeptide of ~8500 Da³. The crystal structure of Ub revealed a distinctive fold, the β-grasp fold, which is also present in a group of proteins with distinct functions: ubiquitin-like (Ubl) proteins⁴⁻⁶.

Through the sequential action of three enzymes a target protein is modified by covalent ligation to Ub (Figure1). In the first step of the ubiquitination pathway, Ub is activated by a specific activating enzyme (E1) UBA1. UBA1 first binds MgATP and Ub and catalyzes Ub C-terminal acyl-adenylation. Secondly, the catalytic cysteine residue in the E1 attacks the ubiquitin-adenylate

to form the activated ubiquitin-E1 complex via a high-energy thioester bond. In the second step of the ubiquitination pathway, the Ub loaded E1 engages one of up to tens of related E2 conjugating enzymes and then transfers the activated Ub to an active site cysteine residue of the E2. Finally the Ub is covalently linked by its C-terminus in an amide isopeptide linkage to an ε-amino group of a lysine residue of a target protein, which is catalyzed through the coordinated function of E3 Ub ligases. There are three different types of E3 ligase, RING (the Really Interesting New Gene), U-box and HECT (Homologous with E6-associated protein C-Terminus) domains and contain binding sites for both charged E2s and ubiquitinated substrates. For the largest class of E3s the RING family and the RING-related U-box family an ε-amino group of a lysine residue in the associated substrate attacks the thioester of the transiently associated charged E2 to make an isopeptide bond with Ub. The discharged E2 then dissociates from the E3, allowing a second charged E2 to interact with the E3. This facilitates a second round of Ub transfer, either by attack of a lysine residue on Ub itself or by attack of a different lysine residue on the substrate⁷⁻¹¹.

In addition, through a similar cascade of reactions catalyzed by evolutionary related enzymes, the Ubl proteins (URM1, ATG12, Nedd8, SUMO, FAT10, ISG15 etc.) can also be conjugated to target proteins^{9,11-16}.

Because Ub itself contains seven acceptor lysines that can be a target of Ub conjugation, different types and lengths of Ub chains can be formed. Thus target proteins not only are ubiquitinated with a single Ub on a single lysine residue

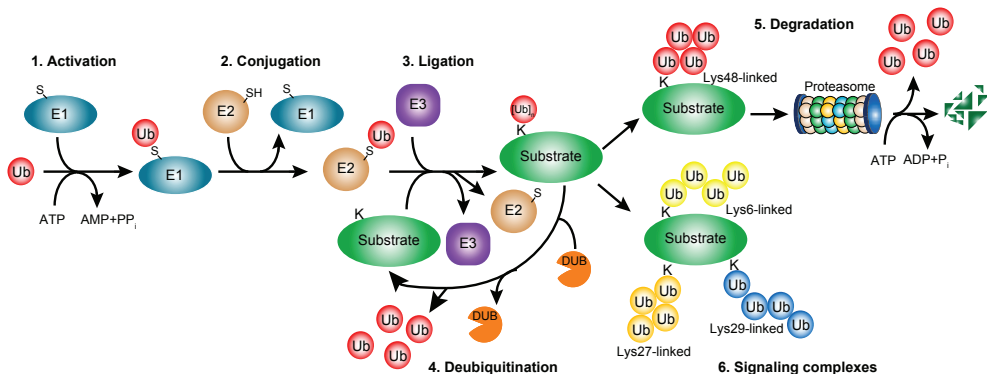


Figure 1. The enzymes and reactions of the (de)ubiquitination pathway. Image adapted from¹⁷.

(mono-ubiquitination) or on multiple lysine residues (multi-mono-ubiquitination), but they are also modified with different types of poly-ubiquitin chains (Figure 2).

In addition Ub chains can be assembled in a head-to-tail or linear configuration through the α -amino group at the N-terminus. An important difference between linear and lysine-linked chains is the chemistry of the linkage (isopeptide compared with peptide bond). To add to the complexity of ubiquitination, quantitative studies have shown the existence of branched Ub chains, although the specific pathways in which these more complex poly-ubiquitin chains are involved remain poorly understood¹⁸⁻²¹.

Deubiquitination pathway

Protein ubiquitination, similar to other regulated targeting pathways, is a reversible process and in the last decade protein deubiquitination has emerged as an important regulatory step in the ubiquitin-dependent pathways. In this deubiquitination process the isopeptide bond between Ub and a target protein or between Ub molecules in a poly-ubiquitin chain, is hydrolyzed by proteases named deubiquitinases (DUBs) (Figure 1)²²⁻²⁵.

Proteases

Proteases likely arose at the earliest stages of protein evolution as simple destructive enzymes necessary for protein catabolism and the generation of amino acids in primitive organisms. However, many years of studies on proteases have shown their relevance in the control of multiple biological processes in all living organisms. Thus proteases regulate the fate, localization and activity of many proteins, modulate protein-protein interactions, create new bioactive molecules and generate, transduce and amplify molecular signals. Because of their essential roles in different cellular processes, alterations in the structure and expression patterns of proteases underlie many human pathological conditions such as cancer, neurodegenerative disorders, and inflammatory and cardiovascular diseases²⁶⁻²⁹.

Based on the mechanism of catalysis, proteases are classified into six distinct classes: aspartic, glutamic, metalloproteases, cysteine, serine and threonine proteases. The first three classes utilize an activated water molecule as a nucleophile to attack the peptide bond of the substrate.

In contrast to the remaining protease classes, the nucleophile is an amino acid residue (Cys, Ser or Thr) located in the active site³⁰. Most proteases hydrolyse the α -peptide bonds between naturally occurring amino acids, but there are some proteases that perform slightly different reactions. In particular, the DUBs are able to hydrolyze the isopeptide bonds in Ub and Ubl protein conjugates.

DUBS

The human genome encodes more than 100 putative DUBs that are predicted to be active³¹. Even though there is a lack of knowledge about the regulation and roles of many DUBs, several generalizations have emerged in recent years.

Most DUB activity is cryptic. That is DUBs require substrate association or a scaffolding protein to achieve competent conformation. So like most other proteases, their activity is carefully controlled to prevent unnecessary cleavage of non-substrates³². Other DUBs are covalently modified by phosphorylation, ubiquitination or sumoylation, which are likely to influence activity, localization and half-life.

In addition to their active-site core domains, most DUBs contain insertions within the catalytic domain and N- and C-terminal extensions, which participate in the substrate binding and recognition and direct the assembly of multi-protein complexes that localize DUBs and assist in substrate selection. These extensions contain predicted ubiquitin-binding domains (UBDs), including the zinc finger ubiquitin-specific protease domain (ZnF-UBP domain), the ubiquitin-interacting motif (UIM) and the ubiquitin-associated domain (UBA domain)^{33,34}. The presence of one or multiple Ubl domains is also widely predicted³⁵.

DUB activities fall into three major functional categories (Figure 2). First, Ub can be transcribed from several genes as a linear fusion of multiple Ub molecules or with ribosomal proteins, such that the generation of free Ub requires DUB activity (Figure 2a). Second, DUBs can remove Ub chains from post-translationally modified proteins, leading to reversal of Ub signaling or to protein stabilization by rescue from degradation (Figure 2b, c). However, once proteins are targeted for degradation, associated DUB activities can prevent degradation of Ub and maintain Ub homeostasis (recycle of Ub) (Figure 2d,e)^{36,37}. Third, DUBs can

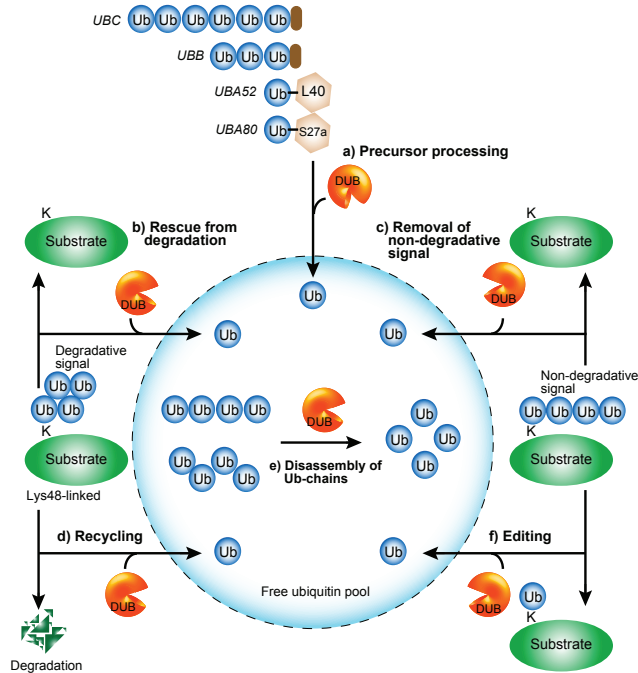


Figure 2. Schematic diagram of DUB function. Image adapted from³⁸.

be used to edit the form of Ub modification by trimming Ub chains and thereby help to exchange one type of Ub signal for another (Figure 2f)^{38,39}.

The DUB family can be classified into five distinct subfamilies: ubiquitin C-terminal hydrolyases (UCHs), ubiquitin-specific proteases (USPs), ovarian tumor proteases (OTUs), Josephins and JAB1/MPN/MOV34 metalloenzymes (JAMMs). The UCH, USP, OTU and Josephin subfamilies are Cys proteases, whereas the JAMM family members are zinc metalloproteases. A more comprehensive view on these five subfamilies of DUBs will be given in **chapter 2**: A genomic and function inventory of deubiquitinating enzymes.

Ubiquitin signaling

Types of ubiquitination

Depending on the type of Ub modification (attachment of a single Ub molecule or a Ub chain), a target protein can undergo different cellular fates (Figure 3). Multi-mono-ubiquitination has been shown to be involved in triggering the internalization of cell-surface receptors and their subsequent degradation in lysosomes or recycling to the cell surface⁴⁰. Mono-ubiquitination is also involved in

the DNA-damage response pathway, where histones or the DNA sliding clamp, PCNA (Proliferating-Cell Nuclear Antigen), are mono-ubiquitinated^{41,42}.

The most well studied example of Ub signaling is the Ub chain conjugation through the lysine at position 48 of Ub which leads to the proteasomal degradation of the modified target protein^{7,43-45}.

Also, proteins modified with K11-linked poly-ubiquitin chains are targeted for degradation by the proteasome. In addition proteins from diverse cellular processes were identified as being modified and regulated by K11-linked chains, suggesting that K11 is employed in many different pathways (e.g. in ERAD (Endoplasmic-Reticulum-Associated Degradation) and in the cell cycle regulation^{21,46,47}).

Another degradation signal is the K29-linked poly-ubiquitination. Proteins conjugated with K29-linked chains are degraded by lysosomal rather than proteasomal degradation pathways^{48,49}. K29-linked poly-ubiquitin chains are also implicated in the UFD (Ubiquitin Fusion Degradation) pathway, in which the N-terminus of target proteins are attached to a Ub leading to the extension with a K29- or K48-linked Ub chain, resulting in efficient degradation of the fusion protein⁵⁰. Besides

playing a role in protein degradation pathways, the K29-linked poly-ubiquitination also is involved in kinase modification, blocking their activity⁵¹.

In contrast to the degradation signals of K11-, K29- and K48-linked Ub chains, K63-linked poly-ubiquitin chains participate in endocytosis, in DNA repair and in signaling kinase complexes⁵²⁻⁵⁹.

While several reports show K6-linked poly-ubiquitination, mediated by the heterodimeric RING E3 ligase complex, BRCA1/BARD1, might be involved in DNA repair⁶⁰⁻⁶².

Although mass spectrometry proteomics did find K27- and K33-linked Ub chains, no clear cellular role has been associated with these types of Ub chains²¹. A U-box E3 ligase, Ufd2, was found to catalyze the formation of K27- and K33-linked Ub chains, which suggests a role in the UFD pathway⁶³. The K33-linked Ub chains have also been shown to be involved in kinase modification⁵¹.

The most recently described type of Ub polymer is the linear Ub chains, which are assembled by a specific ligase complex called the linear Ub-chain assembly complex (LU BAC) and are crucial for NF- κ B signaling^{19,64-66}.

Mass spectrometry proteomics has also shown that Ub chains can have more complex topologies. Doubly modified Ub peptides indicative of branched Ub chains have been detected⁶⁷. The ubiquitination of lysine residues in close proximity of each other as a product of *in vitro* reactions were detected and the K27/K29 forks have been found in yeast cells⁶⁸. It is still unclear which type of signals these branched Ub chains mediate, however they show the complexity of the Ub system.

The function, structure and physiological roles of K48- and K63-linked chains in ubiquitination have been studied and published extensively. However, relatively only a few reports deal with the remaining chain types, some of which have not been studied at all. A likely reason is that only K48- and K63-linked chains have been available and protocols for generation of these Ub chains have been published⁶⁹⁻⁷². El Oualid and colleagues recently published the chemical synthesis of all types of di-ubiquitin⁷³, which in **chapter 4** are utilized for investigating the differential modulation of the activity of a sub-family of DUBs.

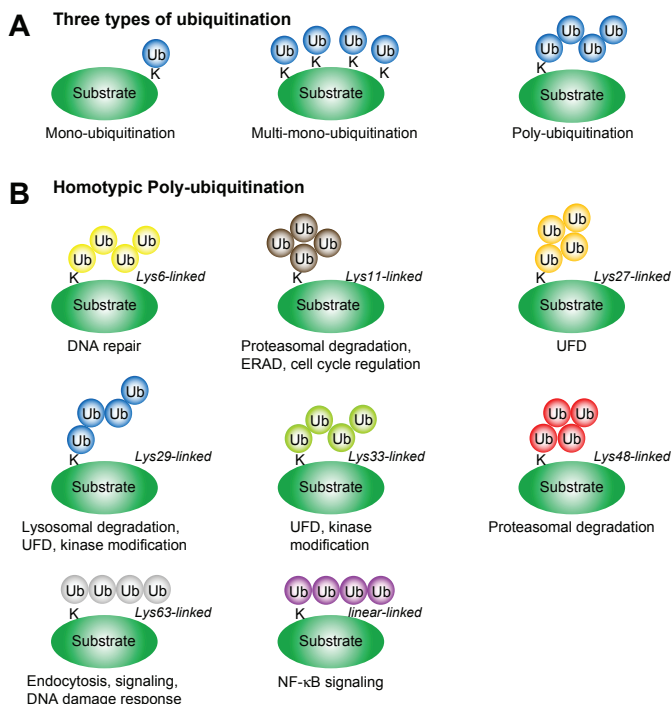


Figure 3. Different types of ubiquitination. Image adapted from²⁰.

Reading out of ubiquitin signals in different cellular processes

In all the processes described above, Ub acts as a signaling component that can trigger molecular events. This is achieved by operating as a reversible and highly versatile regulatory signal for ubiquitin-binding domains (UBDs) in cellular proteins. The effects of protein ubiquitination are mediated through a class of specific UBDs, with more than twenty different families identified to date. UBDs are diverse modules in a protein that can bind, and often distinguish, different types of Ub modifications. The UBDs differ both in structure and in the type of Ub recognition that they use. Most commonly, they fold into α -helical structures that bind a hydrophobic patch in the β -sheet of Ub. Other UBDs bind Ub through two discontinuous α -helices. It is currently unknown why so many variations of helical structures have evolved to interact with Ub and regulate its downstream signaling^{34,74}. The structures of many UBDs in complex with mono-ubiquitin have been determined revealing interactions with multiple surfaces on Ub and not just the Ile44 hydrophobic patch region. The affinities of the mono-ubiquitin binding of these domains span a wide range ($K_d = 1-100\mu\text{M}$). As a crude generalization binding domains in enzymes with activities in or regulated by ubiquitination tend to have affinities in the low micromolar range. Adaptors that bind ubiquitinated proteins contain domains that typically bind mono-ubiquitin with affinities of about $100\mu\text{M}$ or lower⁷⁴⁻⁷⁷.

Linkage-specific Ub recognition contributes to the diverse set of functional cellular processes associated with ubiquitination. Although some UBDs showed little discrimination between different Ub chain types, others do prefer certain ubiquitin-linkages. Several UBDs can selectively bind to K63-linked Ub chains. For example, NZF domains of TAK1-binding protein 2 (TAB2; also known as TRAF-binding protein domain) preferentially bind to K63- over K48-linked Ub chains⁷⁸.

Linker regions in tandem repeats of UBDs can also define linkage specificity. For example, the receptor associated protein 80 (RAP80) targets BRCA1 to DNA damage-induced foci through its two UIMs, which bind K63-linked Ub chains, but not K48-linked ones^{62,79,80}. The sequence between the two UIMs of RAP80 promotes an appropriate protein conformation such that the UIMs are positioned for efficient binding across

a single K63 linkage, thus defining selectivity. As mentioned in the previous paragraph, the linear Ub chains have been implicated in the activation of NF- κ B signaling pathway. Several proteins that regulate this pathway, including NF- κ B essential modulator (NEMO), A20-binding inhibitor of NF- κ B proteins (ABIN) and optineurin, contain the Ub binding in ABIN and NEMO domain (UBAN domain), which specifically binds to linear Ub chains^{66,81,82}. Specific mutations of NEMO that block interactions with linear Ub chains impair the activation of I κ B kinase (IKK) and NF- κ B in response to tumor necrosis factor- α (TNF- α) stimulation.

UBDs in DUBs

As stated previously, also DUBs contain UBDs, which might directly regulate their activity or specificity. USP25 for example requires UIMs to efficiently hydrolyze poly-ubiquitin chains⁸³. UIMs can also play a role in Ub linkage specificity. The UIM of ATXN3 for instance is necessary for K63 selectivity⁸⁴. Another common UBD found in DUBs is the ZnF-UBP domain, which in the case of USP5, binds to proximal Ub in the chain and induces an allosteric conformational change leading to an increased catalytic rate for Ub chain processing⁸⁵. Additionally, USP5 also possess two UBA domains, which are involved in binding two different poly-ubiquitin chains, linear and K48-linked^{86,87}. Recently, the crystal structure of the yeast Ubp8 (USP22) in complex with the SAGA (Spt-Ada-Gcn5 acetyltransferase) module was solved showing how the ZnF-UBP domain acts as a scaffold for complex assembly by holding all subunits of the module together^{88,89}. New classes of UBDs are continuously being reported, revealing new information not only about their functionality but also about the mechanisms of intermolecular regulation. The accumulated knowledge of Ub-UBD interactions will also have an impact on pharmacological and medical applications, as several UBDs have now been linked to various human pathologies, including cancer and immune deficiencies, thus becoming interesting as putative drug targets.

Cancer and disease

Implication of ubiquitination

It has been recognized that the ubiquitination of

cellular proteins is a major post-translational modification that can have profound effects on protein stability, localization or interaction pattern. These changes in the fate of individual proteins can cause alterations in cell signaling, which regulate cell cycle, proliferation or apoptosis⁷⁷. Tampering with the ubiquitination machinery has been observed in various cancers and neurological diseases^{90,91}. Multiple Ub pathway proteins, which directly control stability of key signaling molecules, have been identified as tumor suppressors or oncogenes^{77,92}.

The best studied example in which the deregulation of ubiquitination plays an important role in tumorigenesis and cell death is the p53 signaling pathway. It is a highly complex, multi-component signaling network that is of fundamental importance in tumor biology. p53, commonly known as 'the guardian of the genome', is a tumor suppressor that is capable of inducing cell-cycle arrest, cell senescence and apoptosis⁹³. Loss of p53 expression causes cells to lose pivotal signaling responses to DNA damage events, hypoxia and aberrant oncogene expression as seen in a large percentage of human tumors. The proliferation of oncogenic cells results in the repression of p53 expression and activation. P53 is predominantly regulated through the ubiquitin-proteasome pathway and maintained at low protein levels during normal homeostasis. The major player in controlling p53 levels is Mdm2. Mdm2 is a RING finger domain containing protein that exhibits E3 ubiquitin-protein ligase activity and is capable of regulating its own protein levels through auto-ubiquitination⁹³. Genotoxic stress can induce high levels of p53 promoting the expression of many proteins associated with apoptosis and cell-cycle arrest to counteract the stressors causing DNA damage. On the contrary, if p53 is overactive, the cell will die, so the p53-mediated increase in Mdm2 level helps to regulate p53 levels by polyubiquitination and targeting p53 for proteasomal degradation. Besides Mdm2 a few more E3 ligases have been reported to have similar activities in regulating p53 levels. COP1, Pirh2 and ARF-BP1 directly interact with p53 and target p53 for proteasome-mediated degradation⁹⁴⁻⁹⁹. Decreased p53 levels and mutations in p53 have been linked to high incidences of cancer, thus p53 levels being elevated act as a mechanism of tumor suppression¹⁰⁰. Mdm2-dependent and independent ubiquitinations that target p53 for degradation are considered oncogenic and prevent p53

from regulating the cell cycle or inducing apoptosis.

Recent examples of the implication of ubiquitination in cancer include TRAF6-mediated K63-linked poly-ubiquitination of the kinase Akt, which is required for the membrane localization and activation of this proto-oncogene. Mutations in Akt in tumor cells, have shown to enhance its non-degradative ubiquitination and thus promote oncogenic signaling¹⁰¹. Another example of the implication of the ubiquitination machinery in cancer is the NF- κ B signaling pathway. The NF- κ B transcription factor is activated through K63-linked poly-ubiquitination and its anti-apoptotic activity has been associated with tumor progression, chemotherapy resistance and metastasis¹⁰²⁻¹⁰⁴. The key event in NF- κ B activation is the degradation of the inhibitor of NF- κ B (I κ B) which releases NF- κ B from its sequestration in the cytoplasm. Various pro-inflammatory stimuli, including TNF- α , IL-1, and DNA damage activate the IKK (I κ B kinase) complex that phosphorylates I κ B and recruits the SCF Ub ligase. In turn, this SCF Ub ligase mediates the I κ B ubiquitination and proteasomal degradation. The recruitment of the IKK complex depends on the K63-linked poly-ubiquitination of adaptor proteins TRAF2 and RIP, where TRAF2 is the responsible E3 ligase. Respectively, NF- κ B signaling can be terminated via either deubiquitination of the adaptor proteins or their regulated degradation. Deregulation of either mechanism can lead to tumor formation. Thus, SCF E3 ligase, which ubiquitinates IKK β and down regulates NF- κ B signaling, has been found mutated in a high percentage of human malignancies.

Mediation of DNA repair is another established function of non-degradative Ub signaling. And it has been shown that non-repaired DNA lesions can lead to tumorigenesis and defects in the DNA repair system are common in several cancer predisposition syndromes. BRCA1 is a tumor suppressor whose mutation leads to a high incidence of breast and ovarian cancers¹⁰⁵. And together with BARD1, BRCA1 forms a heterodimeric E3 ligase, which synthesizes poly-Ub chains of different topology. This activity of BRCA1 plays an important role in the homologous recombination (HR) DNA repair pathway¹⁰⁶. In the absence of BARD1, BRCA1 is destabilized and degraded by the proteasome. UBE2T, the E2 conjugating enzyme, and HERC2, the E3 ligase enzyme, are the newly identified factors that mediate pro-

teasomal degradation of BRCA1^{107,108}. HERC2 is also the E3 ligase that is necessary for the Ub signaling at the DNA damage sites. It forms a complex with other Ub ligases, RNF8 and RNF168 (mutated in the RIDDLE syndrome) thereby facilitating the recruitment of the E2 conjugating enzyme Ubc13 to the sites of DNA damage¹⁰⁹. After detection of DNA damage, the Ubc13/RNF8 complex initiates poly-ubiquitination of histone H2A, thereby promoting the recruitment of Ub-binding proteins, including RAP80 and RNF168. RNF168, amplifies histone ubiquitination increasing the local concentration of K63-linked Ub chains and ensuring the recruitment of other DNA repair factor, such as BRCA1 and 53BP1 to the sites of DNA damage^{110,111}.

More recently, the Ub machinery has been implicated in the other major degradation system: autophagy. Autophagy is an evolutionary conserved lysosomal degradation pathway that targets bulky cargos, such as protein aggregates and mitochondria¹¹². Tumors resort to the autophagy to survive hypoxia and lack of nutrition. Yet, in normal mammalian cells, autophagy is more important for cell cleansing of aggregated proteins and damaged organelles¹¹³. Inhibition of autophagy in healthy tissues leads to accumulation of ubiquitinated protein aggregates and damaged mitochondria. This process has been linked to neoplastic transformation, which has shown to be associated with enhanced mutagenesis and deregulated cell signaling¹¹⁴. The inhibition of autophagy in cancer cells, besides limiting their survival in the face of hypoxia and starvation, could lead to accumulation of damaged mitochondria and protein aggregates due to the inhibition of the selective, Ub-regulated forms of autophagy. This could sensitize tumor cells to cancer therapies that aim at inducing apoptosis¹¹⁵.

It has become clear that the deregulation of the Ub-proteasome system (UPS) plays a vital role in the most important age-related neurodegenerative diseases, Alzheimer's disease. In Alzheimer's disease, hyper-phosphorylation of the microtubule-associated protein tau results in the accumulation of paired helical tau filaments involved in the formation of neurofibrillary tangles and neuritic plaques. Relative dysfunction or inhibitory overloading of the UPS may contribute to the abnormal accumulation of phosphorylated and ubiquitinated tau¹¹⁶. Interestingly, a frameshift mutant of Ub, Ub+1, found in some sporadic and hereditary Alzheimer

disease patients, inhibits the UPS and enhances the toxic protein aggregation in a yeast model¹¹⁷.

Implication of DUBs

There is a growing recognition of DUBs that are mutated in human cancers playing an important role as oncogenes and tumor suppressors. As mentioned previously, stabilization of p53 activates downstream targets to initiate cell-cycle control, DNA repair mechanisms and apoptosis. This p53 stabilization can be achieved by inhibiting Mdm2-mediated ubiquitination. Alternatively stabilization can also be achieved by deubiquitination catalyzed by DUBs to reduce ubiquitination of p53. Several USPs, including USP7 (HAUSP), USP2 and USP10, have been reported to regulate p53 and/or Mdm2¹¹⁸⁻¹²¹.

HAUSP was the first USP identified to deubiquitinate p53, with over-expression of HAUSP resulting in p53 stabilization leading to the induction of p53-dependent cell growth repression and apoptosis¹¹⁸. However, depletion of HAUSP in cells doesn't decrease p53 levels as predicted, but rather increases p53 levels, apparently because of HAUSP's ability to bind and deubiquitinate Mdm2^{119,122}. The relationship of HAUSP and cancer was complicated by the demonstration of HAUSP mediated regulation of Akt antagonist PTEN¹²³. Reduced nuclear localization of PTEN is a common feature in aggressive cancers, including advanced stage prostate cancer. PTEN nucleo-cytoplasmic shuttling is regulated by PTEN ubiquitination. HAUSP, which is overexpressed in prostate cancer, was shown to deubiquitinate PTEN leading to reduced nuclear localization. These data suggest that HAUSP may in some instances act as a tumor suppressor by stabilizing p53 or as an oncogene by stabilizing Mdm2 and re-distributing PTEN.

In a yeast-two hybrid screen, USP2 was found to complex with Mdm2. USP2 deubiquitinates Mdm2 leading to its stabilization¹²⁰. OncoPrint data suggest that many cancers have reduced expression of USP2 including cancers of the colon, pancreas and head/neck¹²⁴. Interestingly, USP2 was linked to prostate cancer through a study to isolate androgen sensitive DUBs from a prostate cancer cell line¹²⁵. USP2 was found to bind and stabilize fatty acid synthase, a protein that is often found overexpressed in aggressive prostate cancers^{125,126}.

USP10 is overexpressed in breast cancer tissue compared to adjacent normal tissue and

in glioblastoma samples^{127,128}. Recently, USP10 was identified as a DUB for p53. In unstressed cells, USP10 mainly localizes in the cytoplasm and regulates p53 homeostasis. After DNA damage, USP10 translocates to the nucleus and contributes to p53 activation. Increased USP10 expression in mutant p53 background increases p53 levels and promotes cancer cell proliferation, while downregulation of USP10 inhibits cancer cell growth. Increased expression of USP10 could be another mechanism responsible for increased mutant p53 expression in human cancers¹²¹.

Another example of the implication of DUBs in cancer is the familial cylindromatosis tumor suppressor gene, *CYLD*. Patients with familial cylindromatosis have the predisposition for developing multiple skin tumors of the head and neck. Germline mutations in the *CYLD* gene were identified in patients and most likely abolish the catalytic activity of *CYLD*^{129,130}. *CYLD* negatively regulates NF- κ B signaling through its deubiquitinating activity. As noted above, several intermediates of the NF- κ B pathway become K63-linked poly-ubiquitinated. By removing these K63-linked Ub chains, *CYLD* dampens the NF- κ B signaling¹³¹⁻¹³⁴.

The importance of the DUB activity in tumor progression is also illustrated by the recent findings that USPs are often overexpressed in tumors to stabilize oncogenic potential. USP9X for example was found overexpressed in various hematological malignancies. Initially USP9X in mammals was found to have a variety of functions including important intersections with cancer pathways: the Wnt and TGF β pathway¹³⁵⁻¹³⁸. Whether USP9X mediated deubiquitination plays a role in tumorigenesis remained unclear, and one could predict that overexpressed USP9X would enhance tumorigenesis by enhancing the Wnt and TGF β signaling. Recent findings by Schwickart and co-workers support this idea and found USP9X overexpressed in various hematological malignancies¹³⁹. USP9X overexpression leads to the promotion of cell survival by removing K48-linked poly-ubiquitin chains that would otherwise target the pro-survival BCL-2 member, MCL1, for proteasomal degradation. This contributes to the disease progression and chemoresistance¹³⁹.

Other USPs have been identified to be involved in tumorigenesis, however how these USPs are implicated remains unclear. The increase of USP6 transcription has been shown

to lead to the development of bone tumors¹⁴⁰. USP1 has been identified as a negative regulator of FANCD2 (an important factor in Fanconi Anemia) mono-ubiquitination and DNA repair and was also found to deubiquitinate PCNA, an important component of the trans-lesion synthesis (TLS) repair pathway¹⁴¹⁻¹⁴³. The OncoPrint database reveals the overexpression of USP28 in primary colon and breast cancer samples¹²⁴. USP28 has been identified to deubiquitinate Myc, a central player in many forms of cancer, thereby salvaging it from proteasomal degradation^{144,145}.

It is clear that the ubiquitination and deubiquitination pathway is tightly regulated and the deregulation in both processes has been shown to play a direct or indirect role in tumorigenesis and several inherited neurological diseases.

USP family

The ubiquitin-specific protease subclass represents the largest of the DUB family encoded by the human genome¹⁴⁶. In the last decade the crystal structures of the catalytic domain of several USPs, with or without Ub bound, have been solved (Figure 4) (USP8CD [PDB code: 2GFO], USP7CD [1NB8 & 1NBF], USP14CD [2AYN & 2AYO], USP2CD [2HD5], USP21CD [3I3T], Ubp8 [3M99 & 3MHH] and *CYLD* [2VHF])^{88,89,147-150}. The catalytic domain structures revealed several common structural features between the different USPs. First, despite the low sequence similarity the overall structure of the catalytic domain is highly conserved. Three well-defined sub-domains: the 'Fingers', the 'Thumb' and the 'Palm' domain form a structure that resembles a right-hand (Figure 4). Secondly, the catalytic centre resides at the interface between the Thumb and the Palm regions. The Thumb is predominantly α -helical and contains the Cys Box, a motif that includes the active site cysteine. The Palm is composed of β -strands supported by α -helices and contains the remaining active site residues that form the catalytic triad: a His and an Asp or Asn residue. The junction between the Thumb and the Palm domains forms a cleft that accommodates the C-terminal tail of Ub and the active site residues involved in the catalysis. Third, the Finger domain is composed of four β -strands and in USP8, USP2 and USP21 it contains a CXXCXnCXXC motif that chelates one zinc ion and form the so-called

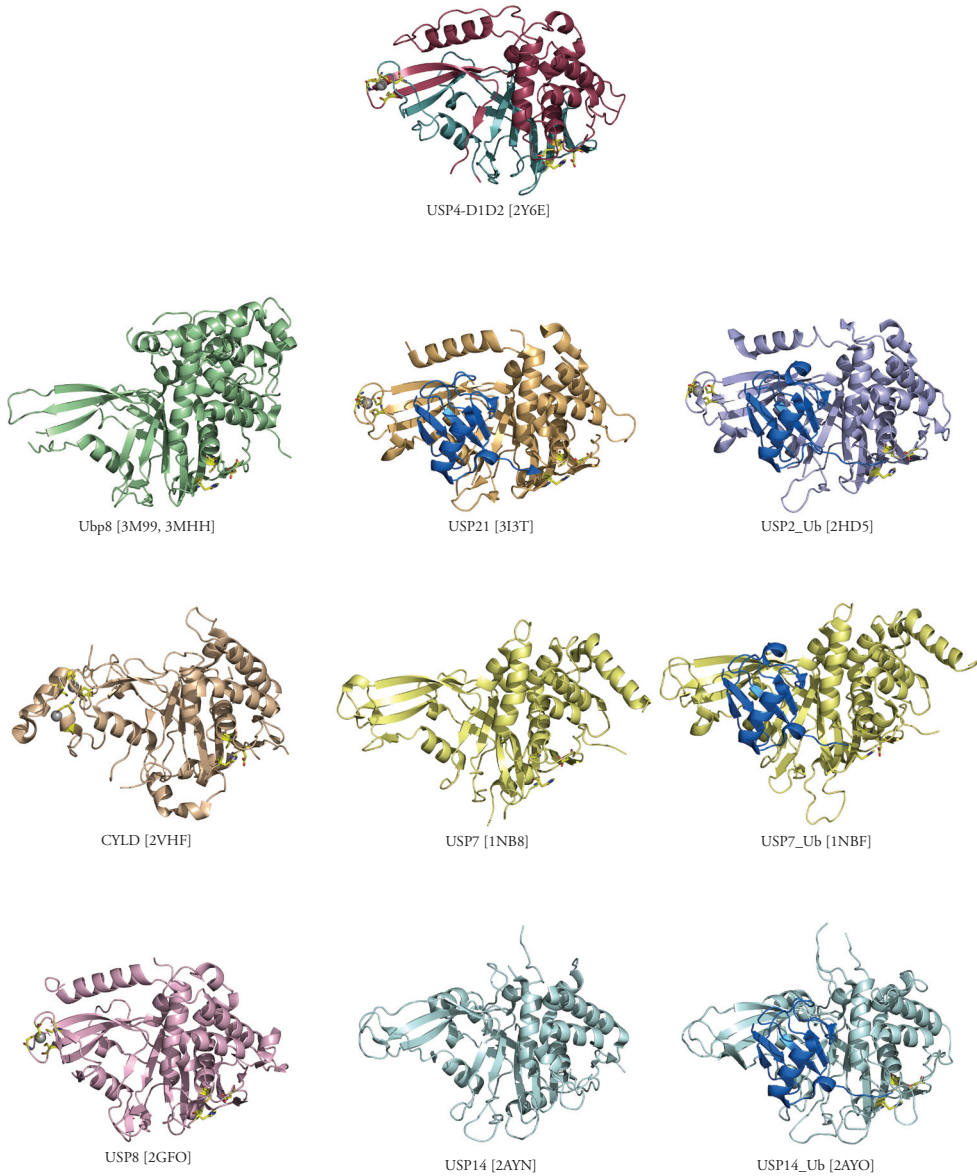


Figure 4. Crystal structures of the catalytic domains of USPs.

Zinc Finger ribbon^{147,150}. Although not all of the solved structures contain this motif, the overall fold of the Finger domain is maintained. The CXX-CXnCXXC motif is lacking in nine of the 54 putative human USPs, suggesting that the zinc binding ability is dispensable for the integrity of the Finger domain fold¹⁴⁶. The role of the Finger domain is to serve as a scaffold that contacts the globular body of Ub and the Zinc Finger ribbon does not appear to be involved in catalysis¹⁵¹. Interestingly, the Finger domain of CYLD is significantly smaller due to the shortening of the β -strands. CYLD also differs from the other USPs by the insertion of a Zn binding domain that closely resembles a B-box. The B-box is not required for deubiquitinating activity, but instead appears to be important for the cytoplasmic localization of CYLD¹³⁴.

Furthermore multiple studies have demonstrated that the catalytic activity of USPs is regulated by substrate- or scaffold-induced conformational changes. For example USP7 in the unliganded form has a misaligned catalytic triad configuration. The active site cysteine is approximately 10Å away from the active site histidine, too far for catalysis to occur. Upon binding to Ub a major conformational change occurs in the catalytic core domain causing the active site cysteine and histidine to be positioned within hydrogen bond distance from one another, rendering the enzyme catalytically competent¹⁴⁸.

The structure of USP14 in the presence and absence of Ub reveals a different type of activation mechanism. Unlike USP7, the catalytic triad of the free USP14 is productively aligned, indicating that the active site is catalytically competent. However, the binding groove that accommodates the C-terminal tail of Ub is blocked by two surface loops that undergo significant conformational changes upon Ub binding¹⁴⁹.

A third conformational change is thought to occur in USP8. In the structure of the unliganded form, the tip of the Zinc finger ribbon of USP8 is positioned inward toward the Palm resulting in a closed conformation that leaves insufficient room for Ub. Unlike the other USPs, USP8 and USP2 have a unique α -helix juxtaposed to the finger and this helix may be involved in stabilizing the closed conformation^{147,150}. Although there is no structure available of USP8 in complex with Ub, the closely related catalytic domain of USP2 has been solved in the presence of Ub. In this structure

the Finger domain is displaced outward to adopt the conformation observed in the other USPs¹⁵⁰. It is possible that upon target protein binding, the Finger domain of USP8 moves to the position observed in the other USPs, allowing the activation of the protease and subsequent binding to Ub.

Recently, the crystal structure of the yeast Ubp8 (USP22) in complex with the SAGA module was solved both in presence and absence of Ub. The structures showed that the Finger domain that binds Ub in the complex remains in an open conformation in the apo form. The Finger domain doesn't collapse and occlude the Ub-binding pocket as seen in USP8. Furthermore, the active site residues are in their catalytically competent orientation in both the presence and absence of Ub. Interestingly, several residues located adjacent to the Ub C-terminus are disordered in the absence of Ub and a small loop containing the active site cysteine (Cys-loop) move inward toward the Ub tail-binding groove. Both the Cys-loop and the disordered region contain residues that contact Ub directly. Ubp8 is activated by binding of the Sgf11 subunit of the SAGA module to the catalytic domain of Ubp8 near the active site, supporting the construction of a competent catalytic center of the enzyme^{88,89}.

The USP family members have modular domain architecture and besides having the conserved catalytic domain they also feature additional protein-protein and localization domains. A number of domains outside the catalytic domain have been identified and characterized, for example the TRAF-like domain of USP7, the DUSP (domain in USPs) domain of USP15 and as described previously several UBDs found in USPs^{87,152,153}. Interestingly, Ubl domains were recently predicted in a subset of USPs³⁵.

Ubl domain

In a sequence analysis integrated ubiquitin-like (Ubl) domain were identified in a large number of USPs³⁵. The integrated Ubl domain is a member of a subfamily of the Ub superfold family. Despite the poor sequence conservation for all members of the Ub superfold family, they all share the conserved β -grasp fold^{6,154}. The integrated Ubl folds are stretches of 45-80 amino acids and are found in a wide array of eukaryotic proteins. Only a small number of these integrated Ubl domains have been studied and characterized functionally. These integrated

Ubl domains are present in proteasomal shuttle factors like Rad23 and Dsk2 and are believed to play a role in recruitment of ubiquitinated proteins to the proteasome. Integrated Ubl domains in other proteins such as Parkin and USP14 can also be recruited to the proteasome. However, the integrated Ubl folds not only function in recruitment but also play a role in enzymatic activities of certain immune-response inducible kinases, such as IKK β ^{155,156}.

The Ubl domains found in the USP family are located at the N-terminus, within or at the C-terminus of the catalytic domain. Till recently only the Ubl domain at the N-terminus of USP14 has been characterized. It has been shown to be involved in proteasome binding, which promotes the DUB activity of USP14¹⁴⁹. In **chapter 5** a Ubl domain located within the catalytic domain of a USP is described and its effect on DUB activity.

USP4

Like USP14, USP4 has a Ubl domain N-terminal of its catalytic domain, but more interestingly it has a second Ubl domain within the catalytic domain. Furthermore, the DUSP domain is located N-terminal of the first Ubl domain. Not much is known about the structure and function of USP4, previously known as UNP for ubiquitous nuclear protein. It has been identified as a proto-oncogene related to *tre-2/tre-17* (USP6) by its ability to transform NIH3T3 cells and lead to increased tumorigenesis in nude mice^{157,158}. In a study of primary human lung tumor tissue, USP4 was observed to have a consistently elevated gene expression levels in small cell tumors and adenocarcinomas of the lung, suggesting a possible causative role for USP4 in neoplasia¹⁵⁹.

Besides the described domains of USP4, it also possesses functional nuclear import/export signals, the basis of its ability to shuttle between nucleus and cytoplasm¹⁶⁰. Because of this ability, USP4 seems to have different cellular functions depending on its localization. When located in the cytoplasm, it has been reported that knockdown of USP4 activates the β -catenin-associated transcription¹⁶¹. By interacting with two known Wnt signaling components Nemo-like kinase and T-cell factor 4, USP4 may play a role in the Wnt signaling pathway in a variety of physiological conditions.

Interestingly, Song and co-workers show that USP4 is recruited to the spliceosome by form-

ing a complex with Sart3¹⁶². The N-terminal DUSP domain and the adjacent DUF1055 domain (amino acids 27-216) of USP4 is primarily responsible for this interaction with Sart3. The Sart3 protein is a recycling factor of the U4/U6 spliceosomal snRNP, which promotes the re-annealing of U4 and U6 snRNPs. The crystal structure of the N-terminus of USP4 (PDB: 3JYU) shows that the DUF1055 domain is actually a Ubl domain which interacts extensively with the DUSP domain. It is likely that binding to the Sart3 protein might abolish this interaction and hence recruit USP4 to the spliceosome complex where it preferentially deubiquitinates K63-linked chains on the U4 component Prp3. The deubiquitination of Prp3 most likely facilitates the release of Prp3 from the spliceosome during maturation of its active site¹⁶².

In addition to its cytoplasmic roles, recent evidence shows that USP4 also plays important nuclear roles. Fan and co-workers show that the tumor necrosis factor- α (TNF α), a pro-inflammatory cytokine, induces association of USP4 with the transforming growth factor- β -activated kinase 1 (TAK1), which leads to the deubiquitination of Lys63-linked polyubiquitinated TAK1 and thereby down-regulating the TAK1-mediated NF- κ B activation¹⁶³.

Furthermore, Zhang and co-workers recently identified a new important role for USP4. They show that USP4 interacts directly with and deubiquitinates ARF-BP1, leading to the stabilization of ARF-BP1 and subsequent reduction of p53 levels¹⁶⁴. ARF-binding protein 1 (ARF-BP1; also known as HUWE1) was recently identified as another critical E3 Ub ligase in regulating p53 levels⁹⁹. ARF-BP1 is a HECT domain-containing E3 Ub ligase, which interacts directly and ubiquitinates the p53 protein. This p53 ubiquitination is strongly repressed by the binding of ARF to ARF-BP1. The inactivation of ARF-BP1 stabilizes p53 and induces apoptosis.

It seems that USP4 plays several important cellular roles depending on its location in the cell. And it is therefore interesting to see what future research will unveil on how USP4 function is being regulated. **Chapter 5** shows how the catalytic activity of USP4 is being regulated.

Structural genomics

In the 21st century with the rise of new efficient

genome sequencing techniques, microarray experiments and new proteomics technologies, biology has seen huge increase in DNA sequence, gene expression and proteomics data. The Human Genome and other genome sequencing projects continue to deliver new protein sequences in a rapid pace. New protein families are being discovered in newly sequenced genomes, for which a large fraction of these new protein families we virtually don't have any functional or structural data.

To counteract this trend a number of structural genomics (SG) programs were created with the aim to determine rapidly a large number of novel structures in order to expand structural and functional knowledge for proteins found in genomes. The largest SG centers are funded by Japan (RIKEN), the United States [Protein Structure Initiative] (PSI and PSI2) and by an international consortium of governments, charitable foundations and industry [the Structural Genomics Consortium] (SGC), while in Europe The Structural Proteomics In Europe (SPINE and SPINE2) was set-up. These SG centers are using different approaches to structurally characterize the protein world¹⁶⁵⁻¹⁶⁸. RIKEN and the SGC focuses on the human proteome¹⁶⁵, while PSI and PSI2 target the representative members of the largest protein families, proteins from human parasite and Mycobacterium tuberculosis^{168,169}. SPINE and SPINE2 introduced high-throughput proteomics in a wide collaborative platform in which SPINE initially was focused on targets of medical relevance. SPINE2 continued and extended these methodologies to study macromolecular complexes¹⁷⁰.

Additionally, most SG centers have dedicated a significant part of their efforts in the development of high-throughput methods, which may now also be used for fast and more accurate determination of structures by both X-ray crystallography and NMR techniques in laboratories not involved in SG efforts. The work on thousands of target proteins has led to the development of efficient protocols for each of the steps of the structure determination process^{167,171}. New experimental protocols that were developed through SG efforts have shifted over time the so-called 'bottlenecks' in the pipeline and it seems that at present the analysis of 3D structures in the context of all biological and bioinformatics information is the slowest step of the whole process.

As part of the SPINE network, we did

our share of work in developing new tools and efficient protocols to aid the initial steps of structure determination and are described in **chapter 3**.

Outline of this thesis

Ubiquitination is a reversible protein modification that plays a central role in many important cellular functions. The enzymes involved in this ubiquitination process have been the main focus of many studies for several decades. However, deubiquitinases (DUBs), responsible for the removal and processing of ubiquitin, have been shown to be equally important. Over the last decade a lot of progress has been made in the characterization of this large family of isopeptidases. Because of their roles in key regulatory processes, these DUBs are actively pursued as new drug targets. The aim of this thesis was to study the structure and function of members of the ubiquitin-specific protease family.

In **Chapter 2** we give a comprehensive overview of putative DUBs encoded by the human genome. Furthermore, the function, specificity and the regulation of DUB activity is discussed.

In order to study a large number of USPs in parallel, high-throughput tools and methods needed to be developed. In **Chapter 3** a description of a set of protein expression vectors for ligation-independent cloning is given and their use on a large number of the USP family members.

In **Chapter 4** a set of twelve USPs in presence and absence of modulators have been analyzed for their enzyme activity using synthetic reagents. Among these reagents are all seven wild-type lysine-linked di-ubiquitins and the first comprehensive analysis comparing Ub chain preference is given.

In **Chapter 5** we present the crystal structure of the catalytic domain of USP4 and we show a new function of its Ubl domain located within the catalytic core.

A summary of the findings, concluding remarks and implications for future research are presented in **Chapter 6**.

References

1. Weissman, A.M. Themes and variations on ubiquitylation. *Nat Rev Mol Cell Biol* **2**, 169-78 (2001).
2. Sun, L. & Chen, Z.J. The novel functions of ubiquitination in signaling. *Curr Opin Cell Biol* **16**, 119-26 (2004).
3. Giles, J. Chemistry Nobel for trio who revealed molecular death-tag. *Nature* **431**, 729 (2004).
4. Vijay-Kumar, S., Bugg, C.E., Wilkinson, K.D. & Cook, W.J. Three-dimensional structure of ubiquitin at 2.8 Å resolution. *Proc Natl Acad Sci U S A* **82**, 3582-5 (1985).
5. Vijay-Kumar, S., Bugg, C.E. & Cook, W.J. Structure of ubiquitin refined at 1.8 Å resolution. *J Mol Biol* **194**, 531-44 (1987).
6. Burroughs, A.M., Balaji, S., Iyer, L.M. & Aravind, L. Small but versatile: the extraordinary functional and structural diversity of the beta-grasp fold. *Biol Direct* **2**, 18 (2007).
7. Hershko, A. & Ciechanover, A. The ubiquitin system. *Annu Rev Biochem* **67**, 425-79 (1998).
8. Pickart, C.M. Mechanisms underlying ubiquitination. *Annu Rev Biochem* **70**, 503-33 (2001).
9. Dye, B.T. & Schulman, B.A. Structural mechanisms underlying post-translational modification by ubiquitin-like proteins. *Annu Rev Biophys Biomol Struct* **36**, 131-50 (2007).
10. Deshaies, R.J. & Joazeiro, C.A. RING domain E3 ubiquitin ligases. *Annu Rev Biochem* **78**, 399-434 (2009).
11. Schulman, B.A. & Harper, J.W. Ubiquitin-like protein activation by E1 enzymes: the apex for downstream signalling pathways. *Nat Rev Mol Cell Biol* **10**, 319-31 (2009).
12. Kerscher, O., Felberbaum, R. & Hochstrasser, M. Modification of proteins by ubiquitin and ubiquitin-like proteins. *Annu Rev Cell Dev Biol* **22**, 159-80 (2006).
13. Furukawa, K., Mizushima, N., Noda, T. & Ohsumi, Y. A protein conjugation system in yeast with homology to biosynthetic enzyme reaction of prokaryotes. *J Biol Chem* **275**, 7462-5 (2000).
14. Mizushima, N. et al. A protein conjugation system essential for autophagy. *Nature* **395**, 395-8 (1998).
15. Kamitani, T., Kito, K., Nguyen, H.P. & Yeh, E.T. Characterization of NEDD8, a developmentally down-regulated ubiquitin-like protein. *J Biol Chem* **272**, 28557-62 (1997).
16. Dohmen, R.J. SUMO protein modification. *Biochim Biophys Acta* **1695**, 113-31 (2004).
17. Vucic, D., Dixit, V.M. & Wertz, I.E. Ubiquitylation in apoptosis: a post-translational modification at the edge of life and death. *Nat Rev Mol Cell Biol* **12**, 439-52 (2011).
18. Ikeda, F. & Dikic, I. Atypical ubiquitin chains: new molecular signals. 'Protein Modifications: Beyond the Usual Suspects' review series. *EMBO Rep* **9**, 536-42 (2008).
19. Kirisako, T. et al. A ubiquitin ligase complex assembles linear polyubiquitin chains. *Embo J* **25**, 4877-87 (2006).
20. Komander, D. The emerging complexity of protein ubiquitination. *Biochem Soc Trans* **37**, 937-53 (2009).
21. Xu, P. et al. Quantitative proteomics reveals the function of unconventional ubiquitin chains in proteasomal degradation. *Cell* **137**, 133-45 (2009).
22. Amerik, A.Y. & Hochstrasser, M. Mechanism and function of deubiquitinating enzymes. *Biochim Biophys Acta* **1695**, 189-207 (2004).
23. D'Andrea, A. & Pellman, D. Deubiquitinating enzymes: a new class of biological regulators. *Crit Rev Biochem Mol Biol* **33**, 337-52 (1998).
24. Wilkinson, K.D. Ubiquitination and deubiquitination: targeting of proteins for degradation by the proteasome. *Semin Cell Dev Biol* **11**, 141-8 (2000).
25. Wing, S.S. Deubiquitinating enzymes—the importance of driving in reverse along the ubiquitin-proteasome pathway. *Int J Biochem Cell Biol* **35**, 590-605 (2003).
26. Urban, S. Rhomboid proteases: conserved membrane proteases with divergent biological functions.

- 1**
- Genes Dev* **20**, 3054-68 (2006).
27. Ehrmann, M. & Clausen, T. Proteolysis as a regulatory mechanism. *Annu Rev Genet* **38**, 709-24 (2004).
 28. Siegel, R.M. Caspases at the crossroads of immune-cell life and death. *Nat Rev Immunol* **6**, 308-17 (2006).
 29. Page-McCaw, A., Ewald, A.J. & Werb, Z. Matrix metalloproteinases and the regulation of tissue remodelling. *Nat Rev Mol Cell Biol* **8**, 221-33 (2007).
 30. Barrett A.J., R.N.D., Woessner J.F. *Handbook of proteolytic enzymes*, 1666 (Academic Press, 1998).
 31. Nijman, S.M. et al. A genomic and functional inventory of deubiquitinating enzymes. *Cell* **123**, 773-86 (2005).
 32. Liz, M.A. & Sousa, M.M. Deciphering cryptic proteases. *Cell Mol Life Sci* **62**, 989-1002 (2005).
 33. Reyes-Turcu, F.E. & Wilkinson, K.D. Polyubiquitin binding and disassembly by deubiquitinating enzymes. *Chem Rev* **109**, 1495-508 (2009).
 34. Hurley, J.H., Lee, S. & Prag, G. Ubiquitin-binding domains. *Biochem J* **399**, 361-72 (2006).
 35. Zhu, X., Menard, R. & Sulea, T. High incidence of ubiquitin-like domains in human ubiquitin-specific proteases. *Proteins* **69**, 1-7 (2007).
 36. Swaminathan, S., Amerik, A.Y. & Hochstrasser, M. The Doa4 deubiquitinating enzyme is required for ubiquitin homeostasis in yeast. *Mol Biol Cell* **10**, 2583-94 (1999).
 37. Verma, R. et al. Role of Rpn11 metalloprotease in deubiquitination and degradation by the 26S proteasome. *Science* **298**, 611-5 (2002).
 38. Komander, D., Clague, M.J. & Urbe, S. Breaking the chains: structure and function of the deubiquitinases. *Nat Rev Mol Cell Biol* **10**, 550-63 (2009).
 39. Heyninck, K. & Beyaert, R. A20 inhibits NF-kappaB activation by dual ubiquitin-editing functions. *Trends Biochem Sci* **30**, 1-4 (2005).
 40. Haglund, K. et al. Multiple monoubiquitination of RTKs is sufficient for their endocytosis and degradation. *Nat Cell Biol* **5**, 461-6 (2003).
 41. Alpi, A.F., Pace, P.E., Babu, M.M. & Patel, K.J. Mechanistic insight into site-restricted monoubiquitination of FANCD2 by Ube2t, FANCL, and FANCI. *Mol Cell* **32**, 767-77 (2008).
 42. Sigismund, S., Polo, S. & Di Fiore, P.P. Signaling through monoubiquitination. *Curr Top Microbiol Immunol* **286**, 149-85 (2004).
 43. Finley, D. Recognition and processing of ubiquitin-protein conjugates by the proteasome. *Annu Rev Biochem* **78**, 477-513 (2009).
 44. Petroski, M.D. & Deshaies, R.J. Mechanism of lysine 48-linked ubiquitin-chain synthesis by the cullin-RING ubiquitin-ligase complex SCF-Cdc34. *Cell* **123**, 1107-20 (2005).
 45. Chen, Z. & Pickart, C.M. A 25-kilodalton ubiquitin carrier protein (E2) catalyzes multi-ubiquitin chain synthesis via lysine 48 of ubiquitin. *J Biol Chem* **265**, 21835-42 (1990).
 46. Baboshina, O.V. & Haas, A.L. Novel multiubiquitin chain linkages catalyzed by the conjugating enzymes E2EPF and RAD6 are recognized by 26 S proteasome subunit 5. *J Biol Chem* **271**, 2823-31 (1996).
 47. Jin, L., Williamson, A., Banerjee, S., Philipp, I. & Rape, M. Mechanism of ubiquitin-chain formation by the human anaphase-promoting complex. *Cell* **133**, 653-65 (2008).
 48. Chastagner, P., Israel, A. & Brou, C. AIP4/Itch regulates Notch receptor degradation in the absence of ligand. *PLoS One* **3**, e2735 (2008).
 49. Chastagner, P., Israel, A. & Brou, C. Itch/AIP4 mediates Deltex degradation through the formation of K29-linked polyubiquitin chains. *EMBO Rep* **7**, 1147-53 (2006).
 50. Johnson, E.S., Ma, P.C., Ota, I.M. & Varshavsky, A. A proteolytic pathway that recognizes ubiquitin as a degradation signal. *J Biol Chem* **270**, 17442-56 (1995).
 51. Al-Hakim, A.K. et al. Control of AMPK-related kinases by USP9X and atypical Lys(29)/Lys(33)-linked polyubiquitin

- chains. *Biochem J* **411**, 249-60 (2008).
52. Deng, L. et al. Activation of the Ikap- α B kinase complex by TRAF6 requires a dimeric ubiquitin-conjugating enzyme complex and a unique polyubiquitin chain. *Cell* **103**, 351-61 (2000).
 53. Hofmann, R.M. & Pickart, C.M. Non-canonical MMS2-encoded ubiquitin-conjugating enzyme functions in assembly of novel polyubiquitin chains for DNA repair. *Cell* **96**, 645-53 (1999).
 54. Chen, Z.J. & Sun, L.J. Nonproteolytic functions of ubiquitin in cell signaling. *Mol Cell* **33**, 275-86 (2009).
 55. Duncan, L.M. et al. Lysine-63-linked ubiquitination is required for endolysosomal degradation of class I molecules. *Embo J* **25**, 1635-45 (2006).
 56. Moldovan, G.L., Pfander, B. & Jen-
tsch, S. PCNA, the maestro of the replication fork. *Cell* **129**, 665-79 (2007).
 57. Mailand, N. et al. RNF8 ubiquitylates histones at DNA double-strand breaks and promotes assembly of repair proteins. *Cell* **131**, 887-900 (2007).
 58. Panier, S. & Durocher, D. Regulatory ubiquitylation in response to DNA double-strand breaks. *DNA Repair (Amst)* **8**, 436-43 (2009).
 59. Skaug, B., Jiang, X. & Chen, Z.J. The role of ubiquitin in NF- κ B regulatory pathways. *Annu Rev Biochem* **78**, 769-96 (2009).
 60. Nishikawa, H. et al. Mass spectrometric and mutational analyses reveal Lys-6-linked polyubiquitin chains catalyzed by BRCA1-BARD1 ubiquitin ligase. *J Biol Chem* **279**, 3916-24 (2004).
 61. Morris, J.R. & Solomon, E. BRCA1 : BARD1 induces the formation of conjugated ubiquitin structures, dependent on K6 of ubiquitin, in cells during DNA replication and repair. *Hum Mol Genet* **13**, 807-17 (2004).
 62. Sobhian, B. et al. RAP80 targets BRCA1 to specific ubiquitin structures at DNA damage sites. *Science* **316**, 1198-202 (2007).
 63. Hatakeyama, S., Yada, M., Matsumoto, M., Ishida, N. & Nakayama, K.I. U box proteins as a new family of ubiquitin-protein ligases. *J Biol Chem* **276**, 33111-20 (2001).
 64. Tokunaga, F. et al. Involvement of linear polyubiquitylation of NEMO in NF- κ B activation. *Nat Cell Biol* **11**, 123-32 (2009).
 65. Iwai, K. & Tokunaga, F. Linear polyubiquitination: a new regulator of NF- κ B activation. *EMBO Rep* **10**, 706-13 (2009).
 66. Rahighi, S. et al. Specific recognition of linear ubiquitin chains by NEMO is important for NF- κ B activation. *Cell* **136**, 1098-109 (2009).
 67. Kim, H.T. et al. Certain pairs of ubiquitin-conjugating enzymes (E2s) and ubiquitin-protein ligases (E3s) synthesize nondegradable forked ubiquitin chains containing all possible isopeptide linkages. *J Biol Chem* **282**, 17375-86 (2007).
 68. Peng, J. et al. A proteomics approach to understanding protein ubiquitination. *Nat Biotechnol* **21**, 921-6 (2003).
 69. Virdee, S., Ye, Y., Nguyen, D.P., Komander, D. & Chin, J.W. Engineered diubiquitin synthesis reveals Lys29-isopeptide specificity of an OTU deubiquitinase. *Nat Chem Biol* **6**, 750-7 (2010).
 70. Ye, Y. et al. Polyubiquitin binding and cross-reactivity in the USP domain deubiquitinase USP21. *EMBO Rep* **12**, 350-7 (2011).
 71. Pickart, C.M. & Raasi, S. Controlled synthesis of polyubiquitin chains. *Methods Enzymol* **399**, 21-36 (2005).
 72. Bremm, A., Freund, S.M. & Komander, D. Lys11-linked ubiquitin chains adopt compact conformations and are preferentially hydrolyzed by the deubiquitinase Cezanne. *Nat Struct Mol Biol* **17**, 939-47 (2010).
 73. El Oualid, F. et al. Chemical synthesis of ubiquitin, ubiquitin-based probes, and diubiquitin. *Angew Chem Int Ed Engl* **49**, 10149-53 (2010).
 74. Dikic, I., Wakatsuki, S. & Walters, K.J. Ubiquitin-binding domains - from structures to functions. *Nat Rev Mol Cell Biol* **10**, 659-71 (2009).
 75. Hicke, L., Schubert, H.L. & Hill, C.P. Ubiquitin-binding domains. *Nat Rev Mol Cell Biol* **6**, 610-21 (2005).

76. Harper, J.W. & Schulman, B.A. Structural complexity in ubiquitin recognition. *Cell* **124**, 1133-6 (2006).
77. Kirkin, V. & Dikic, I. Role of ubiquitin- and Ubl-binding proteins in cell signaling. *Curr Opin Cell Biol* **19**, 199-205 (2007).
78. Komander, D. et al. Molecular discrimination of structurally equivalent Lys 63-linked and linear polyubiquitin chains. *EMBO Rep* **10**, 466-73 (2009).
79. Wang, B. et al. Abraxas and RAP80 form a BRCA1 protein complex required for the DNA damage response. *Science* **316**, 1194-8 (2007).
80. Sims, J.J. & Cohen, R.E. Linkage-specific avidity defines the lysine 63-linked polyubiquitin-binding preference of rap80. *Mol Cell* **33**, 775-83 (2009).
81. Wagner, S. et al. Ubiquitin binding mediates the NF-kappaB inhibitory potential of ABIN proteins. *Oncogene* **27**, 3739-45 (2008).
82. Lo, Y.C. et al. Structural basis for recognition of diubiquitins by NEMO. *Mol Cell* **33**, 602-15 (2009).
83. Meulmeester, E., Kunze, M., Hsiao, H.H., Urlaub, H. & Melchior, F. Mechanism and consequences for paralog-specific sumoylation of ubiquitin-specific protease 25. *Mol Cell* **30**, 610-9 (2008).
84. Winborn, B.J. et al. The deubiquitinating enzyme ataxin-3, a polyglutamine disease protein, edits Lys63 linkages in mixed linkage ubiquitin chains. *J Biol Chem* **283**, 26436-43 (2008).
85. Reyes-Turcu, F.E. et al. The ubiquitin binding domain ZnF UBP recognizes the C-terminal diglycine motif of unanchored ubiquitin. *Cell* **124**, 1197-208 (2006).
86. Reyes-Turcu, F.E., Shanks, J.R., Komander, D. & Wilkinson, K.D. Recognition of polyubiquitin isoforms by the multiple ubiquitin binding modules of isopeptidase T. *J Biol Chem* **283**, 19581-92 (2008).
87. Bonnet, J., Romier, C., Tora, L. & Devys, D. Zinc-finger UBPs: regulators of deubiquitylation. *Trends Biochem Sci* **33**, 369-75 (2008).
88. Samara, N.L. et al. Structural insights into the assembly and function of the SAGA deubiquitinating module. *Science* **328**, 1025-9 (2010).
89. Kohler, A., Zimmerman, E., Schneider, M., Hurt, E. & Zheng, N. Structural basis for assembly and activation of the heterotetrameric SAGA histone H2B deubiquitinase module. *Cell* **141**, 606-17 (2010).
90. Chung, K.K., Dawson, V.L. & Dawson, T.M. The role of the ubiquitin-proteasomal pathway in Parkinson's disease and other neurodegenerative disorders. *Trends Neurosci* **24**, S7-14 (2001).
91. Schwartz, A.L. & Ciechanover, A. The ubiquitin-proteasome pathway and pathogenesis of human diseases. *Annu Rev Med* **50**, 57-74 (1999).
92. Hoeller, D. & Dikic, I. Targeting the ubiquitin system in cancer therapy. *Nature* **458**, 438-44 (2009).
93. Brooks, C.L. & Gu, W. p53 ubiquitination: Mdm2 and beyond. *Mol Cell* **21**, 307-15 (2006).
94. Jones, S.N., Roe, A.E., Donehower, L.A. & Bradley, A. Rescue of embryonic lethality in Mdm2-deficient mice by absence of p53. *Nature* **378**, 206-8 (1995).
95. Montes de Oca Luna, R., Wagner, D.S. & Lozano, G. Rescue of early embryonic lethality in mdm2-deficient mice by deletion of p53. *Nature* **378**, 203-6 (1995).
96. Leng, R.P. et al. Pirh2, a p53-induced ubiquitin-protein ligase, promotes p53 degradation. *Cell* **112**, 779-91 (2003).
97. Dornan, D. et al. COP1, the negative regulator of p53, is overexpressed in breast and ovarian adenocarcinomas. *Cancer Res* **64**, 7226-30 (2004).
98. Dornan, D. et al. The ubiquitin ligase COP1 is a critical negative regulator of p53. *Nature* **429**, 86-92 (2004).
99. Chen, D. et al. ARF-BP1/Mule is a critical mediator of the ARF tumor suppressor. *Cell* **121**, 1071-83 (2005).
100. Horn, H.F. & Vousden, K.H. Coping with stress: multiple ways to activate p53. *Oncogene* **26**, 1306-16 (2007).
101. Yang, W.L. et al. The E3 ligase TRAF6 regulates Akt ubiquitination and activation. *Science* **325**, 1134-8 (2009).
102. Wu, Y. et al. Stabilization of snail by NF-kappaB is required for inflammation-induced cell migration and inva-

103. Wertz, I.E. & Dixit, V.M. Signaling to NF-kappaB: regulation by ubiquitination. *Cold Spring Harb Perspect Biol* **2**, a003350 (2010).
104. Lee, D.F. et al. KEAP1 E3 ligase-mediated downregulation of NF-kappaB signaling by targeting IKKbeta. *Mol Cell* **36**, 131-40 (2009).
105. Futreal, P.A. et al. BRCA1 mutations in primary breast and ovarian carcinomas. *Science* **266**, 120-2 (1994).
106. Ulrich, H.D. & Walden, H. Ubiquitin signalling in DNA replication and repair. *Nat Rev Mol Cell Biol* **11**, 479-89 (2010).
107. Ueki, T. et al. Ubiquitination and downregulation of BRCA1 by ubiquitin-conjugating enzyme E2T overexpression in human breast cancer cells. *Cancer Res* **69**, 8752-60 (2009).
108. Wu, W. et al. HERC2 is an E3 ligase that targets BRCA1 for degradation. *Cancer Res* **70**, 6384-92 (2010).
109. Bekker-Jensen, S. et al. HERC2 coordinates ubiquitin-dependent assembly of DNA repair factors on damaged chromosomes. *Nat Cell Biol* **12**, 80-6; sup pp 1-12 (2010).
110. Doil, C. et al. RNF168 binds and amplifies ubiquitin conjugates on damaged chromosomes to allow accumulation of repair proteins. *Cell* **136**, 435-46 (2009).
111. Stewart, G.S. et al. The RIDDLE syndrome protein mediates a ubiquitin-dependent signaling cascade at sites of DNA damage. *Cell* **136**, 420-34 (2009).
112. Kirkin, V., McEwan, D.G., Novak, I. & Dikic, I. A role for ubiquitin in selective autophagy. *Mol Cell* **34**, 259-69 (2009).
113. Mathew, R., Karantza-Wadsworth, V. & White, E. Role of autophagy in cancer. *Nat Rev Cancer* **7**, 961-7 (2007).
114. Mathew, R. et al. Autophagy suppresses tumorigenesis through elimination of p62. *Cell* **137**, 1062-75 (2009).
115. Dikic, I., Johansen, T. & Kirkin, V. Selective autophagy in cancer development and therapy. *Cancer Res* **70**, 3431-4 (2010).
116. Keck, S., Nitsch, R., Grune, T. & Ullrich, O. Proteasome inhibition by paired helical filament-tau in brains of patients with Alzheimer's disease. *J Neurochem* **85**, 115-22 (2003).
117. Tank, E.M. & True, H.L. Disease-associated mutant ubiquitin causes proteasomal impairment and enhances the toxicity of protein aggregates. *PLoS Genet* **5**, e1000382 (2009).
118. Li, M. et al. Deubiquitination of p53 by HAUSP is an important pathway for p53 stabilization. *Nature* **416**, 648-53 (2002).
119. Li, M., Brooks, C.L., Kon, N. & Gu, W. A dynamic role of HAUSP in the p53-Mdm2 pathway. *Mol Cell* **13**, 879-86 (2004).
120. Stevenson, L.F. et al. The deubiquitinating enzyme USP2a regulates the p53 pathway by targeting Mdm2. *Embo J* **26**, 976-86 (2007).
121. Yuan, J., Luo, K., Zhang, L., Chevillet, J.C. & Lou, Z. USP10 regulates p53 localization and stability by deubiquitinating p53. *Cell* **140**, 384-96 (2010).
122. Cummins, J.M. et al. Tumour suppression: disruption of HAUSP gene stabilizes p53. *Nature* **428**, 1 p following 486 (2004).
123. Song, M.S. et al. The deubiquitinylation and localization of PTEN are regulated by a HAUSP-PML network. *Nature* **455**, 813-7 (2008).
124. Rhodes, D.R. et al. OncoPrint 3.0: genes, pathways, and networks in a collection of 18,000 cancer gene expression profiles. *Neoplasia* **9**, 166-80 (2007).
125. Graner, E. et al. The isopeptidase USP2a regulates the stability of fatty acid synthase in prostate cancer. *Cancer Cell* **5**, 253-61 (2004).
126. Baron, A., Migita, T., Tang, D. & Loda, M. Fatty acid synthase: a metabolic oncogene in prostate cancer? *J Cell Biochem* **91**, 47-53 (2004).
127. Deng, S. et al. Over-expression of genes and proteins of ubiquitin specific peptidases (USPs) and proteasome subunits (PSS) in breast cancer tissue observed by the methods of RFDD-PCR and proteomics. *Breast Cancer Res Treat* **104**, 21-30 (2007).
128. Grunda, J.M. et al. Increased expression of thymidylate synthetase (TS), ubiquitin specific protease 10 (USP10)

- and survivin is associated with poor survival in glioblastoma multiforme (GBM). *J Neurooncol* **80**, 261-74 (2006).
129. Sagar, S. et al. CYLD mutations in familial skin appendage tumours. *J Med Genet* **45**, 298-302 (2008).
130. Bignell, G.R. et al. Identification of the familial cylindromatosis tumour-suppressor gene. *Nat Genet* **25**, 160-5 (2000).
131. Trompouki, E. et al. CYLD is a deubiquitinating enzyme that negatively regulates NF-kappaB activation by TNFR family members. *Nature* **424**, 793-6 (2003).
132. Kovalenko, A. et al. The tumour suppressor CYLD negatively regulates NF-kappaB signalling by deubiquitination. *Nature* **424**, 801-5 (2003).
133. Brummelkamp, T.R., Nijman, S.M., Dirac, A.M. & Bernards, R. Loss of the cylindromatosis tumour suppressor inhibits apoptosis by activating NF-kappaB. *Nature* **424**, 797-801 (2003).
134. Komander, D. et al. The structure of the CYLD USP domain explains its specificity for Lys63-linked polyubiquitin and reveals a B box module. *Mol Cell* **29**, 451-64 (2008).
135. Murray, R.Z., Jolly, L.A. & Wood, S.A. The FAM deubiquitylating enzyme localizes to multiple points of protein trafficking in epithelia, where it associates with E-cadherin and beta-catenin. *Mol Biol Cell* **15**, 1591-9 (2004).
136. Taya, S., Yamamoto, T., Kanai-Azuma, M., Wood, S.A. & Kaibuchi, K. The deubiquitinating enzyme Fam interacts with and stabilizes beta-catenin. *Genes Cells* **4**, 757-67 (1999).
137. Gumbiner, B.M. Carcinogenesis: a balance between beta-catenin and APC. *Curr Biol* **7**, R443-6 (1997).
138. Dupont, S. et al. FAM/USP9x, a deubiquitinating enzyme essential for TGFbeta signaling, controls Smad4 monoubiquitination. *Cell* **136**, 123-35 (2009).
139. Schwickart, M. et al. Deubiquitinase USP9X stabilizes MCL1 and promotes tumour cell survival. *Nature* **463**, 103-7 (2010).
140. Oliveira, A.M. et al. USP6 (Tre2) fusion oncogenes in aneurysmal bone cyst. *Cancer Res* **64**, 1920-3 (2004).
141. Nijman, S.M. et al. The deubiquitinating enzyme USP1 regulates the Fanconi anemia pathway. *Mol Cell* **17**, 331-9 (2005).
142. Huang, T.T. et al. Regulation of monoubiquitinated PCNA by DUB autocleavage. *Nat Cell Biol* **8**, 339-47 (2006).
143. Brown, S., Niimi, A. & Lehmann, A.R. Ubiquitination and deubiquitination of PCNA in response to stalling of the replication fork. *Cell Cycle* **8**, 689-92 (2009).
144. Popov, N., Herold, S., Llamazares, M., Schulein, C. & Eilers, M. Fbw7 and Usp28 regulate myc protein stability in response to DNA damage. *Cell Cycle* **6**, 2327-31 (2007).
145. Popov, N. et al. The ubiquitin-specific protease USP28 is required for MYC stability. *Nat Cell Biol* **9**, 765-74 (2007).
146. Quesada, V. et al. Cloning and enzymatic analysis of 22 novel human ubiquitin-specific proteases. *Biochem Biophys Res Commun* **314**, 54-62 (2004).
147. Avvakumov, G.V. et al. Amino-terminal dimerization, NRDPI-rhodanese interaction, and inhibited catalytic domain conformation of the ubiquitin-specific protease 8 (USP8). *J Biol Chem* **281**, 38061-70 (2006).
148. Hu, M. et al. Crystal structure of a UBP-family deubiquitinating enzyme in isolation and in complex with ubiquitin aldehyde. *Cell* **111**, 1041-54 (2002).
149. Hu, M. et al. Structure and mechanisms of the proteasome-associated deubiquitinating enzyme USP14. *Embo J* **24**, 3747-56 (2005).
150. Renatus, M. et al. Structural basis of ubiquitin recognition by the deubiquitinating protease USP2. *Structure* **14**, 1293-302 (2006).
151. Krishna, S.S. & Grishin, N.V. The finger domain of the human deubiquitinating enzyme HAUSP is a zinc ribbon. *Cell Cycle* **3**, 1046-9 (2004).
152. de Jong, R.N. et al. Solution structure of the human ubiquitin-specific protease 15 DUSP domain. *J Biol Chem* **281**, 5026-31 (2006).
153. Zapata, J.M. et al. A diverse family of proteins containing tumor necrosis fac-

- tor receptor-associated factor domains. *J Biol Chem* **276**, 24242-52 (2001).
154. Kiel, C. & Serrano, L. The ubiquitin domain superfold: structure-based sequence alignments and characterization of binding epitopes. *J Mol Biol* **355**, 821-44 (2006).
155. May, M.J., Larsen, S.E., Shim, J.H., Madge, L.A. & Ghosh, S. A novel ubiquitin-like domain in I κ B kinase beta is required for functional activity of the kinase. *J Biol Chem* **279**, 45528-39 (2004).
156. Grabbe, C. & Dikic, I. Functional roles of ubiquitin-like domain (ULD) and ubiquitin-binding domain (UBD) containing proteins. *Chem Rev* **109**, 1481-94 (2009).
157. Gupta, K., Chevrette, M. & Gray, D.A. The Unpp proto-oncogene encodes a nuclear protein. *Oncogene* **9**, 1729-31 (1994).
158. Gupta, K., Copeland, N.G., Gilbert, D.J., Jenkins, N.A. & Gray, D.A. Unp, a mouse gene related to the tre oncogene. *Oncogene* **8**, 2307-10 (1993).
159. Gray, D.A. et al. Elevated expression of Unph, a proto-oncogene at 3p21.3, in human lung tumors. *Oncogene* **10**, 2179-83 (1995).
160. Soboleva, T.A., Jans, D.A., Johnson-Saliba, M. & Baker, R.T. Nuclear-cytoplasmic shuttling of the oncogenic mouse UNP/USP4 deubiquitylating enzyme. *J Biol Chem* **280**, 745-52 (2005).
161. Zhao, B., Schlesiger, C., Masucci, M.G. & Lindsten, K. The ubiquitin specific protease 4 (USP4) is a new player in the Wnt signalling pathway. *J Cell Mol Med* **13**, 1886-95 (2009).
162. Song, E.J. et al. The Prp19 complex and the Usp4Sart3 deubiquitinating enzyme control reversible ubiquitination at the spliceosome. *Genes Dev* **24**, 1434-47 (2010).
163. Fan, Y.H. et al. USP4 targets TAK1 to downregulate TNF α -induced NF- κ B activation. *Cell Death Differ* (2010).
164. Zhang, X., Berger, F.G., Yang, J. & Lu, X. USP4 inhibits p53 through deubiquitinating and stabilizing ARF-BP1. *Embo J* **30**, 2177-89 (2011).
165. Edwards, A. Large-scale structural biology of the human proteome. *Annu Rev Biochem* **78**, 541-68 (2009).
166. Sugahara, M. et al. High-throughput crystallization-to-structure pipeline at RIKEN SPring-8 Center. *J Struct Funct Genomics* **9**, 21-8 (2008).
167. Xiao, R. et al. The high-throughput protein sample production platform of the Northeast Structural Genomics Consortium. *J Struct Biol* **172**, 21-33 (2010).
168. Dessailly, B.H. et al. PSI-2: structural genomics to cover protein domain family space. *Structure* **17**, 869-81 (2009).
169. Ioerger, T.R. & Sacchettini, J.C. Structural genomics approach to drug discovery for Mycobacterium tuberculosis. *Curr Opin Microbiol* **12**, 318-25 (2009).
170. Albeck, S. et al. SPINE bioinformatics and data-management aspects of high-throughput structural biology. *Acta Crystallogr D Biol Crystallogr* **62**, 1184-95 (2006).
171. Elsliger, M.A. et al. The JCSG highthroughput structural biology pipeline. *Acta Crystallogr Sect F Struct Biol Cryst Commun* **66**, 1137-42.

A Genomic and Functional Inventory of Deubiquitinating Enzymes

Sebastian M.B. Nijman^{1,*}, Mark P.A. Luna-Vargas¹, Arno Velds¹, Thijn R.
Brummelkamp², Annette M.G. Dirac¹,
Titia K. Sixma¹, and René Bernards^{1*}

Cell 2005;123(5):773-86 Review

¹Division of Molecular Carcinogenesis and Center for Biomedical Genetics,
The Netherlands Cancer Institute, Plesmanlaan 121, 1066 CX Amsterdam, The Netherlands

²Whitehead Institute for Biomedical Research, Nine Cambridge Center, Cambridge, MA 02142, USA

*Contact: s.nijman@nki.nl (S.M.B.N.), r.bernards@nki.nl (R.B.)

2



Abstract

Posttranslational modification of proteins by the small molecule ubiquitin is a key regulatory event, and the enzymes catalyzing these modifications have been the focus of many studies. Deubiquitinating enzymes, which mediate the removal and processing of ubiquitin, may be functionally as important but are less well understood. Here, we present an inventory of the deubiquitinating enzymes encoded in the human genome. In addition, we review the literature concerning these enzymes, with particular emphasis on their function, specificity, and the regulation of their activity.

Introduction

Over the last few decades, protein modification by ubiquitin (Ub) and ubiquitin-like (Ubl) molecules has emerged as a critical regulatory process in virtually all aspects of cell biology. Indeed, the 2004 Nobel Prize in Physiology or Medicine was awarded for the discovery of Ub-mediated proteolysis.

More than a dozen different Ub and Ubl modifications have been described, and up to 20% of yeast proteins are conjugated to Ub under standard culture conditions^{1,2}. In yeast, potentially all seven conserved lysines of Ub itself (K6, 11, 27, 29, 33, 48, and 63) are used as branching sites for the generation of Ub polymers.

The topic of ubiquitination, the proteins involved, and their functions in various pathways and signaling networks has been well reviewed^{3,4}. Here, we discuss the enzymes that remove Ub from polypeptides. These deubiquitinating enzymes (DUBs) play key regulatory roles in a multitude of processes from hereditary cancer to neurodegeneration. Despite the importance of DUBs, our knowledge of their mode of regulation and substrate specificity is surprisingly scant. A detailed annotation of individual family members of this enzyme group is an important step toward elucidating the molecular functions of DUBs in health and disease. To this end, we provide a comprehensive overview of putative DUBs encoded in the human genome. In addition, we discuss the lacunae in our understanding of these enzymes by drawing on examples from yeast and higher eukaryotes.

In our attempt to classify these enzymes, we have made some arbitrary decisions as to which genes to include or exclude as potential DUBs. Therefore, we present three caveats to this list. First, we cannot exclude the fact that proteins or protein families not included in this overview can remove Ub from polypeptides. For instance, a recent *in silico* effort to predict new Ub signaling components suggested a

previously undetected family of Ub peptidases⁵. Second, protein domain prediction based on gene transcripts depends on consensus sequences. Thus, divergent but true family members can be missed due to low homology scores. Finally, we wish to emphasize that it is unlikely that all predicted DUBs are truly specific for Ub: some will display additional activity or exclusive activity toward Ubl molecules.

DUBs Are Proteases

DUBs belong to the superfamily of proteases, of which an estimated 561 members are present in the human genome⁶. Based on the mechanism of catalysis, proteases are divided into five classes—aspatic, metallo, serine, threonine, and cysteine proteases—and further subdivided based on phylogeny.

Two classes of proteases (cysteine and metallo) contain DUBs, although most DUBs are cysteine proteases. By definition, the enzymatic activity of cysteine proteases relies on the thiol group of a cysteine in the active site. Deprotonation of this cysteine is assisted by an adjacent histidine, which is polarized by an aspartate residue. These three residues make up the catalytic triad. During catalysis, the cysteine performs a nucleophilic attack on the carbonyl of the scissile peptide bond, which, in the case of DUBs, is between the target and Ub. The intermediate, which contains an oxyanion, is stabilized in the so-called oxyanion hole. This oxyanion hole is generally provided by a glutamine, glutamate, or asparagine residue and the main chain of the catalytic cysteine. The result of the reaction is release of the target protein and formation of a covalent intermediate with the Ub moiety. Reaction of this intermediate with a water molecule results in the release of the free enzyme and Ub.

In contrast to cysteine proteases, metalloproteases generally use a Zn²⁺ bound po-

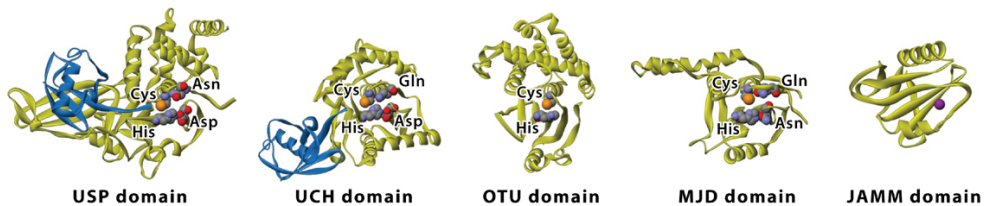


Figure 1. Structures of the Catalytic Domains of the Five Subclasses of Ub-Specific Proteases (Yellow) with Ub (Blue) Structures show the remarkable variability in secondary structure between the DUB classes. Catalytic centers are shown as Van der Waals spheres (carbon, gray; nitrogen, blue; oxygen, red; sulfur, orange; zinc, purple) and have been aligned for easy comparison. The OTU domain of OTU2 lacks the conserved Asp in the catalytic center and the Asn/Glu/Gln that is normally used to stabilize the oxyanion hole in these proteases. For detailed structural information see Amerik and Hochstrasser (2004). Protein Databank (PDB) codes: USP7, 1nbf; UCH-L3, 1xd3; OTU2, 1tff; Ataxin-3, 1yzb; JAMM, 1r5x.

2

larized water molecule to generate a noncovalent intermediate with the substrate. The metal atom is primarily stabilized by an aspartate and two histidine residues⁷. The intermediate is further broken down by proton transfer from a water molecule causing the release of the DUB.

The Human DUB Genes

The cysteine protease DUBs can be further organized into four subclasses based on their Ub-protease domains: ubiquitin-specific protease (USP), ubiquitin C-terminal hydrolase (UCH), Otubain protease (OTU), and Machado-Joseph disease protease (MJD). All DUBs that are metalloproteases have a Ub protease domain called JAMM (JAB1/MPN/Mov34 metalloenzyme). The structures of the catalytic domains of the different subclasses of DUBs reveal an impressive diversity in secondary structure (Figure 1).

We used the ENSEMBL human genome database (v32, July 2005) to retrieve all putative DUBs from the human genome by selecting genes whose transcripts encode one of the five Ub protease domains. Our search identified all known DUBs except two DUBs with OTU domains (*Otubain-1* and *Otubain-2*). This analysis indicated that the human genome encodes approximately 95 putative DUBs, including many that have not been previously reported. These can be broken down into 58 USP, 4 UCH, 5 MJD, 14 OTU, and 14 JAMM domain-containing genes, many of which are associated with multiple transcripts (see Table S1 in the Supplemental Data available with this article online). For six unnamed genes, we have

submitted gene names to the HUGO gene nomenclature committee (HGNC) (Table S1). To determine whether the putative DUB genes are expressed, we searched NCBI human-expressed sequence tag (EST) databases for transcripts corresponding to the predicted protein sequence. We obtained further evidence for expression of a number of genes with relatively low numbers of ESTs from additional sources (such as SAGE and UniGene). For five predicted DUBs, we could not find any convincing data supporting transcription.

Next, we generated sequence alignments to ensure conservation of the catalytic residues and made an inventory of DUBs reported to display Ub protease activity. This indicated that of the 90 putative DUBs that are expressed, 11 are unlikely to display Ub-protease activity. Together, these data indicate that humans express approximately 79 putative DUBs that are functional (Table S1).

To investigate sequence homology between the various putative DUBs, we used two strategies. We used CLANS (Cluster analysis of sequences) software to visualize pairwise all-against-all sequence BLAST matches⁸. As expected, very few positive BLAST results were found between the five subclasses, whereas the members within the subclasses clustered together (Figure 2A). This analysis revealed that within the subclasses some relatively divergent members are present (for example, *Otubain-1* and *Otubain-2*, USP55, and CYLD). Similar results were obtained using the CLUSTAL alignment algorithm (Figure 2B).

The Five DUB Subclasses

Three-dimensional structures of DUB catalytic domains from all subclasses, some of them in complex with Ub derivatives, have been solved (Figure 1). These studies reveal intriguing similarities and differences between the four cysteine protease subclasses. This topic, including the structure of a JAMM domain, has recently been extensively reviewed by Amerik and Hochstrasser⁹. Here, we comment on the new structural features of the DUB subclasses.

Ubiquitin C-Terminal Hydrolases (UCHs)
 The human UCH subclass of DUBs consists of four proteins that share close homology in their catalytic domains. Structural and biochemical studies have indicated that the UCH subclass of DUBs prefers to cleave relatively small protein substrates (up to 20– 30 amino acids) from Ub⁹. This size limit is thought to be imposed by a loop that partially occludes the active site of these enzymes. However, recent biochemical and structural studies show that certain large substrates can nevertheless be accommodated¹⁰.

Although UCHs were the first described DUBs, their specific functions remain poorly understood. UCHs are thought to mainly act in the recycling of Ub when Ub is inappropriately conjugated to intracellular nucleophiles (for example, glutathione, polyamines). They also may be involved in the processing of newly synthesized Ub, which is translated either as a polyubiquitin precursor or fused to ribosomal protein precursors. However, other DUBs also display *in vitro* activity toward linear Ub fusions, suggesting that processing of newly synthesized Ub is performed by multiple DUBs.

Some studies suggest a role for UCHs in specific Ub-regulated processes. Mutations in UCH-L1 (a UCH

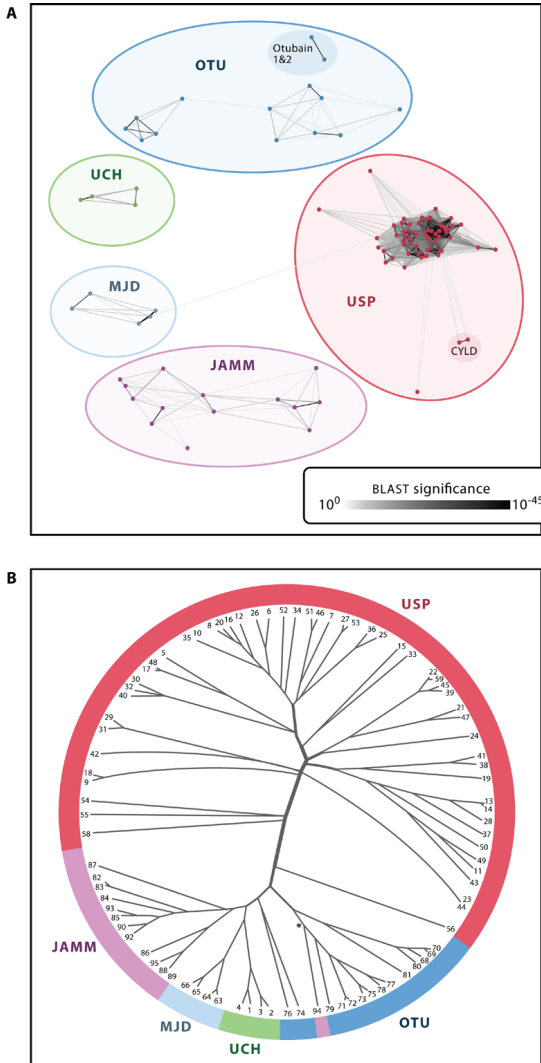


Figure 2. Phylogenetic Map of Human DUBs (A) Graphic two-dimensional representation of sequence similarities between all Ub protease domains of DUBs using CLANS software. CLANS performs all-against-all BLAST searches and uses the significant high-scoring segment pairs (HSPs) to draw a three-dimensional graph represented here in two dimensions. Each node represents a Ub protease domain and each edge (line) represents a significant HSP (edges are shaded according to p value). DUB subclasses are highlighted in the graph. The start and end positions of the DUB Ub-protease domains, as defined by Interpro, were used to generate the protein sequences. Proteins with a partial or short and misaligning DUB domain were excluded from the analysis. **(B)** Unrooted dendrogram of the DUBs using Clustal software. Clustal generates a multiple sequence alignment file based on pairwise alignments. From this information a phylogenetic tree can be constructed. The robustness of the phylogenetic relations can be assessed by “bootstrapping,” a mathematical technique that introduces noise in the alignment and measures how often the phylogenetic relationships reproduce. An asterisk indicates a bootstrapping percentage <10% (lowest branch only). The numbers correspond to the genes in Table S1.

specifically expressed in neurons) that reduce its DUB activity have been described in two siblings with Parkinson's disease (PD), and a polymorphism in this gene has been linked to reduced PD risk^{11,12}. However, not all studies have found a strict relationship between UCH-L1 activity and PD. Furthermore, although mice that have a mutation in *Uch-L1* exhibit neurodegeneration, they do not display PD-like symptoms¹³.

Ubiquitin-Specific Proteases (USPs)

The USP subclass represents the bulk of the DUBs encoded by the human genome. As the number of Ub E3 ligases (the third factor in the ubiquitination cascade that determines target specificity) increased during evolution, so did the number of USPs, suggesting an intimate relationship between the two resulting in their co-evolution¹⁴.

The catalytic domain of USPs contains two short and well-conserved motifs, called Cys and His boxes, which include the residues critical for catalysis. However, the size of the complete domain varies from approximately 300 to 800 amino acids due to the large unrelated sequences that are interspersed between the two motifs, which may serve a regulatory function (Figure 3).

Upon closer examination of the catalytic domains of USPs, we noted that a subset (USP16, USP30, USP39, USP45, and USP52) lack catalytic residues previously thought to be critical for protease activity (Figure S1). USP30 and USP16 lack only the aspartate in the catalytic triad but retain enzymatic activity against a model substrate (Table S1 and M.P.A.L.-V. and T.K.S., unpublished data). This indicates that, as is the case for the Otubain-2 protein, USP30 and USP16 may use a different residue to stabilize the active site histidine. Additional structural information about USPs may shed light on this issue.

USP39 (also known as SAD1) does not contain the conserved catalytic cysteine or histidine and does not cleave a model substrate *in vitro*, indicating that USP39 is not a bona fide DUB (M.P.A.L.-V. and T.K.S., unpublished data). However, USP39 plays a critical role in spliceosome maturation in both yeast and human cells, and many of the other residues within the catalytic domain are conserved^{15,16}. Therefore, it is tempting to speculate that USP39 can still inter-

act with Ub. An analogous situation exists in Ub conjugation. Here, a Ub interaction motif known as UEV (ubiquitin-conjugating enzyme variant) strongly resembles the catalytic domain of E2s (the second enzyme in the ubiquitination cascade) but lacks activity¹⁷. In keeping with this nomenclature, these catalytically inactive USP domains are hereby referred to as USPV (ubiquitin-specific protease variant). The functions of these variants with respect to Ub await further investigation.

Machado-Joseph Disease Protein Domain Proteases (MJDPs)

A bioinformatics search for other classes of Ub proteases identified Ataxin-3 and a number of Ataxin-3-like proteins¹⁸. Experiments *in vitro* confirmed that wild-type Ataxin-3, but not a mutant with the active site cysteine mutated, could deubiquitinate a model substrate¹⁹. Sequence similarity between the catalytic domain of Ataxin-3 and other DUBs is low (Figure 2A), but recent NMR structures show that the overall arrangement of the catalytic triad is conserved (Figure 1)^{20,21}.

Instability of a CAG nucleotide repeat in the *Ataxin-3* gene leads to a hereditary neurological condition known as spinocerebellar ataxia type-3 or Machado-Joseph disease (OMIM 607047). Like other polyglutamine neurodegenerative disease-associated genes, expansion of the CAG repeat in *Ataxin-3* leads to protein misfolding, resulting in aggregation and cellular toxicity. Some experimental evidence indicates that the normal function of Ataxin-3 involves transcriptional regulation, but whether its DUB activity plays a role in this process remains unclear²². In evolutionary terms, MJDPs likely represent a relatively late addition to the Ub system, as no homologs have been identified in yeast. However, protease activity of the other family members has not yet been demonstrated, and their biological functions remain unknown.

Ovarian Tumor Proteases (OTUs)

A bioinformatics approach also led to the identification of the Ovarian Tumor (OTU) subclass of Ub proteases²³. The *otu* gene is involved in the development of the *Drosophila melanogaster* ovary where it may regulate the localization and translation of certain RNA transcripts^{24,25}. Using the *Drosophila otu* gene and its homologs as a starting point, Markarova and colleagues found sequence similarity between these genes and those encoding viral cysteine

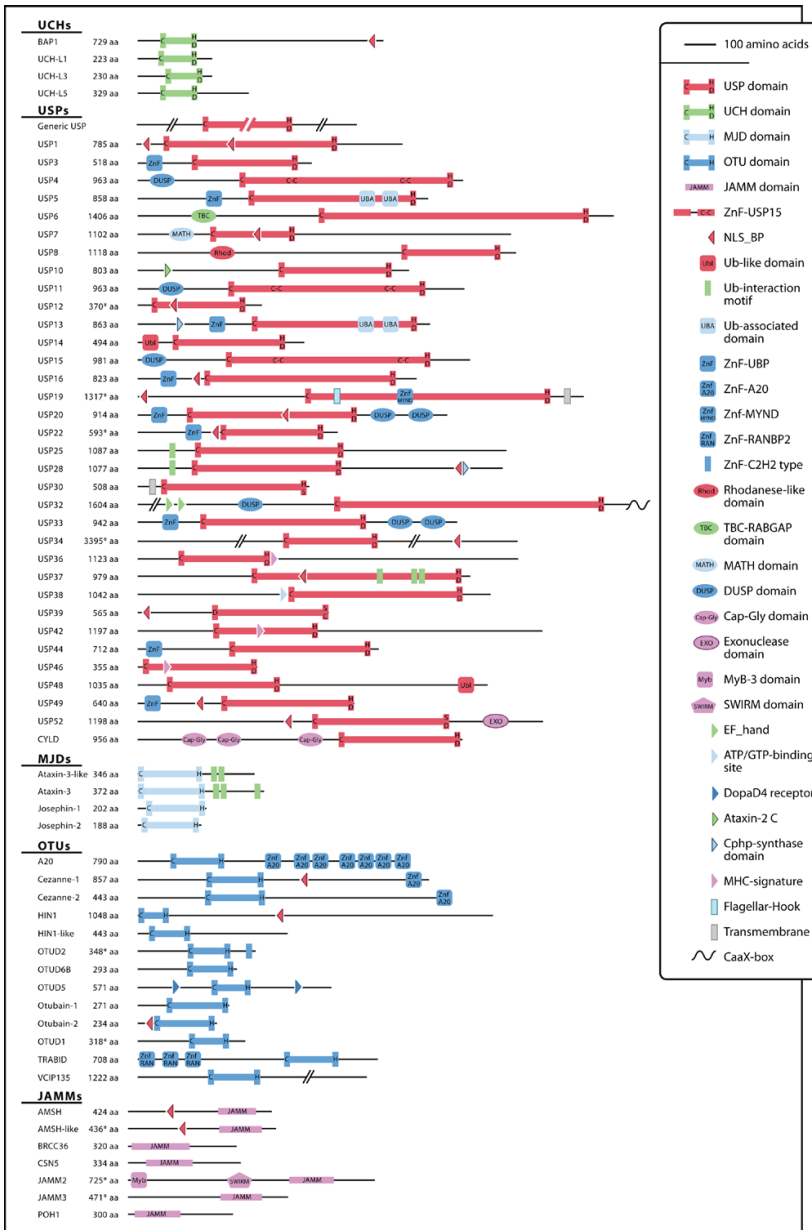


Figure 3. Comparison of the Domain Structures of Putative DUBs For each primary DUB transcript (the transcript associated with the HUGO or RefSeq ID), we retrieved information concerning domain architecture and signal motifs using ENSEMBL, SMART (simple modular architecture research tool; <http://smart.embl-heidelberg.de/>), Pfam (protein families database; <http://www.sanger.ac.uk/Software/Pfam/>), and PROSITE databases. The USPs without additional domains are indicated as “generic USP.” Only JAMM and MJD domain proteins with predicted catalytic activity are shown. An asterisk indicates that the ENSEMBL-predicted translational start site is uncertain. Proteins and domains are plotted on an approximate scale. Select abbreviations: ZnF, zinc finger; NLS_BP, bipartite nuclear localization signal; MATH, meprin and TRAF homology; DUSP, domain in ubiquitin-specific proteases. For additional information concerning the indicated domains visit <http://www.ebi.ac.uk/interpro/>.

proteases²³. A recently solved OTU structure shows that, unlike other cysteine protease DUBs, the catalytic triad is incomplete and is stabilized by a new method involving a hydrogen bonding network²⁶.

Otubain-1 and Otubain-2 were the first two OTU proteins found to display *in vitro* DUB activity²⁷. Shortly thereafter, Cezanne, another OTU-domain containing protein, was found to interact with poly-Ub in a yeast two-hybrid assay and to contain DUB activity *in vitro*, suggesting that this is a general OTU feature²⁸. However, for most OTU proteases, their physiological role *in vivo*, including their putative role as DUBs, remains to be investigated.

JAMM Motif Proteases

The JAMM domain is found in all three major kingdoms of life (bacteria, archaea, and eukarya). However, bacteria do not contain Ub protease activity, and an analogous Ub-like conjugation system has not yet been identified in prokaryotes. This suggests that JAMM domains have adopted new protease functions during evolution and indicates that at least some of the human JAMM proteases may be involved in more than Ub (or Ubl) processing. Indeed, recent work has identified the protein product of the *Mycobacterium tuberculosis* gene *mec+* as a JAMM domain peptidase involved in cysteine biosynthesis by cleaving cysteine from a peptide intermediate²⁹.

Sequence alignment of the JAMM-domain proteins revealed that seven of the 14 members have at least one amino acid change in the conserved Zn²⁺ ion-stabilizing residues, indicating that they may not be functional proteases. Three family members (POH1, CSN5, and AMSH) will be briefly discussed in the section concerning DUB function.

DUB Specificity

Accumulating evidence indicates that most DUBs regulate a limited number of proteins and pathways, suggesting that they target specific substrates (Table 1). In the case of DUBs, specificity can refer to either the Ub or Ubl moiety itself (substrate specificity) or the target protein to which the moiety is conjugated (target specificity). In reality, it may not be possible to separate these types of specificities. It is likely that in many cases a combinatorial mechanism relying on recognition

of both the target and the attached moiety determines overall DUB specificity. Additional mechanisms, such as protein localization and interactions with binding partners, may further contribute to *in vivo* specificity. In the following sections, we will discuss current insights into DUB specificity.

Substrate Specificity: Ubiquitin Polymers

Protein ubiquitination comes in many different flavors that serve distinct functions². Whereas poly-Ub chains linked through the lysine residues of Ub at position 48 (K48) target proteins for proteasomal degradation, the attachment of a single Ub moiety (monoubiquitination) appears to regulate subcellular localization and recruitment of Ub binding proteins. Besides mono- and K48-linked polyubiquitination, other poly-Ub branches using alternative lysines on Ub have been described. The relevance and function of most of these different types of described for a number of mammalian proteins, including RIP, NEMO and TRAFs³⁰. These signaling molecules are involved in activation of NF- κ B signaling, a pathway involved in inflammation, apoptosis, and tumorigenesis. As in the case of mono-Ub, K63 polyubiquitination is required for the activation of downstream molecules, like kinases, or recruitment of other proteins. K63-linked Ub molecules differ remarkably from K48 chains in their three-dimensional structure, which probably accounts for their distinct functions³¹. Furthermore, this suggests that certain DUBs may act on specific Ub branches. Indeed, the yeast DUB Ubp2 prefers K63 over K48-linked Ub chains as a substrate³². Conversely, examples of DUBs cleaving K48 but not K63-linked Ub polymers include USP8 and USP14^{33,34}. Another DUB, UCH-L5 can cleave various types of branches but does not display activity toward linear Ub dimers. Other examples further support the notion that DUBs cleave poly-Ub variants with varying efficiency, at least *in vivo*. One such example is the protein product of the Cyldromatosis tumor-suppressor gene (CYLD), a DUB involved in inhibiting NF- κ B signaling³⁵⁻³⁷. CYLD cleaves linear Ub fusions *in vitro*; yet *in vivo* it appears to be specific for non-K48-linked Ub chains. The basis for the specificity observed *in vivo* remains unclear, but phylogenetic analysis indicates that the catalytic domain of CYLD is relatively divergent from other DUBs, as indicated by its unique protease family identifier, C67 (Table S1 and Figure 2). This information leads us

Table 1. Mammalian DUBs and Their Reported Functions

Name	Substrate(s)	Process	Remarks	References
UCHs				
UCH-L1	Unknown	Parkinson's disease	Homodimer has E3 activity; mutant mice display ataxia	Leroy et al. (1998); Liu et al. (2002); Saigoh et al. (1999)
BAP1	Unknown	Unknown	Binds to BRCA1	Jensen et al. (1998)
UCH-L5	Unknown	Ubiquitin editing, TGF- β signaling?	Binds to proteasome	Lam et al. (1997); Wicks et al. (2005)
USPs				
CYLD	TRAF2/6, NEMO	NF- κ B and JNK signaling	Familial tumor suppressor (cylindromatosis)	Brummelkamp et al. (2003); Kovalenko et al. (2003); Trompouki et al. (2003); Reiley et al. (2004)
USP1	FANCD2	DNA repair		Nijman et al. (2005)
USP2	Fatty acid synthase	Androgen signaling	Circadian-regulated	Graner et al. (2004); Oishi et al. (2003)
USP4	Unknown	Unknown	Transforming activity	Gupta et al. (1994)
USP5	Unknown	Unknown	Binds K29 chains, binds ISG15 and Ub	Hemelaar et al. (2004); Russell and Wilkinson (2004)
USP6	Unknown	Putative oncogene, actin remodeling	Transforming activity; found in cancer	Masuda-Robens et al. (2003); Oliveira et al. (2005); Paulding et al. (2003)
USP7	HDM2, p53, H2B	p53 signaling, Polycomb silencing	Binds herpes virus protein Vmw110	Cummins et al. (2004); Everett et al. (1997); Li et al. (2004); van der Knaap et al. (2005)
USP8	NRDP1	Endocytosis	Oncogenic fusion with p85-PI3K	Janssen et al. (1998); Kato et al. (2000); Wu et al. (2004)
USP9X	β -catenin, epsins, AF-6	Wnt-, Notch signaling, endocytosis		Murray et al. (2004); Overstreet et al. (2004)
USP9Y	Unknown	Spermatogenesis	Mutants associated with azoospermia	Sun et al. (1999)
USP11	BRCA2	DNA repair?	Interacts with RanBPM	Ideguchi et al. (2002); Schoenfeld et al. (2004)
USP14	Unknown	Synapse function	Mutant mice develop ataxia; binds to proteasome	Borodovsky et al. (2001); Wilson et al. (2002)
USP15	RBX1	COP9 signalosome		Herfeld et al. (2005)
USP16	H2A?	Chromosome condensation?		Mimnaugh et al. (2001)
USP18	Unknown	JAK-STAT signaling, immunity, brain function	ISG15-specific; mRNA is induced by IFN- α and IFN- γ	Malakhova et al. (2003); Ritchie et al. (2004); Ritchie et al. (2002)
USP20	DIO2?	Thyroid hormone metabolism, hypoxia signaling	Interacts with pVHL	Curcio-Morelli et al. (2003); Li et al. (2002b)
USP21	Unknown	Unknown	Cleaves Ub and NEDD8 but not SUMO	Gong et al. (2000)
USP26	Unknown	Spermatogenesis	mUsp26 is testis specific	Paduch et al. (2005); Stouffs et al. (2005); Wang et al. (2001)
USP33	HIF1- α DIO2?	Hypoxia signaling	Interacts with pVHL	Curcio-Morelli et al. (2003); Li et al. (2002b); Li et al. (2005)
MJDs				
Ataxin-3	Unknown	MJD disease	Sequence has CAG repeats	Burnett et al. (2003); Scheel et al. (2003)
OTUs				
A20	RIP	NF- κ B signaling	Also E3 ligase	Wertz et al. (2004)
VCIP135	Unknown	Golgi disassembly		Wertz et al. (2004)
JAMMs				
POH1	Unknown	Proteasome		Verma et al. (2002); Yao and Cohen (2002)
AMSH	EGFR?	Endocytosis		McCullough et al. (2004)
CSN5	Cullins	CSN function	Mainly NEDD8 as substrate	Cope et al. (2002); Groisman et al. (2003)
BRCC36	Unknown	G2/M checkpoint signaling	Enhances BRCA1/ BARD1 E3 ligase activity	Dong et al. (2003)

Listed are DUBs that have been linked to specific pathways, processes, and substrates (based on published studies).

to speculate that the architecture of the enzymatic cleft contributes to its specificity. The OTU-type DUB A20 is another potent inhibitor of NF- κ B signaling³⁸. *In vitro*, A20 can cleave both K48- and K63-linked Ub polymers with similar efficiency. Yet *in vivo*, A20 deubiquitinates K63 but not K48 polyubiquitinated RIP (the protein we mentioned previously that is involved in NF- κ B activation). However, given that A20 also contains (K48) E3 ligase activity toward RIP, it is not clear if the apparent K63 DUB activity *in vivo* is due to true substrate preference or simply due to its ability to catalyze the addition of K48-linked Ub polymers.

In at least some cases, domains outside the catalytic domain may contribute to Ub chain specificity³⁹. Splice variants of USP2 and a mutant containing only the core catalytic domain of this DUB cleave both linear Ub fusions and K48-linked Ub polymers. However, their relative efficiency var-

ies considerably. The core domain prefers linear fusions, but full-length USP2b was most efficient in cleaving K48-linked Ub. Although USP2 does not contain an additional, known Ub-interaction motif, it is conceivable that sequences outside the catalytic domain contribute to selection and positioning of specific Ub chains. In fact, Ub-interaction motifs found in some E2 ligases have been implicated in determining linkage specificity. Indeed, it was recently described that a previously unnoticed Ub-interacting Zinc finger domain in USP15 is needed for disassembling branched Ub polymers but not for cleavage of a linear Ub-GFP fusion⁴⁰. Another recent study showed that addition of a UBA domain that recognizes K48-Ub chains to USP5 skewed its substrate preference toward this type of Ub polymer⁴¹. Similarly, other Ub binding domains frequently encountered in DUBs, like UIM and ZnF-UBP (also called PAZ) may also

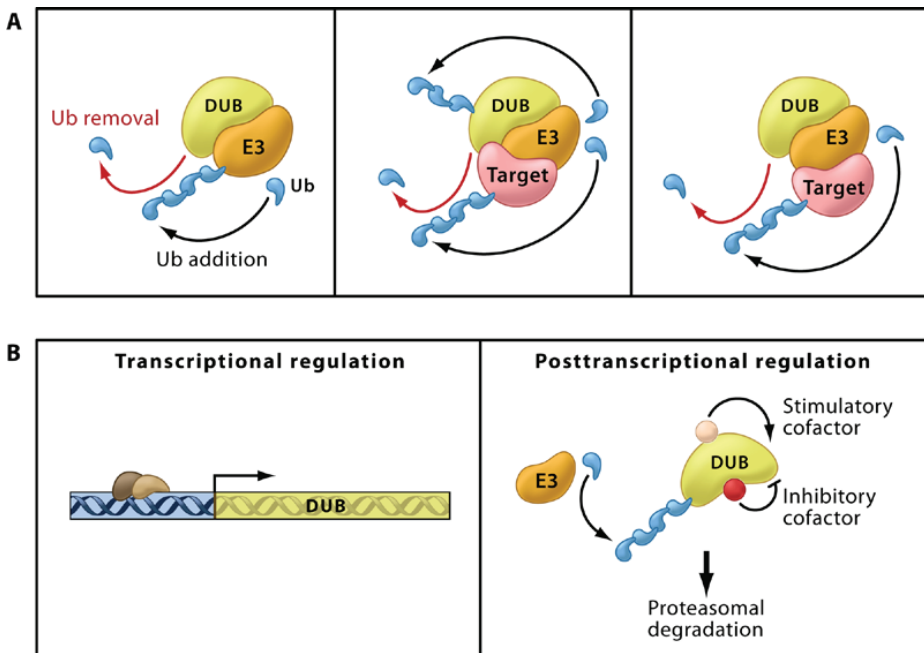


Figure 4. DUB Specificity and Regulation (A) DUB/E3 interactions. DUBs and E3 are often found in a complex together. These interactions, which occur between USP7 and HDM2, for example, serve to reverse E3-mediated autoubiquitination (left panel) or allow the E3 to regulate the target and its DUB simultaneously as in the case of USP20 and pVHL (middle panel). Alternatively, DUB/E3 interactions confer specificity to the DUB, as in the case of Ubp2 and Rsp5 (right panel). E3 Ub-ligase and Ub-protease activity is indicated with black arrows and red arrows, respectively. Ub conjugated to E2 is not shown for clarity. (B) DUB activity is regulated at various levels, including transcription (left panel), degradation, and binding to stimulatory or inhibitory cofactors (right panel). The exact mechanism whereby these cofactors regulate DUB activity is unknown but may occur at multiple levels (for example, phosphorylation, subcellular localization), stimulating conformational changes or conferring specificity.

contribute to Ub chain selection (Figure 3).

Substrate Specificity: Ubiquitin and Ubiquitin-like Molecules

The vast majority of putative DUBs tested so far display Ub protease activity *in vitro* (Table S1). Nonetheless, some predicted DUBs may be active toward Ubl moieties. Therefore, when considering DUB specificity, we wish to extend our discussion to both Ub and Ubl moieties. USP21 and UCH-L3 cleave both Ub and the Ubl molecule NEDD8. USP18 has been proposed to specifically cleave another Ubl, ISG15⁴²⁻⁴⁴. Furthermore, although some circumstantial evidence indicates that CSN5 may contain Ub protease activity, its main proteolytic target is thought to be the Ubl NEDD8⁴⁵⁻⁴⁷. For other Ubl molecules, distinct proteases have been identified. For instance, newly synthesized Ubl Atg8 is processed by a distinct protease (Apg4) of which five family members are found in the genome⁴⁸. Likewise, protease activity toward SUMO (small ubiquitin-like modifier) has thus far been restricted to the SENP family of cysteine proteases, of which seven genes are present in the human genome. However, within this family proteolytic activity is not limited to SUMO; SENP8 (also known as DEN1) is a NEDD8-specific protease^{49,50}.

Our current knowledge of the motifs or residues in these proteases that are responsible for distinguishing Ub from Ubl moieties is limited. Clearly, more *in vitro* and *in vivo* analysis of DUBs and Ubl proteases, including structural information, is required.

Target Specificity and DUB/E3 Interactions

The recognition of targets by DUBs may be directed by sequences and motifs outside the conserved catalytic core. For instance, one of the Cap-Gly domains of CYLD mediates its interaction with NEMO, a potential CYLD substrate (Figure 3)⁵¹. However, like most enzyme/substrate interactions, DUB/target interactions are expected to be weak and transient in nature, making the identification of *in vivo* targets frustrating. A more stable complex between a DUB and its target may occur in the case when proteins are inappropriately K48 polyubiquitinated (Figure 4A, left panel). These proteins need to be continuously deubiquitinated to protect them from unwanted degradation. Autoubiquitination by ring fingertype E3 ligases is a frequently observed phenomenon resulting from nonspecific ubiquitination of proximal lysines (careless gunplay). For

instance, the E3 ligase NRD1 stimulates its own turnover as well as a number of cellular targets. The DUB USP8 associates with NRD1 resulting in its deubiquitination and stabilization, suggesting that interaction with a DUB may simply serve to antagonize this self-inflicted degradation⁵². Similarly, the interaction of USP7 with HDM2 and USP15 with Rbx1 results in the stabilization of these E3 ligases^{40,53-55}. Interestingly, USP7 was also found to stabilize the herpes virus E3 ligase ICP0, indicating that viruses can hijack cellular DUBs to stabilize viral proteins. The importance for controlling Ub dynamics in the herpes virus life cycle is further underscored by the recent finding that the *herpesviridae* contains a distinct class of cysteine protease DUBs without known mammalian homologs⁵⁶.

Not all DUB/E3 interactions strictly serve to regulate E3 ligase stability. The E3 tumor suppressor protein pVHL regulates the stability of HIF1 transcription factors that are important regulators of angiogenesis. USP33 interacts with this E3⁵⁷ and appears to regulate HIF1 stability by deubiquitination⁵⁸. This suggests that, in this case, interaction of the DUB with the E3 allows the E3 ligase to differentially regulate the primary proteasomal target (HIF1) as well as its deconjugating enzyme (Figure 4A, middle panel).

Kee and colleagues recently suggested a third type of DUB/E3 interaction³². They postulated that in some cases the DUB may hitch along with the E3 ligase. They showed that the target specificity of the yeast DUB Ubp2 is strictly dependent on the E3 ligase Rsp5, which is responsible for recognition of the substrate (Figure 4A, right panel). A remarkable variation on this theme is the previously mentioned protein A20. Here, E3 ligase and DUB activity reside in the same polypeptide³⁸.

DUB Function

Gene deletion studies in yeast have indicated that none of the USPs are required for cell growth or viability⁹. Nonetheless, USPs and other DUBs in lower and higher eukaryotes including mammals have been implicated in regulating various critical cellular processes in a nonredundant manner. Human DUBs (or their murine homologs) of particular interest that have been linked to defined cellular processes or substrates are listed in Table 1.

The functions of DUBs at the proteasome lid, in endocytosis and regulation of

chromatin structure, are reasonably well understood and are therefore discussed in some detail in the following sections. In addition, we will propose some directions for future studies.

DUBs and Proteasome Function

Proteins that must undergo fast and dramatic changes in abundance are often regulated by proteolysis. These proteins are targeted to the proteasome by K48-linked polyubiquitination, where they are degraded. The 26S proteasome consists of two 19S regulatory particles and a 20S cylinder-shaped multiprotein complex possessing the proteolytic activity⁵⁹. The 19S subunit restricts access to the interior of the 13 Å cylinder of the proteasome, which is where the catalytic residues for proteolysis are located. Deubiquitination of proteins arriving at the proteasome allows recycling of Ub and is required for protein degradation. In fact, deubiquitination, protein unfolding, translocation into the proteasome and degradation are intimately linked processes. A number of DUBs from various subclasses have been found in complex with the 19S proteasome regulatory component, including the JAMM protease POH1 (Rpn11 in yeast), UCH-L5, and USP14 (Ubp6 in yeast)^{46,60-62}. Interestingly, residents of a paralogous multiprotein structure known as the COP9 signalosome are the JAMM protein CSN5 and USP15^{63,64}. Like the proteasome, the COP9 signalosome has been implicated in a diverse array of biological processes. At least some of these functions can be explained by its ability to inhibit the activity of the cullin family of ubiquitin E3 ligases by CSN5-mediated deneddylation.

The main DUB activity at the proteasome appears to be generated by POH1, since deletion of the gene that encodes this enzyme results in defective proteasomal degradation and is lethal in yeast. The functions of the other DUBs may be partially redundant with POH1, only playing a role in the deubiquitination of specific substrates, or in “Ub editing.” The Ub-editing concept was postulated as a mechanism to rescue proteins that have been mistakenly ubiquitinated (as recognized by having short Ub chains) from destruction. The suggested Ub-editing mechanism would remove Ub polymers, starting at the distal end, independently of the substrate moiety⁶¹. Although UCH-L5 indeed cleaves Ub chains from the distal end, compelling evidence for an Ub-editing function for UCH-L5 has not

yet been provided, and no ortholog of UCH-L5 has been found in *Saccharomyces cerevisiae*.

DUBs and Chromatin Structure

An increasing body of evidence implicates dynamic histone ubiquitination in the regulation of transcription and silencing, and even double-strand-break formation during meiosis⁶⁵. Although most histone proteins can be ubiquitinated, the dynamics of H2B monoubiquitination are best understood. In yeast, deubiquitination of H2B by the DUB Ubp10 is required for telomeric silencing. This in turn allows recruitment of the silencing factor Sir2⁶⁶. Interestingly, a second USP Ubp8 has been implicated in regulating H2B. In contrast to Ubp10, deubiquitination of H2B by Ubp8 correlates with transcriptional activation^{67,68}. At least at some sites of active transcription, Ub-H2B levels are high during activation and subsequently decrease in an Ubp8-dependent manner. Importantly, both the ubiquitination and deubiquitination of H2B are necessary for optimal transcription, indicating a requirement for dynamic H2B modification by Ub⁶⁸.

Similar to yeast Ubp10, *Drosophila* USP7 interacts preferentially with silenced genomic regions, including telomeric domains, where it has been suggested to deubiquitinate H2B and thereby contribute to Polycomb-mediated silencing⁶⁹. In mammals, USP7 associates with HDM2, an E3 ligase critical for regulating p53 turnover, and thereby inhibits degradation of both HDM2 and p53^{54,55}. Indeed, different levels of USP7 can have opposite outcomes with respect to p53 stability. Intermediate inhibition of USP7 result in increased p53 degradation, whereas complete inhibition of USP7 enhances p53 stability. Interestingly, a recent report has suggested that HDM2 can mediate H2B ubiquitination⁷⁰. Together, these data suggest an attractive model in which HDM2/p53/USP7 complexes mediate transcriptional repression by regulating H2B ubiquitination.

DUBs and Endocytosis

Monoubiquitination and, at least in yeast, the attachment of a K63-linked Ub dimer, play an important role in endocytosis of receptors and sorting of proteins^{71,72}. After binding to ligands, receptor tyrosine kinases (RTKs) and adaptor proteins are monoubiquitinated at multiple sites, which triggers their internalization. The RTKs are subse-

quently either recycled or transported to lysosomes for destruction. The E3 ligase for many RTKs is the proto-oncogene Cbl, which can also induce proteasome-dependent degradation by stimulating K48 polyubiquitination⁷³. Repeated addition of Ub or reduced deubiquitination may be the trigger for targeting to the lysosomal compartment, though exactly how ubiquitination determines this decision is unclear. Ub-interacting proteins like Hrs subsequently bind to the monoubiquitinated receptor and recruit protein complexes involved in budding of the endocytic vesicle.

DUBs are implicated in the endocytic pathway at multiple levels and also play important roles in other types of intracellular traffic. In yeast, the DUB Doa4 acts to recycle Ub at the late endosome to rescue Ub from destruction. Inactivation of Doa4 interferes with many Ub-related processes since it results in depletion of free Ub and many of the defects observed on Doa4 mutant cells are restored upon expression of additional Ub⁷⁴. The closest human relative of Doa4 is USP8, which binds the Hrs binding partner (Hbp) and inhibits EGF receptor (EGFR) endocytosis, suggesting that USP8 may act to regulate endocytic traffic^{75,76}. Remarkably, a second Hrs interacting protein is AMSH, a JAMM domain DUB³⁴. Inhibition of AMSH results in the accumulation of endosomal Ub and promotes EGFR endocytosis thereby accelerating EGFR downregulation.

Yet more DUBs are implicated in controlling endocytosis. In *Drosophila*, Fat facets (Faf; the homolog of human USP9X), deubiquitinates Liquid facets (Lqf), resulting in enhanced Lqf activity⁷⁷. Lqf and Faf play a role in *Drosophila* eye development by enhancing the internalization of a receptor implicated in cell patterning, called Delta. In humans, Lqf homologs are known as epsins, adaptor molecules involved in the initial steps of endocytosis.

Ubiquitination and deubiquitination appears to be a common theme in vesicle dynamics; monoubiquitination plays a critical role in budding of some viruses. Additionally, VCIP135, a OTU, has been implicated in Golgi assembly after mitosis⁷⁸.

Other Potential Roles for DUBs

Indications for the function of DUBs may come from various sources, including genetic screens in model organisms, interactome data, and domain-

and signaling-motif predictions. Genetic screens in model organisms like the worm *Caenorhabditis elegans* and the fruit fly *Drosophila* are pointing at new roles for DUBs in various pathways. For instance, screens in *C. elegans* for modulators of RNA interference or longevity suggest an involvement of a USP and a UCH^{79,80}. In addition, a protein with both a USP and OTU domain (Duo-2) has recently been implicated in synapse function⁸¹. These studies further solidify the broad involvement of the Ub conjugation/deconjugation system in biological processes and will certainly spark research into the functions of the human DUB orthologs.

Data derived from large-scale human protein-protein interaction experiments has implicated a number of USPs in several signaling cascades such as the TGF- β and NF- κ B pathways. For instance, USP45 binds specifically to the phosphorylated TGF- β receptor in a mammalian two-hybrid⁸². Similarly, USP11 and USP9 interact with the NF- κ B transcription factors RelB and p100, respectively⁸³. Although the significance of these interactions remains to be determined, these findings suggest that DUBs may play a regulatory role in these pathways.

Hints to the function of DUBs may be obtained from additional domains and signal motifs present in the primary amino acid sequence of these enzymes (Figure 3). For instance, USP7 might be involved in specific signaling pathways as it contains a MATH (meprin and TRAF homology) domain. These domains are found in members of the TRAF family of ring finger E3 ligases which mediates signaling via TNF receptors. Similarly, the JAMM2 protein might play a role in transcription and chromatin remodeling, as it contains domains (SWIRM and Myb DNA binding motif) implicated in these processes.

Regulation of DUBs

In contrast to many proteases, such as caspases that are translated as inactive precursors, DUBs are generally produced as active enzymes. Structural analysis has pointed out that the catalytic triad of UCHs and USPs only assume the active confirmation when bound to Ub, thereby preventing spurious protease activity against other substrates. In addition, various studies show that a diverse array of mechanisms regulates DUB activity and additional ones are likely to be discovered.

In the case of at least two JAMM domain proteins (POH1 and CSN5), it appears that incorporation into higher-order protein structures (the 19S proteasome and COP9 signalosome, respectively) is required for peptidase activity^{46,63}. Similarly, accessibility of the enzymatic cleft of USP14 appears to be regulated by activity of the 26S proteasome, its resident complex⁶⁰.

Bre5, a cofactor for the yeast DUB Ubp3, is largely responsible for its *in vivo* activity toward Sec23, a protein involved in anterograde transport between the endoplasmic reticulum and the Golgi compartment⁸⁴. Bre5 does not bind directly to Sec23, suggesting that the interaction between Bre5 and Ubp3 regulates Ubp3 activity. Surprisingly, the human homolog of Bre5, G3BP1, inhibits the activity of USP10, at least *in vitro*, indicating that cofactors can either restrict or enhance protease activity (Figure 4B, right panel)⁸⁵. A USP7 cofactor called GMP5 that strongly augments USP7 activity was recently identified in *Drosophila*⁶⁹. In addition, USP7 is regulated during apoptosis by cleavage by caspases. This cleavage presumably inactivates USP7⁸⁶.

DUBs have frequently been found to be degraded by the proteasome, indicating that their abundance is an important regulatory mechanism (Figure 4B, right panel). Moreover, some DUBs have been reported to be transcriptionally regulated (Figure 4B, left panel), sometimes in a cell-cycle-regulated manner (for example, USP1) or as part of a negative feedback loop (such as CYLD)^{87,88}.

In another case, inhibitory phosphorylation of CYLD after TNF- α stimulation is required for the accumulation of one of its proposed substrates, K63-ubiquitinated TRAF2. Interestingly, this event does not appear to modulate the affinity of CYLD for TRAF2, suggesting that phosphorylation may directly regulate CYLD activity by an unknown mechanism⁸⁹.

Concluding Remarks

A large number of studies over the last decade have uncovered an unanticipated diversity of protein regulation by Ub and Ubl molecules. Nature has utilized the versatility of Ub in almost any conceivable way. Strikingly, the ubiquitin conjugation/deconjugation system outcompetes the protein phosphorylation system in terms of diversity and complexity.

Although the reversal of ubiquitination by DUBs has been firmly established as a critical regulatory mechanism, we are only beginning to uncover the different mechanisms that control the activity of these enzymes.

Remarkably, the Ub E3 ligases greatly outnumber the DUBs encoded in the human genome. This is in contrast to tyrosine kinases and phosphatases, which are roughly equal in number. One possible explanation is that we have not yet identified all DUBs or their associated cofactors that may determine specificity. Indeed, Serine/Threonine kinases outnumber Serine/Threonine phosphatases, but a large variety of cofactors provide additional specificity to these phosphatases. It is also possible that many DUBs have poor substrate specificity and regulate on average up to 10 times more substrates than the average E3 ligase. However, most DUBs studied thus far appear to regulate a small number of targets. Another more likely explanation for the excess of E3 ligases could be that only a fraction of the targets that are ubiquitinated are regulated by specific deubiquitination. For destruction mediated by K48 Ub polymers, we would predict that many proteins are not deubiquitinated prior to arrival at the proteasome. Unless of course when you have made a mistake, why recycle a protein that you have decided to throw away? Possibly, only proteins that require extremely tight regulation, such as p53, require additional regulation by deubiquitination. Indeed, other types of Ub-based modifications, like K63-linked polymers or monoubiquitin require DUBs to “reset” the protein to its unmodified state and are thus more likely to be critically regulated by DUBs. Undoubtedly, future studies aided by detailed genomic annotation, structural information, and other new tools and methods to characterize this intriguing protein family will result in the demystification of these proteases.

Supplemental Data

Supplemental Data include one figure and one table and can be found with this article online at <http://www.cell.com/cgi/content/full/123/5/773/DC11>.

Acknowledgments

We would like to thank Dr. Tony Huang, Dr. Huib Ovaa, and Dr. Helen Pickers-

gill for critical reading and helpful discussions. This work was supported by grants from The Netherlands Organization for Scientific Research (NWO) to T.K.S. and R.B.

References

1. Peng, J., Schwartz, D., Elias, J.E., Thoreen, C.C., Cheng, D., Marsischky, G., Roelofs, J., Finley, D. & Gygi, S.P. A proteomics approach to understanding protein ubiquitination. *Nat Biotechnol* **21**, 921-6 (2003).
2. Welchman, R.L., Gordon, C. & Mayer, R.J. Ubiquitin and ubiquitin-like proteins as multifunctional signals. *Nat Rev Mol Cell Biol* **6**, 599-609 (2005).
3. Hershko, A. & Ciechanover, A. The ubiquitin system. *Annu Rev Biochem* **67**, 425-79 (1998).
4. Pickart, C.M. & Eddins, M.J. Ubiquitin: structures, functions, mechanisms. *Biochim Biophys Acta* **1695**, 55-72 (2004).
5. Iyer, L.M., Koonin, E.V. & Aravind, L. Novel predicted peptidases with a potential role in the ubiquitin signaling pathway. *Cell Cycle* **3**, 1440-50 (2004).
6. Puente, X.S. & Lopez-Otin, C. A genomic analysis of rat proteases and protease inhibitors. *Genome Res* **14**, 609-22 (2004).
7. Ambroggio, X.I., Rees, D.C. & Deshaies, R.J. JAMM: a metalloprotease-like zinc site in the proteasome and signalosome. *PLoS Biol* **2**, E2 (2004).
8. Frickey, T. & Lupas, A. CLANS: a Java application for visualizing protein families based on pairwise similarity. *Bioinformatics* **20**, 3702-4 (2004).
9. Amerik, A.Y. & Hochstrasser, M. Mechanism and function of deubiquitinating enzymes. *Biochim Biophys Acta* **1695**, 189-207 (2004).
10. Misaghi, S., Galardy, P.J., Meester, W.J., Ovaa, H., Ploegh, H.L. & Gaudet, R. Structure of the ubiquitin hydrolase UCH-L3 complexed with a suicide substrate. *J Biol Chem* **280**, 1512-20 (2005).
11. Leroy, E., Boyer, R., Auburger, G., Leube, B., Ulm, G., Mezey, E., Harta, G., Brownstein, M.J., Jonnalagada, S., Chernova, T., Dehejia, A., Lavedan, C., Gasser, T., Steinbach, P.J., Wilkinson, K.D. & Polymeropoulos, M.H. The ubiquitin pathway in Parkinson's disease. *Nature* **395**, 451-2 (1998).
12. Liu, Y., Fallon, L., Lashuel, H.A., Liu, Z. & Lansbury, P.T., Jr. The UCH-L1 gene encodes two opposing enzymatic activities that affect alpha-synuclein degradation and Parkinson's disease susceptibility. *Cell* **111**, 209-18 (2002).
13. Saigoh, K., Wang, Y.L., Suh, J.G., Yamanishi, T., Sakai, Y., Kiyosawa, H., Harada, T., Ichihara, N., Wakana, S., Kikuchi, T. & Wada, K. Intragenic deletion in the gene encoding ubiquitin carboxy-terminal hydrolase in gad mice. *Nat Genet* **23**, 47-51 (1999).
14. Semple, C.A. The comparative proteomics of ubiquitination in mouse. *Genome Res* **13**, 1389-94 (2003).
15. Lygerou, Z., Christophides, G. & Seraphin, B. A novel genetic screen for snRNP assembly factors in yeast identifies a conserved protein, Sad1p, also required for pre-mRNA splicing. *Mol Cell Biol* **19**, 2008-20 (1999).
16. Makarova, O.V., Makarov, E.M. & Luhrmann, R. The 65 and 110 kDa SR-related proteins of the U4/U6.U5 tri-snRNP are essential for the assembly of mature spliceosomes. *Embo J* **20**, 2553-63 (2001).
17. Hicke, L., Schubert, H.L. & Hill, C.P. Ubiquitin-binding domains. *Nat Rev Mol Cell Biol* **6**, 610-21 (2005).
18. Scheel, H., Tomiuk, S. & Hofmann, K. Elucidation of ataxin-3 and ataxin-7 function by integrative bioinformatics. *Hum Mol Genet* **12**, 2845-52 (2003).
19. Burnett, B., Li, F. & Pittman, R.N. The polyglutamine neurodegenerative protein ataxin-3 binds polyubiquitylated proteins and has ubiquitin protease activity. *Hum Mol Genet* **12**, 3195-205 (2003).
20. Mao, Y., Senic-Matuglia, F., Di Fiore, P.P., Polo, S., Hodsdon, M.E. & De Camilli, P. Deubiquitinating function of ataxin-3: insights from the solution structure of the Josephin domain. *Proc Natl Acad Sci U S A* **102**, 12700-5 (2005).
21. Nicasastro, G., Menon, R.P., Masino, L., Knowles, P.P., McDonald, N.Q. & Pastore, A. The solution structure of the Josephin domain of ataxin-3: structural determinants for molecular recognition. *Proc Natl Acad*

22. Li, F., Macfarlan, T., Pittman, R.N. & Chakravarti, D. Ataxin-3 is a histone-binding protein with two independent transcriptional corepressor activities. *J Biol Chem* **277**, 45004-12 (2002).
23. Makarova, K.S., Aravind, L. & Koonin, E.V. A novel superfamily of predicted cysteine proteases from eukaryotes, viruses and Chlamydia pneumoniae. *Trends Biochem Sci* **25**, 50-2 (2000).
24. Goodrich, J.S., Clouse, K.N. & Schupbach, T. Hrb27C, Sqd and Otu cooperatively regulate gurken RNA localization and mediate nurse cell chromosome dispersion in Drosophila oogenesis. *Development* **131**, 1949-58 (2004).
25. Steinhauer, W.R., Walsh, R.C. & Kalfayan, L.J. Sequence and structure of the Drosophila melanogaster ovarian tumor gene and generation of an antibody specific for the ovarian tumor protein. *Mol Cell Biol* **9**, 5726-32 (1989).
26. Nanao, M.H., Tcherniuk, S.O., Chroboczek, J., Dideberg, O., Dessen, A. & Balakirev, M.Y. Crystal structure of human otubain 2. *EMBO Rep* **5**, 783-8 (2004).
27. Balakirev, M.Y., Tcherniuk, S.O., Jaquinod, M. & Chroboczek, J. Otubains: a new family of cysteine proteases in the ubiquitin pathway. *EMBO Rep* **4**, 517-22 (2003).
28. Evans, P.C., Smith, T.S., Lai, M.J., Williams, M.G., Burke, D.F., Heynink, K., Kreike, M.M., Beyaert, R., Blundell, T.L. & Kilshaw, P.J. A novel type of deubiquitinating enzyme. *J Biol Chem* **278**, 23180-6 (2003).
29. Burns, K.E., Baumgart, S., Dorrestein, P.C., Zhai, H., McLafferty, F.W. & Begley, T.P. Reconstitution of a new cysteine biosynthetic pathway in Mycobacterium tuberculosis. *J Am Chem Soc* **127**, 11602-3 (2005).
30. Sun, C., Skaletsky, H., Birren, B., Devon, K., Tang, Z., Silber, S., Oates, R. & Page, D.C. An azoospermic man with a de novo point mutation in the Y-chromosomal gene USP9Y. *Nat Genet* **23**, 429-32 (1999).
31. Varadan, R., Assfalg, M., Haririnia, A., Raasi, S., Pickart, C. & Fushman, D. Solution conformation of Lys63-linked di-ubiquitin chain provides clues to functional diversity of polyubiquitin signaling. *J Biol Chem* **279**, 7055-63 (2004).
32. Kee, Y., Lyon, N. & Huibregtse, J.M. The Rsp5 ubiquitin ligase is coupled to and antagonized by the Ubp2 deubiquitinating enzyme. *Embo J* **24**, 2414-24 (2005).
33. Hu, M., Li, P., Song, L., Jeffrey, P.D., Chenova, T.A., Wilkinson, K.D., Cohen, R.E. & Shi, Y. Structure and mechanisms of the proteasome-associated deubiquitinating enzyme USP14. *Embo J* **24**, 3747-56 (2005).
34. McCullough, J., Clague, M.J. & Urbe, S. AMSH is an endosome-associated ubiquitin isopeptidase. *J Cell Biol* **166**, 487-92 (2004).
35. Brummelkamp, T.R., Nijman, S.M., Dirac, A.M. & Bernards, R. Loss of the cylindromatosis tumour suppressor inhibits apoptosis by activating NF-kappaB. *Nature* **424**, 797-801 (2003).
36. Kovalenko, A., Chable-Bessia, C., Cantarella, G., Israel, A., Wallach, D. & Courtois, G. The tumour suppressor CYLD negatively regulates NF-kappaB signalling by deubiquitination. *Nature* **424**, 801-5 (2003).
37. Trompouki, E., Hatzivassiliou, E., Tsi-chritzis, T., Farmer, H., Ashworth, A. & Mosialos, G. CYLD is a deubiquitinating enzyme that negatively regulates NF-kappaB activation by TNFR family members. *Nature* **424**, 793-6 (2003).
38. Wertz, I.E., O'Rourke, K.M., Zhou, H., Eby, M., Aravind, L., Seshagiri, S., Wu, P., Wiesmann, C., Baker, R., Boone, D.L., Ma, A., Koonin, E.V. & Dixit, V.M. Deubiquitination and ubiquitin ligase domains of A20 downregulate NF-kappaB signalling. *Nature* **430**, 694-9 (2004).
39. Lin, H., Yin, L., Reid, J., Wilkinson, K.D. & Wing, S.S. Divergent N-terminal sequences of a deubiquitinating enzyme modulate substrate specificity. *J Biol Chem* **276**, 20357-63 (2001).
40. Hetfeld, B.K., Helfrich, A., Kapelari, B., Scheel, H., Hofmann, K., Guterman, A., Glickman, M., Schade, R., Kloetzel, P.M.

- & Dubiel, W. The zinc finger of the CSN-associated deubiquitinating enzyme USP15 is essential to rescue the E3 ligase Rbx1. *Curr Biol* **15**, 1217-21 (2005).
41. Raasi, S., Varadan, R., Fushman, D. & Pickart, C.M. Diverse polyubiquitin interaction properties of ubiquitin-associated domains. *Nat Struct Mol Biol* **12**, 708-14 (2005).
42. Gong, L., Kamitani, T., Millas, S. & Yeh, E.T. Identification of a novel isopeptidase with dual specificity for ubiquitin- and NEDD8-conjugated proteins. *J Biol Chem* **275**, 14212-6 (2000).
43. Malakhov, M.P., Malakhova, O.A., Kim, K.I., Ritchie, K.J. & Zhang, D.E. UBP43 (USP18) specifically removes ISG15 from conjugated proteins. *J Biol Chem* **277**, 9976-81 (2002).
44. Wada, H., Kito, K., Caskey, L.S., Yeh, E.T. & Kamitani, T. Cleavage of the C-terminus of NEDD8 by UCH-L3. *Biochem Biophys Res Commun* **251**, 688-92 (1998).
45. Groisman, R., Polanowska, J., Kuraoka, I., Sawada, J., Saijo, M., Drapkin, R., Kisilev, A.F., Tanaka, K. & Nakatani, Y. The ubiquitin ligase activity in the DDB2 and CSA complexes is differentially regulated by the COP9 signalosome in response to DNA damage. *Cell* **113**, 357-67 (2003).
46. Verma, R., Aravind, L., Oania, R., McDonald, W.H., Yates, J.R., 3rd, Koonin, E.V. & Deshaies, R.J. Role of Rpn11 metalloprotease in deubiquitination and degradation by the 26S proteasome. *Science* **298**, 611-5 (2002).
47. Yao, T. & Cohen, R.E. A cryptic protease couples deubiquitination and degradation by the proteasome. *Nature* **419**, 403-7 (2002).
48. Kirisako, T., Ichimura, Y., Okada, H., Kabeya, Y., Mizushima, N., Yoshimori, T., Ohsumi, M., Takao, T., Noda, T. & Ohsumi, Y. The reversible modification regulates the membrane-binding state of Apg8/Aut7 essential for autophagy and the cytoplasm to vacuole targeting pathway. *J Cell Biol* **151**, 263-76 (2000).
49. Gan-Erdene, T., Nagamalleswari, K., Yin, L., Wu, K., Pan, Z.Q. & Wilkinson, K.D. Identification and characterization of DEN1, a deneddylase of the ULP family. *J Biol Chem* **278**, 28892-900 (2003).
50. Wu, K., Yamoah, K., Dolios, G., Gan-Erdene, T., Tan, P., Chen, A., Lee, C.G., Wei, N., Wilkinson, K.D., Wang, R. & Pan, Z.Q. DEN1 is a dual function protease capable of processing the C terminus of Nedd8 and deconjugating hyper-neddylated CUL1. *J Biol Chem* **278**, 28882-91 (2003).
51. Saito, K., Kigawa, T., Koshihara, S., Sato, K., Matsuo, Y., Sakamoto, A., Takagi, T., Shirouzu, M., Yabuki, T., Nunokawa, E., Seki, E., Matsuda, T., Aoki, M., Miyata, Y., Hirakawa, N., Inoue, M., Terada, T., Nagase, T., Kikuno, R., Nakayama, M., Ohara, O., Tanaka, A. & Yokoyama, S. The CAP-Gly domain of CYLD associates with the proline-rich sequence in NEMO/IKK-gamma. *Structure* **12**, 1719-28 (2004).
52. Wu, X., Yen, L., Irwin, L., Sweeney, C. & Carraway, K.L., 3rd. Stabilization of the E3 ubiquitin ligase Nrdp1 by the deubiquitinating enzyme USP8. *Mol Cell Biol* **24**, 7748-57 (2004).
53. Canning, M., Boutell, C., Parkinson, J. & Everett, R.D. A RING finger ubiquitin ligase is protected from autocatalyzed ubiquitination and degradation by binding to ubiquitin-specific protease USP7. *J Biol Chem* **279**, 38160-8 (2004).
54. Cummins, J.M., Rago, C., Kohli, M., Kinzler, K.W., Lengauer, C. & Vogelstein, B. Tumour suppression: disruption of HAUSP gene stabilizes p53. *Nature* **428**, 1 p following 486 (2004).
55. Li, M., Brooks, C.L., Kon, N. & Gu, W. A dynamic role of HAUSP in the p53-Mdm2 pathway. *Mol Cell* **13**, 879-86 (2004).
56. Kattenhorn, L.M., Korbil, G.A., Kessler, B.M., Spooner, E. & Ploegh, H.L. A deubiquitinating enzyme encoded by HSV-1 belongs to a family of cysteine proteases that is conserved across the family Herpesviridae. *Mol Cell* **19**, 547-57 (2005).
57. Li, Z., Wang, D., Na, X., Schoen, S.R., Messing, E.M. & Wu, G. Identification of a deubiquitinating enzyme subfamily as substrates of the von Hippel-

- Lindau tumor suppressor. *Biochem Biophys Res Commun* **294**, 700-9 (2002).
58. Li, Z., Wang, D., Messing, E.M. & Wu, G. VHL protein-interacting deubiquitinating enzyme 2 deubiquitinates and stabilizes HIF-1 α . *EMBO Rep* **6**, 373-8 (2005).
59. Pickart, C.M. & Cohen, R.E. Proteasomes and their kin: proteases in the machine age. *Nat Rev Mol Cell Biol* **5**, 177-87 (2004).
60. Borodovsky, A., Kessler, B.M., Casagrande, R., Overkleeft, H.S., Wilkinson, K.D. & Ploegh, H.L. A novel active site-directed probe specific for deubiquitylating enzymes reveals proteasome association of USP14. *Embo J* **20**, 5187-96 (2001).
61. Lam, Y.A., Xu, W., DeMartino, G.N. & Cohen, R.E. Editing of ubiquitin conjugates by an isopeptidase in the 26S proteasome. *Nature* **385**, 737-40 (1997).
62. Park, K.C., Woo, S.K., Yoo, Y.J., Wyndham, A.M., Baker, R.T. & Chung, C.H. Purification and characterization of UBP6, a new ubiquitin-specific protease in *Saccharomyces cerevisiae*. *Arch Biochem Biophys* **347**, 78-84 (1997).
63. Cope, G.A., Suh, G.S., Aravind, L., Schwarz, S.E., Zipursky, S.L., Koonin, E.V. & Deshaies, R.J. Role of predicted metalloprotease motif of Jab1/Csn5 in cleavage of Nedd8 from Cul1. *Science* **298**, 608-11 (2002).
64. Zhou, C., Wee, S., Rhee, E., Naumann, M., Dubiel, W. & Wolf, D.A. Fission yeast COP9/signalosome suppresses cullin activity through recruitment of the deubiquitylating enzyme Ubp12p. *Mol Cell* **11**, 927-38 (2003).
65. Yamashita, K., Shinohara, M. & Shinohara, A. Rad6-Bre1-mediated histone H2B ubiquitylation modulates the formation of double-strand breaks during meiosis. *Proc Natl Acad Sci U S A* **101**, 11380-5 (2004).
66. Emre, N.C., Ingvarsdottir, K., Wyce, A., Wood, A., Krogan, N.J., Henry, K.W., Li, K., Marmorstein, R., Greenblatt, J.F., Shilatifard, A. & Berger, S.L. Maintenance of low histone ubiquitylation by Ubp10 correlates with telomere-proximal Sir2 association and gene silencing. *Mol Cell* **17**, 585-94 (2005).
67. Gardner, R.G., Nelson, Z.W. & Gottschling, D.E. Ubp10/Dot4p regulates the persistence of ubiquitinated histone H2B: distinct roles in telomeric silencing and general chromatin. *Mol Cell Biol* **25**, 6123-39 (2005).
68. Henry, K.W., Wyce, A., Lo, W.S., Duggan, L.J., Emre, N.C., Kao, C.F., Pilus, L., Shilatifard, A., Osley, M.A. & Berger, S.L. Transcriptional activation via sequential histone H2B ubiquitylation and deubiquitylation, mediated by SAGA-associated Ubp8. *Genes Dev* **17**, 2648-63 (2003).
69. van der Knaap, J.A., Kumar, B.R., Moshkin, Y.M., Langenberg, K., Krijgsveld, J., Heck, A.J., Karch, F. & Verrijzer, C.P. GMP synthetase stimulates histone H2B deubiquitylation by the epigenetic silencer USP7. *Mol Cell* **17**, 695-707 (2005).
70. Minsky, N. & Oren, M. The RING domain of Mdm2 mediates histone ubiquitylation and transcriptional repression. *Mol Cell* **16**, 631-9 (2004).
71. Haglund, K., Di Fiore, P.P. & Dikic, I. Distinct monoubiquitin signals in receptor endocytosis. *Trends Biochem Sci* **28**, 598-603 (2003).
72. Hicke, L. & Dunn, R. Regulation of membrane protein transport by ubiquitin and ubiquitin-binding proteins. *Annu Rev Cell Dev Biol* **19**, 141-72 (2003).
73. Duan, L., Reddi, A.L., Ghosh, A., Dimri, M. & Band, H. The Cbl family and other ubiquitin ligases: destructive forces in control of antigen receptor signaling. *Immunity* **21**, 7-17 (2004).
74. Swaminathan, S., Amerik, A.Y. & Hochstrasser, M. The Doa4 deubiquitinating enzyme is required for ubiquitin homeostasis in yeast. *Mol Biol Cell* **10**, 2583-94 (1999).
75. Kato, M., Miyazawa, K. & Kitamura, N. A deubiquitinating enzyme UBPY interacts with the Src homology 3 domain of Hrs-binding protein via a novel binding motif PX(V/I)(D/N)RXXKP. *J Biol Chem* **275**, 37481-7 (2000).

76. Mizuno, E., Iura, T., Mukai, A., Yoshimori, T., Kitamura, N. & Komada, M. Regulation of epidermal growth factor receptor down-regulation by UBPY-mediated deubiquitination at endosomes. *Mol Biol Cell* **16**, 5163-74 (2005).
77. Overstreet, E., Fitch, E. & Fischer, J.A. Fat facets and Liquid facets promote Delta endocytosis and Delta signaling in the signaling cells. *Development* **131**, 5355-66 (2004).
78. Wang, Y., Satoh, A., Warren, G. & Meyer, H.H. VCI135 acts as a deubiquitinating enzyme during p97-p47-mediated reassembly of mitotic Golgi fragments. *J Cell Biol* **164**, 973-8 (2004). 79. Hamilton, B., Dong, Y., Shindo, M., Liu, W., Odell, I., Ruvkun, G. & Lee, S.S. A systematic RNAi screen for longevity genes in *C. elegans*. *Genes Dev* **19**, 1544-55 (2005).
80. Kim, J.K., Gabel, H.W., Kamath, R.S., Tewari, M., Pasquinelli, A., Rual, J.F., Kennedy, S., Dybbs, M., Bertin, N., Kaplan, J.M., Vidal, M. & Ruvkun, G. Functional genomic analysis of RNA interference in *C. elegans*. *Science* **308**, 1164-7 (2005).
81. Sieburth, D., Ch'ng, Q., Dybbs, M., Tavazoie, M., Kennedy, S., Wang, D., Dupuy, D., Rual, J.F., Hill, D.E., Vidal, M., Ruvkun, G. & Kaplan, J.M. Systematic analysis of genes required for synapse structure and function. *Nature* **436**, 510-7 (2005).
82. Barrios-Rodiles, M., Brown, K.R., Ozdamar, B., Bose, R., Liu, Z., Donovan, R.S., Shinjo, F., Liu, Y., Dembowy, J., Taylor, I.W., Luga, V., Przulj, N., Robinson, M., Suzuki, H., Hayashizaki, Y., Jurisica, I. & Wrana, J.L. High-throughput mapping of a dynamic signaling network in mammalian cells. *Science* **307**, 1621-5 (2005).
83. Bouwmeester, T., Bauch, A., Ruffner, H., Angrand, P.O., Bergamini, G., Croughton, K., Cruciat, C., Eberhard, D., Gagneur, J., Ghidelli, S., Hopf, C., Huhse, B., Mangano, R., Michon, A.M., Schirle, M., Schlegl, J., Schwab, M., Stein, M.A., Bauer, A., Casari, G., Drewes, G., Gavin, A.C., Jackson, D.B., Joberty, G., Neubauer, G., Rick, J., Kuster, B. & Superti-Furga, G. A physical and functional map of the human TNF-alpha/NF-kappa B signal transduction pathway. *Nat Cell Biol* **6**, 97-105 (2004).
84. Cohen, M., Stutz, F., Belgareh, N., Haguenaer-Tsapis, R. & Dargemont, C. Ubp3 requires a cofactor, Bre5, to specifically de-ubiquitinate the COPII protein, Sec23. *Nat Cell Biol* **5**, 661-7 (2003).
85. Soncini, C., Berdo, I. & Draetta, G. Ras-GAP SH3 domain binding protein (G3BP) is a modulator of USP10, a novel human ubiquitin specific protease. *Oncogene* **20**, 3869-79 (2001).
86. Vugmeyster, Y., Borodovsky, A., Maurice, M.M., Maehr, R., Furman, M.H. & Ploegh, H.L. The ubiquitin-proteasome pathway in thymocyte apoptosis: caspase-dependent processing of the deubiquitinating enzyme USP7 (HAUSP). *Mol Immunol* **39**, 431-41 (2002).
87. Jono, H., Lim, J.H., Chen, L.F., Xu, H., Trompouki, E., Pan, Z.K., Mosialos, G. & Li, J.D. NF-kappaB is essential for induction of CYLD, the negative regulator of NF-kappaB: evidence for a novel inducible autoregulatory feedback pathway. *J Biol Chem* **279**, 36171-4 (2004).
88. Nijman, S.M., Huang, T.T., Dirac, A.M., Brummelkamp, T.R., Kerkhoven, R.M., D'Andrea, A.D. & Bernards, R. The deubiquitinating enzyme USP1 regulates the Fanconi anemia pathway. *Mol Cell* **17**, 331-9 (2005).
89. Reiley, W., Zhang, M., Wu, X., Granger, E. & Sun, S.C. Regulation of the deubiquitinating enzyme CYLD by IkappaB kinase gamma-dependent phosphorylation. *Mol Cell Biol* **25**, 3886-95 (2005).

Enabling high-throughput ligation-independent cloning and protein expression for the family of ubiquitin specific proteases

Mark P.A. Luna-Vargas, Evangelos Christodoulou¹, Andrea Alferi², Willem J. van Dijk, Magda Stadnik, Richard G. Hibbert, Danny D. Sahtoe, Marcello Clerici, Valeria De Marco¹, Dene Littler, Patrick H.N. Celie³, Titia K. Sixma⁴, Anastassis Perrakis*

J Struct Biol 2011; 175(2):113-9

Department of Biochemistry and Centre for Biomedical Genetics,
The Netherlands Cancer Institute, Plesmanlaan 121, 1066 CX Amsterdam, The Netherlands

*Corresponding author: a.perrakis@nki.nl (A. Perrakis).

¹Present address: Division of Molecular Structure, National Institute for Medical Research, The Ridgeway, Mill Hill, London NW7 1AA, UK.

²Present address: Department of Experimental Oncology, European Institute of Oncology, via Adamello 16, I-20139 Milan, Italy.

³Correspondence and requests for all vectors presented in this manuscript should be addressed to P.H.N.C.

⁴Correspondence concerning the USP family and related reagents should be addressed to T.K.S.

3



Abstract

High-throughput methods to produce a large number of soluble recombinant protein variants are particularly important in the process of determining the three-dimensional structure of proteins and their complexes. Here, we describe a collection of protein expression vectors for ligation-independent cloning, which allow co-expression strategies by implementing different affinity tags and antibiotic resistances. Since the same PCR product can be inserted in all but one of the vectors, this allows efficiency in versatility while screening for optimal expression strategies. We first demonstrate the use of these vectors for protein expression in *Escherichia coli*, on a set of proteins belonging to the ubiquitin specific protease (USP) Family. We have selected 35 USPs, created 145 different expression constructs into the pETNKHIS-3C-LIC-kan vector, and obtained 38 soluble recombinant proteins for 21 different USPs. Finally, we exemplify the use of our vectors for bacterial co-expression and for expression in insect cells, with USP4 and USP7 respectively. We conclude that our ligation-independent cloning strategy allows for high-throughput screening for the expression of soluble proteins in a variety of vectors in *E. coli* and in insect cells. In addition, the same vectors can be used for co-expression studies, at least for simple binary complexes. Application in the family of ubiquitin specific proteases led to a number of soluble USPs that are used for functional and crystallization studies.

3

Introduction

The sequences of viral, bacterial and eukaryotic genomes have been unravelled over the last decade, providing a large protein database in demand for structure–function analysis. To meet this challenge, an international effort to understand protein function was initiated, and pioneered by efforts such as the US-based “Protein Structure Initiative” (PSI), the Japan-based RIKEN Structural Genomics Initiative, and private–public open access consortia pioneered by the Structural Genomics Center (SGC) and many others. In Europe, the SPINE project introduced high throughput proteomics in a wide collaborative platform, and SPINE-2-complexes aimed to extend many of these methodologies to the study of macromolecular complexes. A direct consequence of such efforts was the rapid development of new high-throughput technologies for molecular cloning, expression and purification of recombinant proteins, that are crucial in the effort of determining the three-dimensional protein structures on a genomic scale^{1,2}.

Any structure determination project is dependent on the ability to obtain sufficient amounts of soluble recombinant protein. A difference of three amino acids between constructs can already improve either the protein solubility or significantly alter its propensity to crystallize^{3,4}. It is therefore common practice to test many protein constructs, typically combinations of N- and C-terminal truncations and assess them for the amount of protein expressed and solubility. The use of high-

throughput methods enables screening of multiple constructs in parallel, to quickly determine the construct, which produces soluble recombinant protein and is more likely to crystallize.

One technique for molecular cloning that was described two decades ago⁵ but has been popularized in the Structural Genomics field, is Ligation Independent Cloning (LIC). LIC is a procedure for the directional cloning of PCR products that is independent of restriction endonucleases, DNA ligase or alkaline phosphatases. The LIC method takes advantage of the 3'→5' exonuclease activity of T4 DNA Polymerase to create very specific single-stranded overhangs in both the vector and in PCR products of the protein of interest. When vector and insert are transformed into *Escherichia coli* cells, covalent bond formation at the vector-insert junctions occurs within the cell to yield circular plasmid and the resulting construct is ready for expression either in bacteria or in insect cells. Here, we first describe the procedures to design and produce a series of LIC applicable vectors for recombinant protein expression. All but one of the vectors accommodate the same PCR product: this allows to create in parallel a simple hexahistidine tag construct, or a GST tag construct to facilitate solubility, or a Strep-tag II, or a His-tag fused to the Trigger Factor in a cold inducible system that has shown very promising results⁶. At the same time the target vectors have different antibiotic resistance combinations and/or origins of replica-

tion (Fig. 1) making them possible for protein co-expression experiments. The same PCR product can even be used for insertion in vector that can be used for protein production in insect cells. The only vector requiring a different PCR reaction is the his-SUMO2 vector: this peculiarity is necessary to take advantage of the SENP-2 protease property to leave no residual amino-acids after tag cleavage. To enable the high throughput design of PCR primers for these LIC reactions, the web server 'Protein Crystallisation Construct Designer' (ProteinCCD; <http://xtal.nki.nl/ccd>) has been designed⁷.

To exemplify the use of our vector suite, we show our work in the study of the largest sub-family of Deubiquitinating Enzymes (DUBs), the Ubiquitin Specific Protease (USP) family.

DUBs are proteases that are capable of removing ubiquitin (Ub) from Ub conjugated proteins by specifically hydrolyzing ester, thiol ester and amide bonds to the carboxyl group of Glycine-76 of Ubiquitin. The large USP family comprises approximately sixty proteins, which are papain-like proteases that vary greatly in size. These USPs contain three conserved regions surrounding the cysteine, histidine and aspartate/asparagine residues that form the catalytic triad^{8,9}. Only a small number of substrates have been identified and little is known about the substrate specificity and selectivity of the USP family. The large size of the USP family and its associated specificity opens up perspectives for its use as drug target.

We present the expression testing for a large collection of USPs, using one of our vectors. Then, we show the use of a selection of our different bacterial expression vectors for single protein expression and co-expression studies using the minimal catalytic domain of one of the members of the USP family, USP4, which is formed by two domains, USP4-D1 and -D2¹⁰. Finally we illustrate the use of an insect cell expression LIC vector for the production of another member of the USP family, USP7.

Material and methods

The design and construction of the pETNKI-LIC vector suite

An overview of all the vectors used in this study is shown in Fig. 1.

The pETNKI-His-3C-LIC-kan vector is engineered to express the target protein imme-

diately downstream of an N-terminal hexahistidine tag, followed by the human rhinovirus 3C protease (3C protease) cleavage site, enabling removal of all vector-encoded fusion sequences. This vector was based on the popular pET-28a expression vector (Novagen): the sequence between the NcoI and XhoI restriction sites of the original plasmid was replaced with the 5'CCATGGCACATCACCCAC-CACCATCACTCCGCGGCTCTTGAGGTGCTCTTT*CAGGGACCCGGG***TAC-CAAGAACA**AAAACTCATCTCAGAAGAGGATCTGTT**GGTACCCGGGCTTCTCTC**TGAG 3' sequence. This sequence contains two KpnI restriction sites (bold) and the LIC sequences that are used to create the overhanging ends for the annealing reaction (italics). The 5' sequence upstream the first KpnI site encodes the MAHHHHHSAALEVLFQ↓GPG sequence (underlined; ↓ indicates the cleavage site for 3C protease).

To create the pCDFNKI-StrepII-3C-LIC-strep vector, pET52b (Novagen) was cut with XbaI and KpnI to obtain a 109 bp fragment containing the StrepII-tag and 3C protease recognition site. This fragment was ligated into pETNKI-His-3C-LIC-kan that was cut with XbaI and KpnI, to yield pETNKI-StrepII-3C-LIC-kan. The resulting vector was cut with NcoI and XhoI to obtain a 84 bp fragment containing the LIC cassette. This fragment was cloned into the pCDF-Ib expression vector (Novagen) cut with the same enzymes.

To create the pGEXNKI-GST-3C-LIC-amp vector, a PCR reaction was performed using the pETNKI-StrepII-3C-LIC-kan vector as template to obtain a fragment containing the LIC cassette that could be cloned into the pGEX-2T expression vector (GE Healthcare). The forward primer (50-CATAGGGATCCTCCGCGGCTCTTGAGGTG-30) contained a BamHI restriction site and the reverse primer (50-ATCCGAATTCTAAGT-TATTGCTCAGCGG-30) contained an EcoRI site. The 250 bp PCR fragment was digested with BamHI and EcoRI and ligated into the pGEX-2T vector cut with the same enzymes.

To construct the pColdNKI-His-TF-3C-LIC-amp vector containing a hexa-histidine-tagged Trigger Factor (TF) as a solubility tag, pETNKI-His-3C-LIC-kan was digested with SacII and XhoI to obtain a 90 bp SacII-XhoI fragment containing

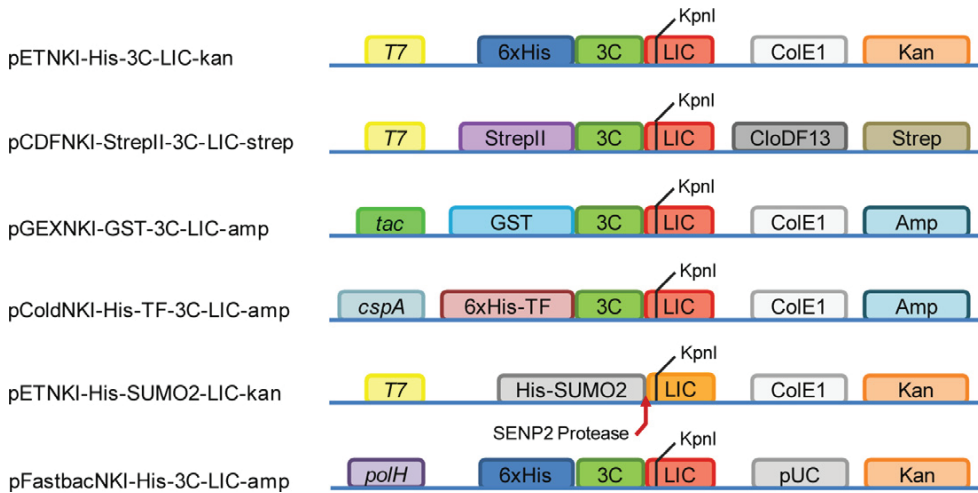


Figure 1. A schematic diagram of the vectors in the NKI suite. Different features of the vectors allowing different affinity purification strategies, better induction mediated or tag mediated solubilisation, or co-expression experiments are indicated: Promoters: T7; *cspA* (Cold-shock protein) promoter; *polH*, polyhedrin. Tags: his, hexa-histidine tag; StrepII, Strep-tag; GST, GST-tag; his-TF, hexa-histidine tagged Trigger Factor; his-SUMO2, hexa-histidine SUMO2 tag. Protease site: 3C, Human Rhinovirus 3C precision protease; SENP2, SUMO-specific protease. Origins of Replications: ColE1; CloDF13; PUC. Resistance markers: Kan, kanamycin; Amp, ampicillin; Strep, streptomycin. LIC cassette (LIC) and KpnI restriction sites to linearize the vector are indicated.

the LIC cassette. This fragment was ligated into the pCOLD™ TF vector (Takara Bio Inc. Otsu, Japan), that was cleaved with the same enzymes.

To create the pET-NKI-His-SUMO2-LIC-kan vector, a Quikchange reaction (Stratagene, CA) was performed with forward primer CCAGCAGCAGACGGAGGGTACC-GGGCTCCGCCCAAGCTTGCGGCCG-CACTCG and the corresponding reverse/complement oligonucleotide according to manufacturers instructions, using the SUMOPRO pSUMO2 vector (LifeSensors, PA), which contains the SMT3A gene in frame with a his-tag, as a template to introduce a LIC cassette. This is the only vector from this collection where different overhangs are required for the PCR fragment.

To create the pFastBac-NKI-His-3C-LIC-amp vector the pETNKIHis-3C-LIC-kan cassette was PCR amplified and inserted in the baculovirus expression vector pFastBac-HTb between the RsrII and HindIII restriction sites using the following primers: forward 5'-GAGACTCGGTCCGAAACCATGGCA-CATCACCACCACATCAC-3' and reverse 5'-ACTTAAAGCTTCTCGAGGAGAAGCCCGGGTA-3'. The start ATG codon was maintained in the same position as in pFastBac-HTb.

Preparation of Linear Plasmid DNA for LIC

An overview of the LIC cloning procedure is depicted in Fig. 2.

Any of these plasmids is transformed into an *E. coli* host strain like DH5a, amplified and retrieved via a midi or maxi plasmid prep kit (Qiagen). The vector DNA (10 µg) is then digested with KpnI for 2–3 h at 37°C in a 100 µL reaction volume and purified with a QIAquick spin column (Qiagen) according to the manufacturer's protocol and eluted in 100 µL TE buffer to achieve DNA concentration of ~100 ng/µL. The linearized vector DNA is then treated with T4 DNA Polymerase to create the single-stand overhangs as follows: In a sterile 1.5-ml micro-centrifuge tube 10 µL of linearized vector, 2 µL 10X T4 DNA Polymerase Buffer (NEB), 2 µL 25 mM dTTP, 1 µL T4 DNA Polymerase (NEB) and 5 µL Nuclease-free water are added to a final volume of 20 µL. The reaction is started by adding the enzyme and incubated at RT for 30 min. The T4 DNA Polymerase is inactivated by incubating at 75°C for 20 min. For the LIC annealing reaction 1 µL of vector prepared in this manner (~50 ng/µL) is annealed with each insert. Starting from the recommended 10 µg of vector, approximately 200 µL of final T4 treated solution is obtained, which is suitable for 200 LIC reactions.

Production of gene products for LIC cloning

To amplify the target gene construct by PCR to create the LIC insert, we typically use the high-fidelity polymerase Pfu from Stratagene. A main requirement here is that the polymerase used needs to be one with minimal activity for the addition of non-templated 30 nucleotides. For all vectors (except pETNKI-His-SUMO2-LIC-kan) the 50-end of the primers must contain the CAGGGACCCGGT sequence upstream of the forward PCR primer and CGAGGAGAAGCCCGGTTA sequence upstream of the reverse primer (which includes a TAA stop codon). For the pETNKI-His-SUMO2-LIC-kan vector the 50-end of the forward PCR primer must contain the CCAGCAGCAGACGGGAGGT sequence upstream of the primer followed by the sequence of the gene of interest; the GCGGCGGAGCCCGTTA sequence is needed upstream at the 5'-end of the reverse primer. Importantly, the SUMO2 tag can be removed from the target protein after treatment with SENP2 protease, leaving no extra amino acid residues at the N-terminus of the sequence of the target protein.

To prepare DNA fragments for the T4 DNA Polymerase treatment, the dNTPs from the PCR product are removed with a spin column kit (QIAquick PCR purification kit) and the purified PCR products are eluted in TE buffer (10 mM Tris-HCl, 0.1 mM EDTA, pH 8.0). In a sterile 1.5-ml microcentrifuge tube (or microwell plate to enable high throughput production) 0.2 pmol of purified PCR DNA (measured in a Nanodrop1000 by ThermoScientific), 2 μ l 10X T4 DNA Polymerase Buffer (NEB), 2 μ l 25 mM dATP and 1 μ l T4 DNA Poly-

merase (NEB) are added to a final volume of 20 μ l. The reaction is started by adding the enzyme and incubated at RT for 30 min. The T4 DNA polymerase is inactivated by incubating at 75°C for 20 min.

Annealing the vector and the LIC insert

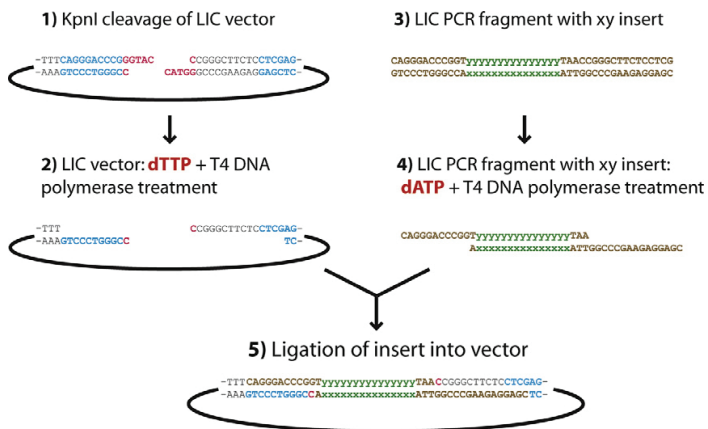
For each construct, 1 μ l vector (50 ng/ μ l) and 2 μ l insert (0.02 pmol) prepared as above are assembled in a sterile reaction plate. The reactions are incubated at RT for 5 min, and stopped by adding 1 μ l of 25 mM EDTA. Typically, half of the annealing reaction (2 μ l) is transformed into NovaBlue competent cells that are plated onto LB agar plates containing the appropriate antibiotic. After overnight incubation at 37°C, two single colonies for each construct are picked and used for plasmid amplification, isolation and sequencing, using standard protocols. Alternatively, colonies containing the insert can be identified using colony PCR and sequence confirmation can be reserved for only constructs that produce soluble protein. It should also be noted that annealing reactions can be transformed directly into the expression strain; or each half of the reaction can go to an expression strain and a DNA amplification strain respectively.

Testing different pETNKI-LIC vectors in medium-throughput co-expression

To identify constructs likely to yield sufficient amounts of soluble protein for scale-up and protein purification, we first performed a small-

Figure 2. A schematic overview of the LIC cloning procedure.

1) Cleavage of the different expression vectors with KpnI (except for the pETNKI-HisSUMO2-LIC).
2) Treatment of the cleaved vector with T4 DNA polymerase in presence of dTTP.
3) Generation of PCR fragment of gene of interest flanked with specific LIC sequences.
4) Treatment of the LIC PCR fragment with T4 DNA polymerase in presence of dATP.
5) Annealing and ligation of insert into expression vector. The sequence of KpnI cleavage site is indicated in pink, the LIC sequence is indicated in blue for the vector and brown for the PCR insert, and the gene of interest is indicated in green.



scale protein expression and solubility screening. 50 μ l *E. coli* Rosetta2(DE3) or BL21(DE3) cells are transformed with 50 ng of plasmid in a Thermowell 96-well PCR microplate (Corning, Inc.) and heat shocked for 40 s at 42°C in a water bath. After incubation on ice for 2 min, 100 μ l SOC medium is added to each well and the 96-well microplate is sealed with a silicone rubber mat (Costar) and incubated at 37°C for 1 h. The transformation reactions are plated out on 6-well LB agar plates (Falcon multiwell, Beckton Dickinson) containing the appropriate antibiotics. After overnight growth at 37°C, single colonies of each construct are picked and grown in 200 μ l auto-induction media (ZYP5052, made in-house)¹¹ (Studier, 2005) with appropriate antibiotics, in a 2 ml 96-deepwell block (Nunc) and sealed with Airpore tape sheets (Qiagen). The 96-deepwell block is incubated in a shaker at 300 rpm for 4 h at 37°C. When the cells reach an OD₆₀₀ of about 2–3, typically after 4 h, the temperature is lowered to 15°C for overnight induction. For higher volume production (in our case for all vector comparison tests) 0.5 ml of overnight pre-culture was used to inoculate 50 ml LB medium (LB Broth (Miller) from Molecular Dimensions Limited) with corresponding antibiotics in 250 ml baffled flasks and grown at 37°C until OD₆₀₀ of 0.8 units is reached. Since USP4 contains two zinc finger motifs, prior to induction we supplement the media with 12.5 μ l 1M ZnCl₂ (250 mM), a practice we know to be beneficial based on prior experience. Finally, we added 25 μ l 1M IPTG (500 mM) to induce protein production and the cells were grown overnight at 15°C.

For high throughput testing, cells are collected by centrifuging the 96-deepwell block at 4000 rpm for 15 min. All liquid handling steps are done by hand with a multi-channel pipette (Matrix Technologies). The pellet in each well is resuspended with 200 μ l lysis buffer (50 mM Tris-HCl pH8.0, 200 mM NaCl, 5 mM imidazole, 0.1% Triton X-100, 2 mM β -mercaptoethanol, 200 U Lysozyme (Novagen)). The 96-deepwell block containing the cell suspension is shaken at 800 rpm for 20 min at room temperature using the thermomixer (Eppendorf). When the cell extract is clear, 10 μ l of MagneHis Ni²⁺-beads (Promega), are added to each well. After 5 min the Magnetight HT96 stand (Novagen) is used to pull down the MagneHis beads to remove unbound proteins. The MagneHis beads

are washed 3 times with 50 μ l wash buffer (50 mM Tris-HCl pH 8.0, 200 mM NaCl, 5 mM imidazole & 2 mM β -mercaptoethanol). Protein elution from the MagneHis-beads is done by adding 20 μ l elution buffer (wash buffer containing 500 mM imidazole) to each well and incubating the 96-deepwell block for 10 min at room temperature. The MagneHis-beads are finally pulled down with the magnetic stand and the eluted proteins removed and analyzed on SDS-page gels.

For higher volume testing (in our case for all vector comparison experiments and co-expression tests), cells are harvested by centrifugation and resuspended with 3 ml lysis buffer (25 mM Hepes pH7.5, 150 mM NaCl, 10 mM Imidazole, 5 mM β -mercaptoethanol and protease inhibitor tablet). The cells are broken by subjecting the cell suspension to a 10 s pulse with a pause of 20 s after each pulse for a total of 2 min using the Misonics sonicator S-4000 at 40% maximum setting. The cell lysate is centrifuged at 13,200 rpm for 25 min at 4°C. The resulting supernatant is incubated with 100 μ l of corresponding resin (Talon resin (Clontech) for His-tag, Glutathione Sepharose resin (GE Healthcare) for GSTtag and Strep Tactin resin (Novagen) for StrepII-tag) for 15 min at 4°C. The resin is washed with 2 times 5 mL lysis buffer and the protein is eluted from the beads with elution buffer (lysis buffer containing 300 mM Imidazole or 25 mM glutathione or 2.5 mM desthiobiotin). Samples of total cells, supernatant cell lysate and eluate are analysed on an SDS-PAGE gel.

Scale-up of expression and protein purification of USP8

As in the small scale expression trials, the *E. coli* host Rosetta2(DE3) was used for the large scale protein expression. 5 ml of overnight pre-culture was used to inoculate 500 ml autoinduction media in 3L baffled flasks and grown at 37°C until OD₆₀₀ of 2–3 units was reached. The temperature was lowered to 15°C for overnight induction. Cells were harvested by centrifugation and resuspended in 200 ml lysis buffer (50 mM Tris-HCl pH8.0, 150 mM NaCl, 10 mM imidazole, 5 mM β -mercaptoethanol and 1 mM PMSF). The cells were broken by subjecting the cell suspension to a 10 s pulse with a pause of 30 s after each pulse for a total of 5 min using the Misonics sonicator S-4000 at 80% maximum setting. The broken cell lysis was centrifuged

Table 1

Summary of the high-throughput cloning and protein expression screen.

Target name	Targets	Constructs designed	Constructs cloned	Soluble proteins (%)	Soluble targets
Human USPs	35	176	145	37 (26%)	21 (60%)

at 48,000 g (J-26XP Avanti Centrifuge, Beckman Coulter) for 30 min at 4°C to remove cellular debris and unbroken cells. The resulting supernatant was incubated with washed 2 ml Talon metal affinity resin (Clontech, Inc., Palo Alto, CA) for 20 min at 4°C and the beads were then washed with 200 ml lysis buffer. The beads were eluted with 20 ml lysis buffer containing 400 mM imidazole. The eluted sample was diluted 10–15 times with 50 mM Bis-Tris pH6.5. The diluted sample was applied to a 5 ml Poros S column equilibrated with buffer A (20 mM BisTris pH6.5, 10 mM NaCl and 5 mM β-mercaptoethanol) and bound protein was eluted with buffer A containing 1 M NaCl using a 60% gradient in 20 column volumes. Peak fractions were pooled and concentrated by ultrafiltration using an Amicon Ultra centrifugal unit (Millipore) and applied to a Superdex 75 16/60 gel filtration column (GE Healthcare) equilibrated with buffer containing 25 mM Tris-HCl pH8.0, 150 mM NaCl and 5mM β-mercaptoethanol. Peak fractions from the gel filtration column were pooled and concentrated in an Amicon Ultra centrifugation unit to a concentration of 10 mg/ml. The concentrated protein was

flash frozen in liquid nitrogen and stored at -80°C.

Small-scale test expression in insect cells

The production and isolation of the recombinant bacmid and the infection of the P0 culture is performed as described in the Invitrogen Bac-to-Bac® Baculovirus Expression System manual. 25 ml of Sf-9 insect cells at 106 cells/ml concentration is infected with 1 ml of P0 culture medium and let grow for 72 h.

Cells are harvested by centrifugation and resuspended with 10 ml lysis buffer (20 mM Hepes pH 8.0, 150 mM NaCl and protease inhibitor tablet). The cells are lysed by sonication in an ice bath for 30 s (5 s pulse with a pause of 40 s) using the Misonics sonicator S-4000 (at 50% maximum setting) and the lysate centrifuged at 48,000g (J-26XP Avanti Centrifuge, Beckman Coulter) for 25 min at 4°C. The supernatant is purified on column using 200 μl of Chelating Sepharose Fast Flow resin loaded with Ni²⁺. Samples of lysate, supernatant and elution are analysed on a SDS-PAGE gel.

Table 2

Medium-throughput testing of different NKI-LIC vectors in single and co-expressions of USP4-D1 and USP4-D2 (c: cloned, E: expression, S: soluble).

Single expression	USP4-D1			USP4-D2		
	C	E	S	C	E	S
pETNKI-His-SUMO2-LIC-kan	√	+++	+	-		
pCDFNKI-StrepII-3C-LIC-strep	-			√	++	-
pCOLDNKI-His-TF-3C-LIC-amp	√	+++	+++	-		
pGEXNKI-GST-3C-LIC-amp	√	+++	+	-		
Co-expression	USP4-D1 & D2					
	E			S		
pETNKI-His-SUMO2-LIC-kan (D1)						
pCDFNKI-StrepII-3C-LIC-strep (D2)	+++			++		
pGEXNKI-GST-3C-LIC-amp (D1)						
pCDFNKI-StrepII-3C-LIC-strep (D2)	+++			++		
pCOLDNKI-His-TF-3C-LIC-amp (D1)						
pCDFNKI-StrepII-3C-LIC-strep (D2)	+++			++		

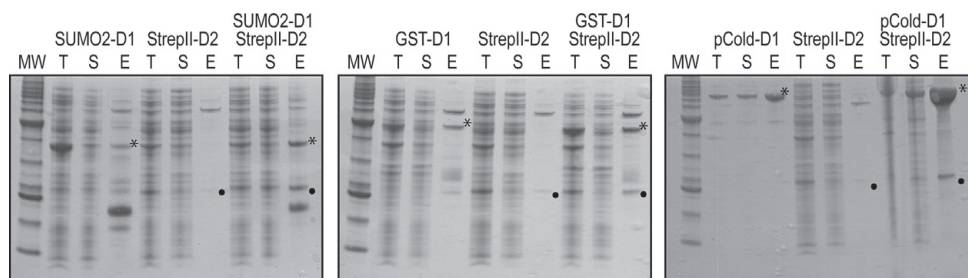


Figure 3. SDS-PAGE assessment of co-expression trials for USP4-D1 and USP4-D2 domains in different NKI-LIC *E. coli* expression vectors. T: total cells; S: supernatant; E: elution. * indicates the D1 fusion protein and • indicates the D2 fusion protein.

Results and discussion

Evaluation of the pET-NKI vectors suite

The pETNKI-His-3C-LIC-kan vector was tested using a set of proteins that we have successfully produced previously in our lab. First, we used our method to clone two different proteins and analyzed 96 colonies from each. The number of clones without an insert was less than 6%, an acceptable rate of false positives to allow high throughput approaches. Expression levels were comparable to other vectors previously used in our lab. The pETNKI-His-3C-LIC-kan vector has thereafter been used successfully to produce well over one thousand expression constructs of different proteins in our lab. In the next section we describe its specific application to the study of the USP family.

Based on the success of the pETNKI-His-3C-LIC-kan system in our lab as well as in other labs, we have created a complementary suite of vectors (Fig. 1) which enable expression of different fusion proteins and which also allow production of protein complexes using co-expression strategies. To evaluate these vectors, we used as a test system the catalytic domain of the deubiquitinating enzyme USP4 (USP4CD) that is made by two domains, D1 and D2, which assemble together to make USP4CD. Neither D1 nor D2 could be obtained as a soluble protein when expressed individually as hexahistidine-tagged fusion proteins. However, upon co-expression of the two domains, a soluble protein complex could be isolated¹⁰. For our vector evaluation experiment, D1 was fused to different N-terminal affinity and solubility tags (His-SUMO2-, GST- and His-TF- tag), whereas D2 was fused only to a StrepII affinity tag. We expressed each protein individually or in different D1-D2 co-expression combinations (Fig. 3, Table 2). For the compari-

son of expression experiments we did not apply any other normalization or optimization, other than using identical culture conditions and volumes in all cases. For His-SUMO2- and GST- D1 fusion constructs, only partially soluble protein could be obtained within the individual expression tests, whereas a fair amount of soluble D1 was obtained when fused to the His-TF-tag. For strepII-tagged D2 protein alone, only a minor portion of the expressed protein appeared in the soluble fraction. However, when D2 was co-expressed together with the D1 constructs, a significant amount of soluble D2 could be co-eluted when D1 was purified via affinity purification (either Talon beads for the his-tag or glutathione Sepharose beads for the GST-tag), demonstrating the presence of a soluble D1-D2 complex. Co-expression improved the solubility of the D1 fragments in all cases. Using the pETNKI-His-SUMO2-LIC-kan and pCDFNKI-StrepII-3C-LICstrep vectors, D1 and D2 were also expressed in similar amounts, representing a stoichiometric ratio of 1:1 as physiologically expected for D1 and D2 being the two parts that constitute USP4CD. These results suggest that the NKI-LIC vector suite can be used to produce soluble proteins and protein complexes when used in co-expression experiments.

The utility of affinity tags has been previously shown to be of great use for purifying recombinant proteins¹². However, most tags come with their own advantages and disadvantages. For example, the use of immobilized metal-ion affinity chromatography (IMAC) sometimes yields insufficiently pure proteins and does not enhance the protein solubility¹³, while the affinity media are very cheap. In contrast, the StrepII-tag displays increased specificity and re-

sults to more pure protein, but the affinity resin is very expensive, while it does not improve protein solubility¹⁴. The GST-, SUMO2- and TF-tags have been developed to aid in protein solubility and folding^{6,15,16}. Furthermore, the SUMO2-tag has been shown to also increase the level of protein expression and solubility. However, also for these tags there are disadvantages: the GST-tagged recombinant protein tends to form dimers, SUMO2 is mostly constrained to *E.coli*, since SUMO proteases that are present in eukaryotes may cleave the fusion protein during expression, and all these tags often result in finally insoluble protein after they are cleaved. Providing a vector suite where the utility of each tag can be tested experimentally easy and with minimal cost (no additional PCR products needed, with the exception of the SUMO2 tag vector) makes the choice of this vector suite particularly appealing. Combining different tags with different origins of replication and antibiotic resistance enables co-expression experiments with the same vectors.

Application to the USP family

The cDNA of 35 different USPs were collected and 176 constructs were designed (Table 1 and Supplementary Table 1). Initial constructs design was enabled by studying existing crystal structures of USP catalytic domains (USP7, 1nb8; USP2, 2hd5; USP8, 2gfo; USP14, 2ayo)¹⁷⁻²⁰ and also based on sequence alignment²¹, secondary structure prediction²² and protein disorder prediction²³. Additional constructs were designed if a link to cancer was found in literature for a specific USP or when a positive but insufficient hit for protein expression was identified. These constructs included the full length protein as well the additional domains found outside the catalytic domain predicted by SMART^{8,24} with variations at the C- and N-terminal ends of the predicted domains. Although PCR problems precluded the amplification of a significant number of constructs (30 out of 176), once PCR products were made, all but one of them have been successfully cloned into the pETNKI-His-3C-LIC-kan vector. The high throughput protein expression and solubility screening of 145 different constructs resulted in 26% of the constructs giving soluble protein for 21 different USPs. Large scale protein production is ongoing to verify whether these constructs can produce soluble protein in amounts suitable for structural studies. In Fig. 4

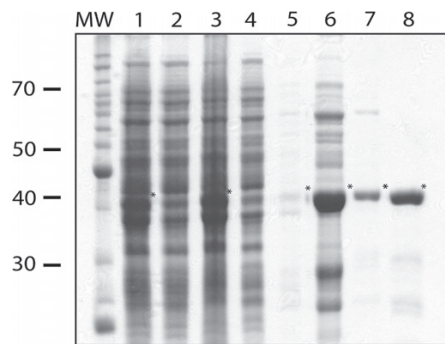


Figure 4. Large scale protein expression and purification profile of the catalytic domain of USP8CD on SDS-PAGE gel. Lane 1, total cells; lane 2, pellet; lane 3, supernatant; lane 4, flow through of washing Talon resin; lane 5, washed Talon resin; lane 6, eluted USP8CD from Talon resin; lane 7, eluted USP8CD of anion exchange column; lane 8, eluted USP8CD of gel filtration column Superdex75 16/60. * indicates the UPS8CD fusion protein.

we exemplify the large scale protein expression and purification of the catalytic domain of USP8.

From all constructs tried, 98 of them (68%) expressed recombinant His-tagged protein for 26 different USPs. Absence of protein expression in the remaining constructs was caused either by failure of transformation reactions or by low cell culture density during protein induction. Of the 98 expressing constructs, 37 constructs produced soluble recombinant protein for 21 different USPs. In some cases only particular constructs were able to give soluble protein. For example, only one construct of USP1 (Supplementary Table 1) expressed soluble protein. This construct lacks the first 29 residues at the N-terminus of the protein, which were predicted to belong to a flexible loop²². The removal of this flexible region seemed to be necessary for the soluble expression of USP1. Also for example, in USP21 the addition and removal of several residues at the N-terminal and C-terminal ends respectively, greatly enhanced expression and solubility compared to the *in silico* (SMART) predicted domain (Supplementary Table 1). USP7 was a particular USP family target that was not expressed in *E.coli* despite significant effort. For convenience we created a vector (pFastBacNKI-His-3C-LIC-amp) to facilitate recombinant virus production for protein expression in insect cells, which could accommodate the exact same PCR product as the *E.coli* vectors we use. We show that this vector can be used straightforwardly for LIC

cloning and will yield viruses that successfully mediated USP7 production in insect cells (Fig. 5).

Initially, all constructs were designed based on the sequence alignment and comparison with the previously determined X-ray crystal structures of several catalytic domains of USPs. However, it is clear that designing and screening several different constructs for a particular USP should also be based on domain prediction, disorder prediction and secondary structure prediction, which can greatly improve the protein expression and solubility. A tool to enable such studies has been developed partially based on this experience and is available from <http://xtal.nki.nl/ccd7>.

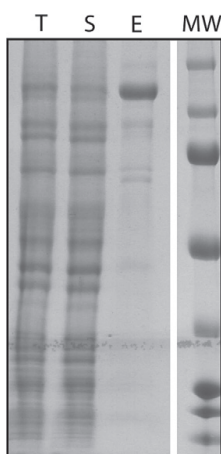
Potential for automation

All described steps were done with a manual multipipette. However all these steps can be automated with the help of robotics²⁵, in which the different steps such as cell lysis, affinity binding and elution of recombinant protein are interlinked. Moreover, the analysis of protein samples by running conventional SDS-PAGE gels is time-consuming and laborious (e.g. pouring gels, pipetting samples, staining and destaining gels). Using other methods for rapid analysis of protein samples such as 96-well gels or microfluidics, might increase the throughput in the last step of identifying soluble recombinant proteins in the high throughput protein expression and solubility screening^{26,27}.

Conclusions

We presented the procedures to create and use a collection of vectors for protein expression, the 'NKI-LIC suite' which can all (but one) accommodate the same PCR product. Combining different affinity and solubility tags with different antibiotic re-

Figure 5. SDS-PAGE assessment of expression and purification of USP7 using the pFastBac-NKI-LIC vector in *Sf9* insect cells. T: total cells; S: supernatant; E: elution.



sistance markers and origins of replication, this enables straightforward and convenient expression strategies. The only vector not compatible with the exact same PCR product contains the small and soluble SUMO2 protein fused to a His-tag for purification purposes. This vector has the advantage that upon cleavage with the SENP protease, no residual residues are left at the N-terminus of the protein of interest. Finally, we show one vector that is suitable to initiate insect cell expression. We showcase the applicability of this strategy to a large collection of targets within the Ubiquitin Specific Protease Family, one of the SPINE-2-complexes priority areas, which enabled the production of many soluble recombinant proteins, suitable for functional and structural studies.

Acknowledgments

Author contributions: MLV identified USP domains, prepared the target list, produced expression clones, performed small scale protein expression and purification, and wrote the manuscript together with AP. EC designed, made and tested the pETNKI-His-3CLIC-kan vector, and initiated the use of the LIC system at the NKI. AA worked on additional USP domains. PvD performed large-scale protein production and purification. MS did the comparative (co-)expression testing of USP4 constructs in all vectors. RGH designed and produced the pETNKI-His-SUMO2-LIC-kan vector. DS and MC designed and tested the pFastBac-NKI-His-3C-LIC-amp vector; VDM and DL participated in testing and establishing the pETNKI-His-3C-LIC-kan for routine use at the NKI. PC designed and produced the pGEXNKI-GST-3C-LIC-amp, pCOLDNKI-His-TF-3C-LICamp and pCDFNKI-StrepII-3C-LIC-strep vectors with various antibiotic resistance markers. TKS initiated and supervised the Ubiquitin Specific Protease project. AP initiated and supervised the high throughput technologies project and wrote the paper with MLV. Funding for this project has been made available through the EC integrated networks SPINE-2 and Rubicon, and through a grant from the KWF (Netherlands).

Appendix A. Supplementary data

Supplementary data associated with this article can be found, in the online version, at [doi:10.1016/j.jsb.2011.03.017](https://doi.org/10.1016/j.jsb.2011.03.017).

References

1. Alzari, P.M. et al. Implementation of semi-automated cloning and prokaryotic expression screening: the impact of SPINE. *Acta Crystallogr D Biol Crystallogr* **62**, 1103-13 (2006).
2. Graslund, S. et al. Protein production and purification. *Nat Methods* **5**, 135-46 (2008).
3. Malawski, G.A. et al. Identifying protein construct variants with increased crystallization propensity--a case study. *Protein Sci* **15**, 2718-28 (2006).
4. Scheich, C. et al. Fast identification of folded human protein domains expressed in *E. coli* suitable for structural analysis. *BMC Struct Biol* **4**, 4 (2004).
5. Aslanidis, C. & de Jong, P.J. Ligation-independent cloning of PCR products (LIC-PCR). *Nucleic Acids Res* **18**, 6069-74 (1990).
6. Qing, G. et al. Cold-shock induced high-yield protein production in *Escherichia coli*. *Nat Biotechnol* **22**, 877-82 (2004).
7. Mooij, W.T., Mitsiki, E. & Perrakis, A. ProteinCCD: enabling the design of protein truncation constructs for expression and crystallization experiments. *Nucleic Acids Res* **37**, W402-5 (2009).
8. Nijman, S.M. et al. A genomic and functional inventory of deubiquitinating enzymes. *Cell* **123**, 773-86 (2005).
9. Quesada, V. et al. Cloning and enzymatic analysis of 22 novel human ubiquitin-specific proteases. *Biochem Biophys Res Commun* **314**, 54-62 (2004).
10. Luna-Vargas, M.P. et al. Ubiquitin-specific protease 4 is inhibited by its ubiquitin-like domain. *EMBO Rep* **12**, 365-72 (2011).
11. Studier, F.W. Protein production by auto-induction in high density shaking cultures. *Protein Expr Purif* **41**, 207-34 (2005).
12. Arnau, J., Lauritzen, C., Petersen, G.E. & Pedersen, J. Current strategies for the use of affinity tags and tag removal for the purification of recombinant proteins. *Protein Expr Purif* **48**, 1-13 (2006).
13. Chaga, G., Bochkariov, D.E., Jokhadze, G.G., Hopp, J. & Nelson, P. Natural poly-histidine affinity tag for purification of recombinant proteins on cobalt(II)-carboxymethylaspartate crosslinked agarose. *J Chromatogr A* **864**, 247-56 (1999).
14. Skerra, A. & Schmidt, T.G. Applications of a peptide ligand for streptavidin: the Strep-tag. *Biomol Eng* **16**, 79-86 (1999).
15. Butt, T.R., Edavettal, S.C., Hall, J.P. & Mattern, M.R. SUMO fusion technology for difficult-to-express proteins. *Protein Expr Purif* **43**, 1-9 (2005).
16. Smith, D.B. & Johnson, K.S. Single-step purification of polypeptides expressed in *Escherichia coli* as fusions with glutathione S-transferase. *Gene* **67**, 31-40 (1988).
17. Avvakumov, G.V. et al. Amino-terminal dimerization, NRDP1-rhodanese interaction, and inhibited catalytic domain conformation of the ubiquitin-specific protease 8 (USP8). *J Biol Chem* **281**, 38061-70 (2006).
18. Hu, M. et al. Structure and mechanisms of the proteasome-associated deubiquitinating enzyme USP14. *EMBO J* **24**, 3747-56 (2005).
19. Hu, M. et al. Crystal structure of a UBP-family deubiquitinating enzyme in isolation and in complex with ubiquitin aldehyde. *Cell* **111**, 1041-54 (2002).
20. Renatus, M. et al. Structural basis of ubiquitin recognition by the deubiquitinating protease USP2. *Structure* **14**, 1293-302 (2006).
21. Plewniak, F. et al. PipeAlign: A new toolkit for protein family analysis. *Nucleic Acids Res* **31**, 3829-32 (2003).
22. Rost, B., Yachdav, G. & Liu, J. The PredictProtein server. *Nucleic Acids Res* **32**, W321-6 (2004).
23. Yang, Z.R., Thomson, R., McNeil, P. & Esnouf, R.M. RONN: the bio-basis function neural network technique applied to the detection of natively disordered regions in proteins. *Bioinformatics* **21**, 3369-76 (2005).
24. Schultz, J., Milpetz, F., Bork, P. & Ponting, C.P. SMART, a simple modular architecture research tool: identification of signaling domains. *Proc Natl Acad Sci U S A* **95**, 5857-64 (1998).

25. Nguyen, H., Martinez, B., Oganesy- an, N. & Kim, R. An automated small-scale protein expression and purification screening provides beneficial information for protein production. *J Struct Funct Genomics* **5**, 23-7 (2004).
26. Feldman, G., Bogoev, R., Shevirov, J., Sartiel, A. & Margalit, I. Detection of tetracysteine-tagged proteins using a bi-arsenical fluorescein derivative through dry microplate array gel electrophoresis. *Electrophoresis* **25**, 2447-51 (2004).
27. Wehr, T., Zhu, M., Rodriguez, R., Burke, D. & Duncan, K. High performance isoelectric focusing using capillary electrophoresis instrumentation. *Am Biotechnol Lab* **8**, 22-9 (1990).

The differential modulation of USP activity by internal regulatory domains, interactors and seven Ubiquitin chain types

Alex C. Faesen^{1,#}, Mark P.A. Luna-Vargas^{1,#}, Paul P. Geurink², Marcello Clerici¹, Remco Merkx², Willem J. van Dijk¹, Dharjath S. Hameed², Farid El Oualid², Huib Ovaa², and Titia K. Sixma^{1,*}

Submitted

¹Division of Biochemistry and Center for Biomedical Genetics, ²Division of Cell Biology, the Netherlands Cancer Institute, Plesmanlaan 121, 1066 CX Amsterdam, the Netherlands.

*Correspondence: t.sixma@nki.nl (T.K.S.)

These authors contributed equally to this study.

4



Abstract

Ubiquitin-specific proteases (USPs) are papain-like isopeptidases with variable inter- and intra-molecular regulatory domains. To understand the effect of these domains on USP activity, we have analyzed enzyme kinetics of a set of twelve USPs in presence and absence of modulators using synthetic reagents. We synthesized all seven wild-type lysine-linked di-ubiquitins and provide the first comprehensive analysis comparing ubiquitin (Ub) chain preference. Our data reveal large variations in both the catalytic turnover and Ub binding between USPs and modest preferences for di-Ub topoisomers. Interestingly, our data show that the preference of USP7 for di-Ub topoisomers can be attributed to the binding affinity (K_M) for the substrate, while the intermolecular activators UAF1 and GMPS mainly increase the catalytic turnover (k_{cat}). Together, this comprehensive kinetic analysis highlights the variability within the USP family.

Introduction

Since the 1980s, the post-translational modification of proteins by Ub has been the focus of many studies due to their important roles in many cellular processes^{1,2}. However, the processing and removal of Ub and thus reversal of the modification of target proteins is equally important and is carried out by De-ubiquitinating enzymes (DUBs).

The human genome encodes nearly 100 putative DUBs, belonging to at least five subfamilies of isopeptidases³. The Ubiquitin-Specific proteases (USP) family is the largest class of DUBs, with more than sixty members^{3,4}. USPs are cysteine proteases that use a papain-like mechanism to hydrolyze the isopeptide bond between the carboxy terminus of Ub and the ϵ -amine of the target lysine.

USPs are variable both in size and their modular domain architecture, which can include substrate binding domains, ubiquitin-like (UBL) domains and other protein-protein interaction domains^{3,5} (Figure 1A). They share a common papain-like fold, but the catalytic domains can have large insertions⁶, possibly directly affecting activity, Ub binding or localization as seen in USP4⁷, USP5⁸, USP14⁹ and CYLD¹⁰. Additionally, some USPs need structural rearrangements to bind their substrate and catalyze hydrolysis¹¹⁻¹⁵.

USPs are often found in large protein complexes and many interaction partners of USPs have been identified¹⁶. Although the function of most interaction partners is still unclear, some play a role in the modulation of USP activity. For example, GMP synthetase (GMPS) interacts and activates USP7¹⁷⁻¹⁹, whereas the WD40-repeat containing UAF1 activates USP1, USP12 and USP46^{20,21}.

With its diversity of domain architectures, internal insertions within the catalytic do-

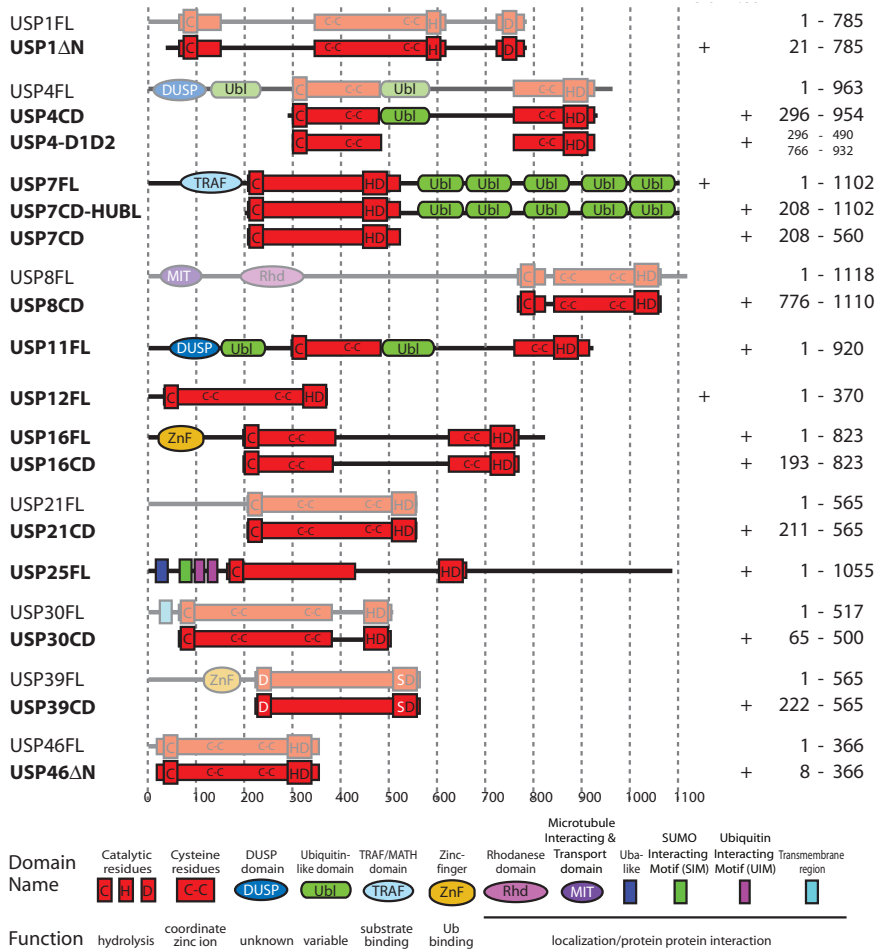
main and external modulators, the USP family apparently requires different levels of regulation. This poses a number of unanswered questions. For instance, what is the variability of the activity between the catalytic domains and the full-length proteins? Are there preferences for Ub-chain types and does this change in the presence of external modulators?

To address these questions, we have developed and produced²² chemical tools, and used these to characterize a set of twelve USPs. This revealed variations of several orders of magnitude in catalytic turnover and Ub binding, and allowed characterizing intra- and inter-molecular activity modulation. Using synthetic di-Ub, we determined the chain preferences of all USPs against all seven lysine-linked topoisomers. This showed a modest chain specificity that was variable between USPs, but did not change in the presence of the modulators. Kinetic analysis of the hydrolysis by USP7 showed that there is no additional Ub binding site, suggesting that the chain preferences are achieved by steric hindrance.

Results

Protein cloning, expression and purification

After protein expression trials²³, we identified constructs suitable for large-scale protein expression of twelve different USPs in either *E.coli* or in *Sf9* insect cells (Figure 1A). In this study we could therefore include sixteen constructs containing either the (almost) full-length constructs (USP1 Δ N, USP7FL, USP11FL, USP12FL, USP16FL, USP25FL and USP46 Δ N, with Δ N and Δ C denoting N- and C-terminal truncations respectively), or the catalytic domain (USP4CD, USP7CD, USP8CD, USP16CD, USP21CD,



B

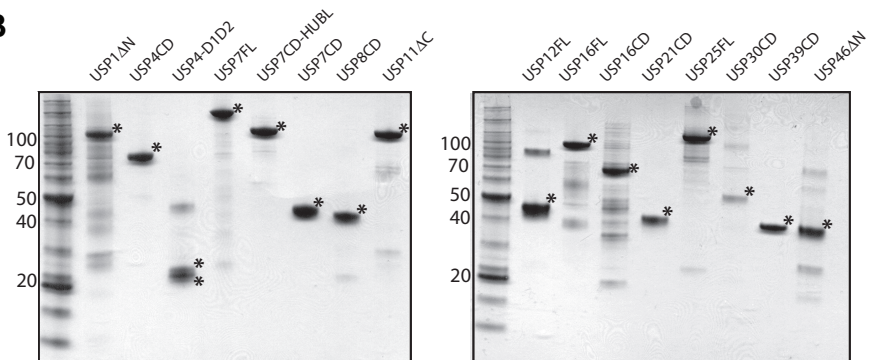


Figure 1. Overview of the characterized USPs. A) Domain architecture of the USPs used in this study. The constructs used in this manuscript are highlighted with corresponding residue numbers and expression system. B) Final purification product of the USP constructs shown on SDS-PAGE gel. An asterisk indicates the expressed USP. USP7FL has an N-terminal GST tag.

USP30CD and USP39CD) (Figure 1A and B). Additionally, we expressed and purified two known USP activity modulators: UAF1²¹ and GMPS¹⁹. Cloning, expression and purification protocols are provided in the materials and methods section.

Large variations in both catalytic turnover and Ub binding

Although USP family members share a homologous catalytic domain, many contain insertions within their catalytic domain or have additional domains that could influence their activity^{6,7} (Figure 1A). To study these effects, we determined the kinetic parameters of all the USPs. To this end, we produced a minimal synthetic Ub substrate with fused at its C-terminus the small molecule 7-amino-4-methyl-

coumarin (UbAMC)^{22,24}. The UbAMC substrate is a widely used reagent to assay DUB activity. Upon hydrolysis by the USP, the free AMC reporter molecule produces a fluorescent signal, which allows for a direct read-out of activity. Since this universal DUB substrate contains an AMC moiety instead of the endogenous USP target, it is suitable for comparing the relative activity among the USP family members. With this substrate, we observed variations of several orders of magnitude in both K_M and k_{cat} between the USP constructs (Figure 2 and Supplemental Figure S1)). Our data are in agreement with earlier reports for USP1, USP4, USP7, USP8 and USP39^{7,11,21,25,26}. Based on their K_M and k_{cat} values, the USPs could be classified in three groups (Figure 2D). Group 1 represents the USPs, whose activity is very limited due to a low k_{cat} (USP1ΔN, USP4CD,

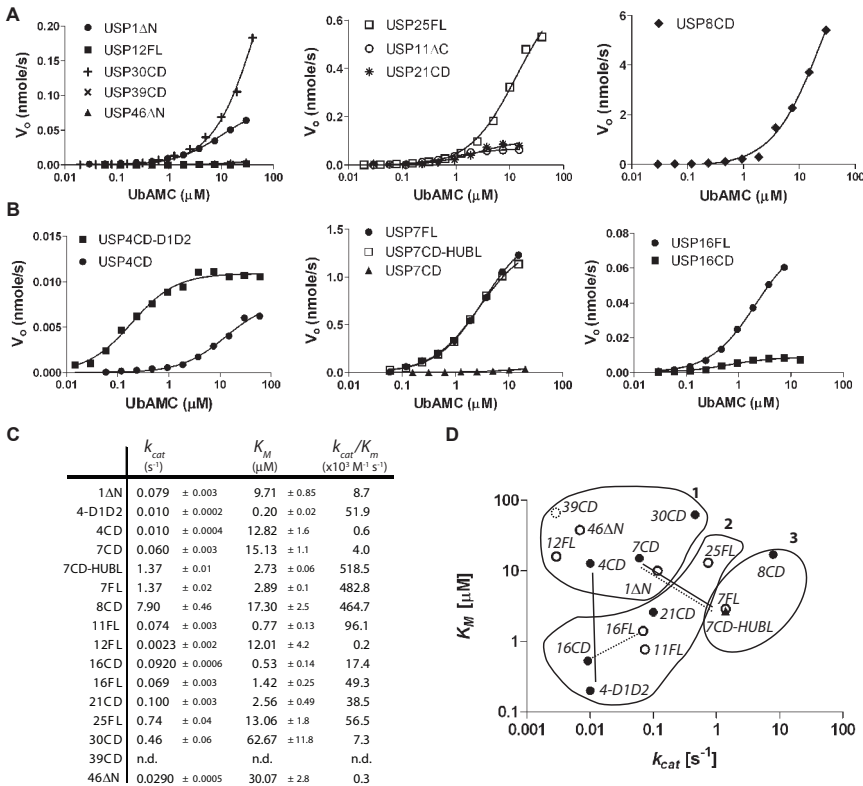


Figure 2. Kinetic parameters using UbAMC. A and B) The Michaelis-Menten curves for the different USPs obtained by determining the initial rates (V_o) at different UbAMC concentration. **B)** shows the USPs with intra-molecular modulation. **C)** Overview of the kinetic parameters (k_{cat} , K_M and K_{cat}/K_M) for the different USPs. **D)** Activity classification of USPs, based on kinetic parameters, where group 1 represents the USPs with the lowest activity; group 2 contains USPs with intermediate activity and group 3 contains the USPs with the highest activity. Dashed lines link the catalytic domains with the corresponding full length USPs. Solid lines show the effect of intra-molecular activating and inhibiting domains.

USP12, USP30CD, USP39CD and USP46ΔN). The “intermediate” group 2 contains the USPs that show moderate activity (USP4-D1D2, USP11FL, USP16CD, USP16FL, USP21CD and USP25FL), and group 3 contains very active USPs (USP7FL, USP7CD-HUBL and USP8CD).

As expected, group 1 contains USP-39CD. It shows no activity, since it lacks the catalytic cysteine and histidine residues³. Group 1 also contains USP1ΔN, USP12FL and USP46ΔN, all three known to have low activity, which is enhanced by the external modulator UAF1^{20,21}. Interestingly, also USP30CD shows very little activity. However, to date there is no known activator for USP30CD, although several interaction partners have been identified¹⁶.

In contrast, group 3 represents the most active USPs, and contains both USP8CD and the USP7 constructs with activating C-terminal HAUSP UBL (HUBL) domain¹⁷. Interestingly, USP8CD has an unusual high K_M , which is possibly due to an inserted α -helix in the catalytic domain, which is suggested to stabilize the observed closed conformation¹¹. However, this is compensated by a very high catalytic turnover, rendering it a very active USP overall.

Intra-molecular modulation of USP activity

Not only do we observe differences in enzymatic behavior between the USPs, but we also observe differential effects of intra-molecular domains on the activity of the (minimal) catalytic domains in USP4, USP7 and USP16 (Figure 2B).

We recently showed that USP4 contains a UBL domain inserted in its catalytic domain⁵ (USP4CD; Figure 1A), which inhibits the activity of USP4CD (group 1; Figure 2B,D). The presence of this UBL domain in USP4CD increases the K_M and is therefore less active than the minimal catalytic domain USP4-D1D2⁷ (group 2; Figure 2D). In contrast, both k_{cat} and K_M are affected in USP7, where the minimal catalytic domain (group 1) shows far less activity than the full-length enzyme (group 3). Here, the activity of USP7 is modulated by its HUBL domain which is essential for both activity and Ub binding *in vitro* and *in vivo*^{17,25,27}. The activity of USP16CD is modulated by the zinc-finger Ub specific protease (ZnF-UBP). Surprisingly, the activity is enhanced by increasing catalytic turnover, rather than the K_M (Figure

2B,D). Since it is a Ub binding domain, the effect of the zinc-finger could be more prominent in poly-Ub processing²⁸, which might add up to a bigger difference than observed here. USP39CD also contains a ZnF-UBP domain, but it is unlikely that this will lead to enzymatic activation since USP39CD does not have the catalytic residues.

Overall, this shows that several intra-molecular domains are able to modulate USPs. The modulation can affect K_M (USP4), k_{cat} (USP16), or both (USP7), and both inhibitory and activating domains are found in USPs. Together, this creates an additional layer of regulation on the catalytic activity of USPs.

Some USPs show small preference for di-Ub topoisomers

Most studies of DUB specificity have focused on processing K48- and K63-linked poly-Ub. However, since the additional linkages serve equally important cellular functions, we synthesized all seven lysine-linked di-Ub topoisomers²² and we used them in a qualitative assay to assess all linkage preferences of the panel of USPs (Figure 3 and Supplemental Figure S2). In agreement with the kinetic parameters from the UbAMC assay, the USPs from group 1 showed very little activity; USP8CD from group 3 is the most active USP, and most USPs from group 2 show an intermediate activity. However, there were two clear changes. Where USP7 was amongst the most active USPs in the UbAMC assay, now it shows an intermediate activity. In contrast, USP21CD showed intermediate activity in the UbAMC assay, but is very active in the di-Ub assay and displays activities almost matching the most active USP; USP8CD.

The USP family seems to be rather promiscuous compared to other DUB families. For example, Cezanne²⁹ (K11), OTUB1^{30,31} (K48) and TRABID³² (K29) from the OTU family display strong linkage preferences for di-Ub topoisomers. However, figure 3 shows that the differential activity of the USPs is smaller. All the active USPs from this study hydrolyze all di-Ub topoisomers. Nevertheless, there are clear differences in efficiency. For instance, most USPs have difficulties in hydrolyzing K27- and, to a lesser extent, K29-linked di-Ub. For example, USP7 has limited activity towards hydrolyzing K27- and K29-linked di-Ub. In contrast, the K6, K11, K48 and K63 Ub topoisomers are hydro-

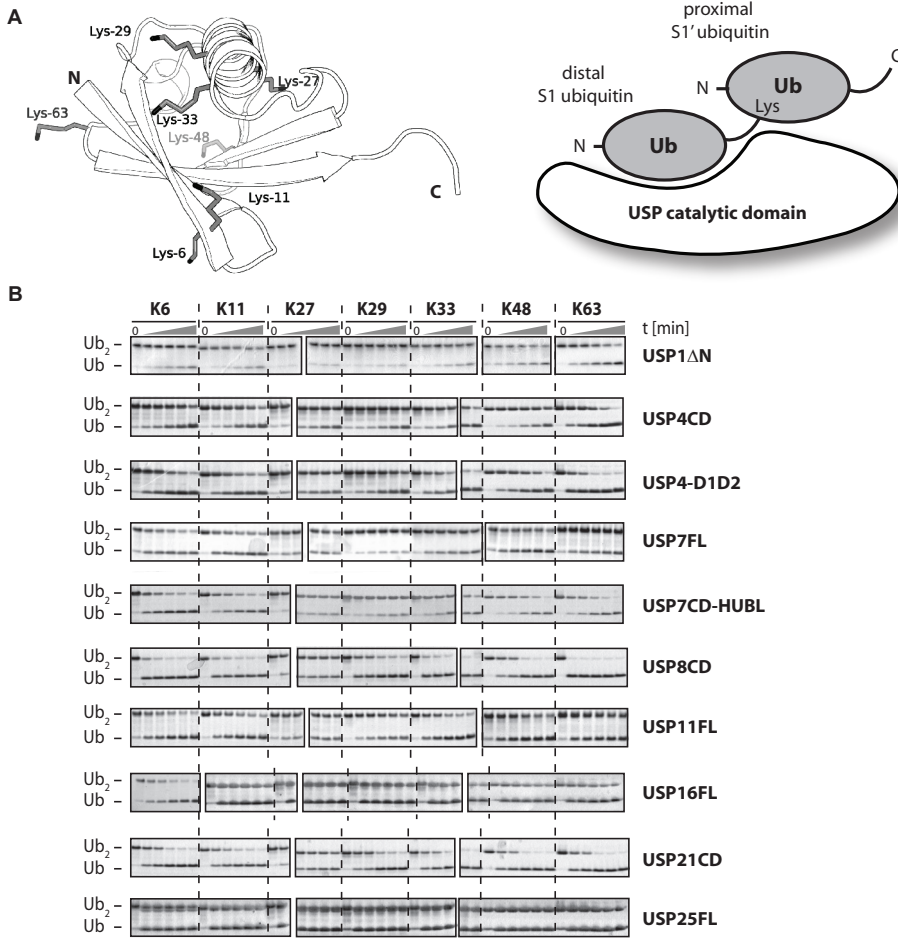


Figure 3. Di-Ub topoisomer preference for the different USPs. A) Ubiquitin (1UBQ) showing all lysines. B) Overview of a time-course using all seven different di-Ub topoisomers (5 μ M) (K6, K11, K27, K29, K33, K48 and K63) for the active USPs (75 nM). Samples from each time-point (0, 5, 10, 30, 60, 180 min) were analyzed on coomassie stained SDS-PAGE gels.

lyzed relatively efficiently. Another clear example is USP4, for which K63-linked di-Ub is a better substrate than K48-linked di-Ub^{7,33}. Apparently, some USPs seem to prefer specific di-Ub isoforms.

We wondered whether the intramolecular modulating domains in USP4, USP7 and USP16 change the linkage preferences. However, this does not seem to be the case. The different USPs respond differently to modulation by internal domains, analogous to what was observed with UbAMC (Figure 3 and Supplemental Figure S2 B,C). However, no change in linkage preference was seen between catalytic domain and longer constructs, showing that the modulation

effects are substrate independent mechanisms.

Overall, this shows that USPs can hydrolyze all Ub lysine-linked di-Ub topoisomers, but with differences in efficiency. Moreover, these differences are preserved in the presence of the intramolecular activity modulators.

In the case of USPs, isopeptide-linked Ub is not representative for di-Ub

To explain the Ub linkage preference, we might not need full-length di-Ub³⁴. To test this in an activity assay, we designed and synthesized a panel of fluorescence polarization-based (FP) di-Ub mimics. In

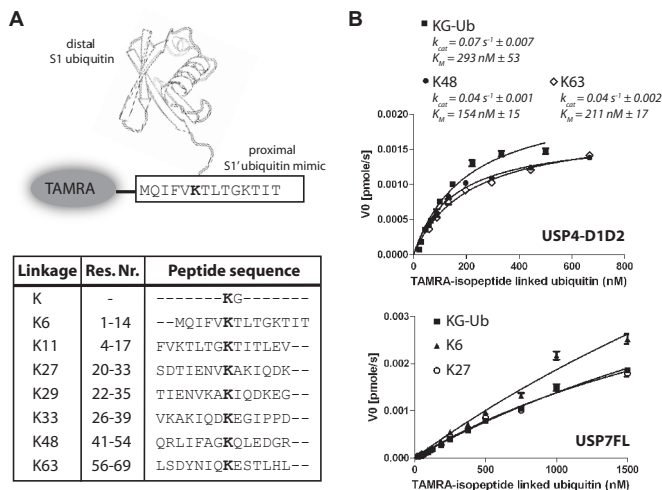


Figure 4. Kinetics of di-Ub hydrolysis. **A)** Schematic view of N-terminal TAMRA labeled ubiquitin peptide (K6) conjugated with ubiquitin. Table shows the peptide sequences used with the corresponding residue numbers for the different types of ubiquitin linkages. The conjugated lysine is highlighted in red. **B)** Michaelis-Menten curves for USP4-D1D2 (top) and USP7FL (bottom) were obtained using the TAMRA labeled ubiquitin peptides in a FP hydrolysis assay. The curves for USP7 could not be fitted.

these reagents, TAMRA-labeled Ub peptides were linked via an isopeptide linkage to the carboxy-terminus of wild-type full-length mono-Ub³⁵ (Figure 4A and Supplemental Figure S3J). Therefore, in contrast to the peptide linkage in UbAMC, these FP-reagents use the natural isopeptide linkage. The proximal Ub is represented by 14-mer peptides, each representing one of the seven lysines of Ub (Figure 3A and 4A, Table). In addition, the di-peptide (KG) was prepared to serve as a minimal substrate. Mass spectrometry and SDS-PAGE analysis of these new Ub substrates showed that the synthesis was successful for all eight different TAMRA labeled isopeptide-linked Ub FP-reagents (Supplemental Figure S3F).

As a proof of principle, we used the minimal 'KG' FP-reagent to determine the kinetic parameters of USP4-D1D2 (Figure 4B and Supplemental Figure S3H). With this reagent we determined K_M (293 nM) and k_{cat} (0.07 s^{-1}) values similar to the kinetic parameters obtained using UbAMC. Only the k_{cat} is higher, possibly due to the difference in the chemical nature of the linkage, since the FP-reagents contain a natural isopeptide linkage in contrast to the UbAMC reagent. However, since the K_M values are similar, both represent comparable Ub reagents.

In the di-Ub time course assay, we observed linkage preferences of USP4-D1D2 and USP7; e.g. USP7 prefers the hydrolysis of K6-over K27-linked di-Ub, and USP4-D1D2 prefers K63-over K48-linked di-Ub (Figure 3B). Although

difficult to fit for USP7, with our FP-reagents we observed no difference in activity for either USP4-D1D2 or USP7, and therefore could not recapitulate the preferences observed in the di-Ub assay (Figure 3B and Supplemental Figure S3G). This shows that these FP reagents do not contain the required information to mimic di-Ub for USPs (Figure 4C and Supplemental Figure S3).

The proximal Ub does not contribute, but rather hinders binding to USP7

Since the FP-reagents were not sufficient to reproduce the observed linkage preference, we used full-length di-Ubs to determine the kinetic parameters directly. We determined K_M and k_{cat} of the hydrolysis of all seven lysine linked di-Ubs by USP7, using initial rate experiments that monitored the appearance of mono-Ub (Figure 5). These experiments showed that the linkages that are efficiently hydrolyzed by USP7 (K6, K11, K33, K48 and K63) have similar kinetic behavior (Figure 5B). Interestingly, the K_M and k_{cat} values are similar to the minimal substrate UbAMC, which contains only a single Ub moiety. This suggests that there is no induced binding or catalysis effect by the proximal Ub moiety.

In the initial di-Ub assay, two linkages (K27 and K29) showed a clear delay in hydrolysis by USP7 (Figure 3). This was nicely reproduced in this kinetic di-Ub assay. Interestingly, there was hardly any change in k_{cat} , but rather the K_M increased far above the concentrations used in our assays. This suggests that the preference for the di-Ub topoisomers arises from steric hindrance, rather than an

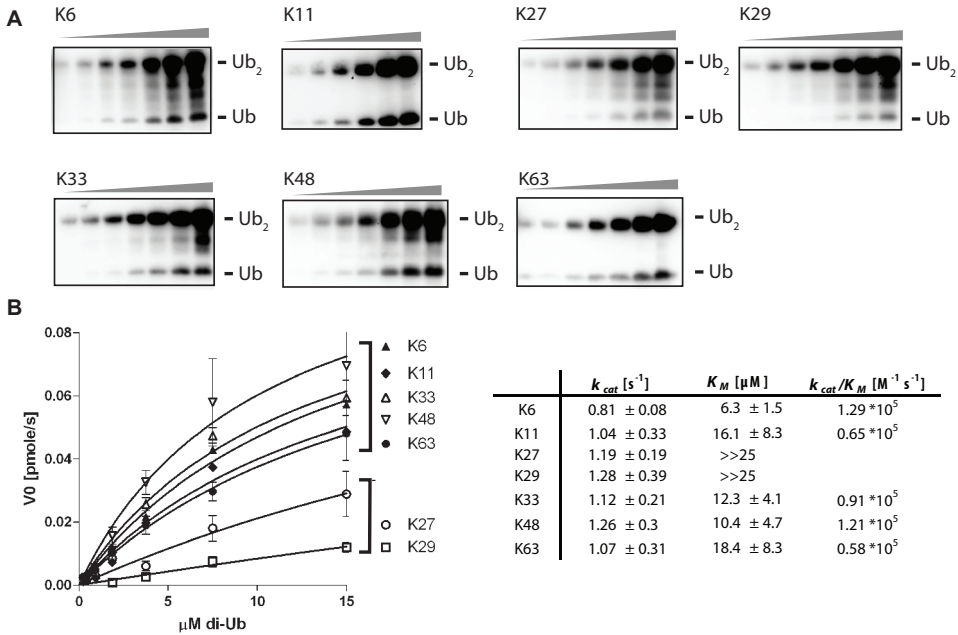


Figure 5. Michaelis-Menten kinetics of di-Ub hydrolysis by USP7. **A** Representative western-blot Michaelis-Menten analysis di-Ub hydrolysis USP7. Assay performed using 2-fold dilutions of the di-Ub starting at 15 μM for 5 minutes at 37 degrees. **B.** Michaelis-Menten analysis for USP7FL for di-ubiquitin hydrolysis. Initial rate (V_0) of di-Ub conversion into mono-Ub was determined at different substrate concentration from Western Blots shown in A. The conversion to mono-Ub was quantified using the di-Ub signal corrected for conversion. **C. and D.** Michaelis-Menten analysis of USP8/21CD (C) and USP11 (D).

additional binding site for the proximal Ub moiety. Therefore, the binding of some linkages to the catalytic domain is impaired, resulting in lower activity.

Intermolecular activation of USPs by UAF1 and GMPS only affects k_{cat}

Besides their intrinsic activity, some USPs are activated by intermolecular modulation. For example, USP1, USP12 and USP46 are activated by the WD40-repeat containing UAF1, and USP7 is activated by GMPS^{17,19-21}. Here, we used the UbAMC assay to quantify this activation (Figure 6A,B and Supplemental Figure S4). In agreement with previous data, we observe mainly a k_{cat} increase (7-fold) of USP1 ΔN activity in the presence of UAF1. The USP1 used in this work has a mutation in the self-cleavage site (Gly671,672Ala)²¹. UAF1 also activates USP12FL and USP46 ΔN , where the k_{cat} is increased by 66- and 70-fold, respectively. Also in the case of USP7 we observed a k_{cat} increase (5.5-fold) in the presence of its modulator GMPS. Interestingly, in contrast to variable modulation invoked by internal

domains (Figure 2D), intermolecular modulation is achieved mainly by an increase in the catalytic turnover rather than in substrate binding (Figure 6B).

To investigate whether this activation also induces new linkage preferences of these USPs, we repeated the di-Ub assay in the presence of UAF1 or GMPS (Figure 6C). As expected from the UbAMC kinetics, USP1 ΔN shows limited activity in the absence of UAF1, while USP12FL and USP46 ΔN show no activity. However, in the presence of UAF1, the activity of all three USPs is increased, albeit not to the same level. In complex with their activators, USP1 ΔN and USP7CD-HUBL show most activity, but no change in chain type preference by UAF1 or GMPS. This agrees well with an activation mechanism that only increases k_{cat} , but does not induce binding, which should translate in changing K_M values.

Discussion

In this study, we used chemical reagents to determine the kinetic parameters of substrate inde-

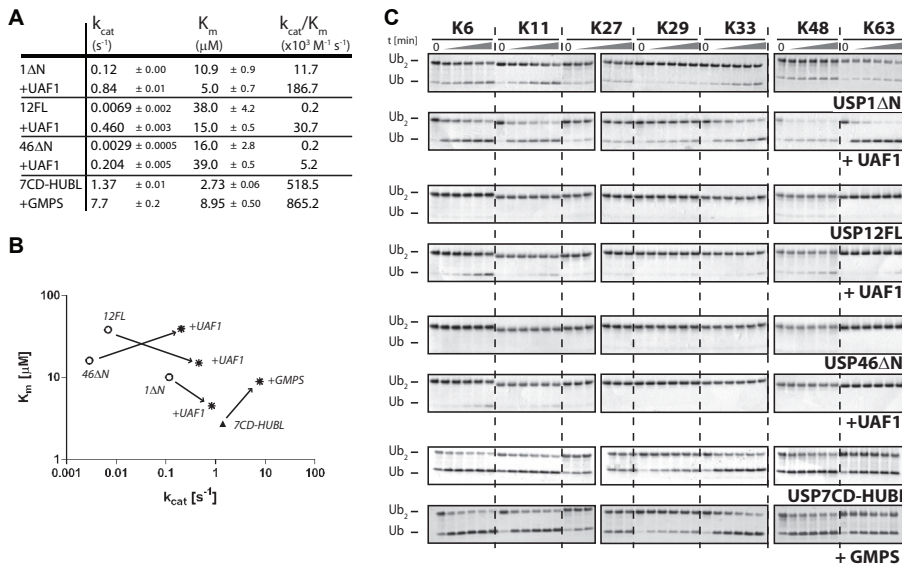


Figure 6. Intermolecular USP activity modulation is achieved by increasing k_{cat} . A) Kinetic parameters (k_{cat} , K_M and k_{cat}/K_M) using UbAMC as substrate for USP1 ΔN , USP12FL and USP46 ΔN in presence of UAF1 and USP7CD-HUBL in presence of GMPS. B) Alternative representation of the kinetic parameters comparing the USP activity between the USPs and in the presence of their modulator. C) Activity modulation by UAF1 and GMPS towards all seven di-Ub topoisomers. Samples from each time-point (0, 5, 10, 30, 60, 180 min) were analyzed on coomassie stained SDS-PAGE gels.

pendent activity of 12 USPs, their di-Ub linkage preference and characteristics of both intra- and intermolecular activity modulation. We observe large variations in both the catalytic turnover (k_{cat}) and Ub binding (K_M) between USPs, which can of the DUBs so far has been tested for all Ub linkages, some DUBs show remarkable specificity. For example the OTU protease DUBA⁴¹ is K63-specific, OTUB1^{30,31} is K48-specific, while AMSH⁴² a small preference for individual di-Ub topoisomers. We show that in USP7 there is no additional Ub binding site, but rather that the differences in hydrolysis of the topoisomers are achieved by hindering binding (K_M) sterically. The combined data provide insights in the variation in the biochemical behavior of the USP enzyme family.

Based on their specific catalytic efficiency (Figure 2), the USPs can be classified into three groups: (1) a group of USPs showing very low DUB activity, (2) an 'intermediate' group and (3) USPs that exhibit high activity. This variability in activity can be explained in several ways. First, the

activity can be affected by structural rearrangements in both Ub binding sites and active sites, as shown by structural studies^{11,12}. Secondly, intra-molecular domains of USPs can modulate the DUB activity, as seen here for USP4, USP7 and USP16. External modulator proteins can further regulate the activity of the USP by enhancing its activity, as seen for USP1, USP7, USP12 and USP46 (Figure 6A,B).

Here we report a few cases where intra-molecular modulators regulate the USP catalytic efficiency: either insertions within or additional domains outside the catalytic domain. For both USP7 and USP16 the enzymatic behavior is regulated by intra-molecular domains (the HUBL and ZnF-UBP domain, respectively) outside the catalytic domain, resulting in the increase of the activity. Additionally, variations in kinetics can be induced by (large) insertions in the catalytic domains themselves, as demonstrated for USP4, where a UBL containing insert is inhibiting the catalytic efficiency⁷. These variations and intra-molecular modulations result in the unique activity of each USP.

For the last decade, the focus on DUB specificity has been on K48- and K63-linked poly-Ub chains. However, different Ub linkage topoisomers

mers can result in different cellular fates, some of which are very specific³⁶⁻³⁸ and others requiring a minimal chain length to invoke its function^{39,40}. Our study presents the first complete and comprehensive study on di-Ub preference of all seven linkages for USP family members. Although none of the DUBs so far has been tested for all Ub linkages, some DUBs show remarkable specificity. For example the OTU protease DUBA⁴¹ is K63-specific, OTUB1^{30,31} is K48-specific, while AMSH⁴² and BRCC3⁴³ both from the JAMM/MPN+ family are K63-specific. Next to CYLD¹⁰, the USPs do not have strict chain-type specificity, but rather have preferences. Kinetic studies on USP7 showed us that there is no proximal S1' Ub binding site to induce Ub topoisomers preference, but rather the proximal Ub moiety induces steric constraints for binding to the USP in the case of K27 or K29 linkages. However, it is possible that linkage specificity is increased when using longer Ub chains.

Overall, the hydrolysis efficiency of the USPs towards K6-, K11-, K48- and K63-linked Ub was higher than for K27- and, to a lesser extent, K29- and K33-linked di-Ub. These residues localize in distinct regions on Ub (Figure 3A). The lysine residues involved in the easiest hydrolyzed linkages (K6, K11, K48 and K63) are in the β -sheet or loops. In contrast, the lysine residues of the more difficult linkages (K27, K29 and K33) are positioned on the other side of the Ub molecule, and are all in the α 1-helix. Additionally, K27 is barely accessible, which possibly induces a steric constraint, resulting in the lower activity. This interesting bi-polar behavior needs future investigation.

Previous studies suggested that Ub-peptide reagents were sufficient to mimic di-Ub and discriminate between topoisomers in binding³⁴. However, in our activity assays with the FP Ub-peptide reagents, we observed no difference between Ub linkages. This suggests that the peptides do not contain enough information to mimic the proximal Ub for the USPs. Nevertheless, they may be sufficient for DUBs from families with more pronounced Ub specificity and be useful tools in those cases. In addition, the 'KG' FP-reagent might prove a good alternative for UbAMC, as the kinetic parameters are similar, while it contains the natural isopeptide linkage, which is not present in UbAMC.

This study confirmed that two known intermolecular USP activity modulators UAF1 and

GMPS activate USP1, USP12, USP46, and USP7 respectively. This activation is mainly by increasing the k_{cat} . However, the biological roles of the UAF1 and GMPS activation are distinct. UAF1 activation is almost essential for USP activity of USP1, USP12 and USP46. This resembles the Ubp8 activation by Sgf11^{14,15}. Surprisingly, USP12 in complex with UAF1 is still not very active, possibly requiring additional partners, like WDR20⁴⁴. In a different manner, GMPS hyper-activates USP7, by allosterically stabilizing the active state of the enzyme induced by the HUBL domain¹⁷. Besides a general activation, the GMPS activity modulation most likely has additional substrate specific roles, as it induces H2B de-ubiquitination.

Although the function of an increasing number of USPs is elucidated, they still represent a relatively uncharacterized enzyme family. To aid in the biochemical understanding of these enzymes, we here report the large variations in kinetics and intra-molecular modulation (k_{cat} and K_M), the modest but surprising differential activity towards the seven di-Ub topoisomers (K_M), and a characterization of the activation by intermolecular interactions (k_{cat}).

Significance

Ubiquitination is a dynamic process, which is involved in numerous key cellular processes. The removal of the Ub molecules is an integral part of this process, and is carried out by Deubiquitinating enzymes (DUBs). These are increasingly recognized as interesting drug targets. However, to date we lack the markers to predict the biochemical behavior based on sequence alignments and therefore a need exists for comprehensive kinetic studies. This is where chemical tools that allow fast and accurate read-outs will contribute to answer these biological questions. In this study, we designed and produced several of such chemical reagents to determine the kinetics and di-Ub linkage preferences of twelve USPs. Despite the homologous catalytic domain, the kinetic data underline the large variability within the USP family, and the intra- and intermolecular activity modulators create an additional layer of regulation.

In addition this study for the first time reports the linkage preference of twelve USPs against all seven-lysine linked di-Ubs. Kinetic analysis of the hydrolysis of the di-Ub topoisomers, suggest

that within the USP family the preferences are induced by steric hindrance, rather than the induced binding, as seen in other DUB families.

Together, this data provides insight in the biochemical behaviour in the USP family, and validates the chemical tools that now also can be applied in characterizing other DUB families.

Material and Methods

General

General reagents were obtained from Sigma Aldrich, Fluka and Acros and used as received. Solvents were purchased from Biosolve or Aldrich. Peptide synthesis reagents were purchased from Novabiochem. USP25 cDNA was provided by Erik Meulmeester and Frauke Melchior.

General plasmids and proteins

Di-Ub moieties were produced as previously described²². USP4CD (aa 296-954), USP4-D1D2 (aa 296-490/766-932), USP8CD (aa 776-1110), USP11FL (aa 1-920), USP16FL (aa 1-823), USP16CD (aa 193-823), USP21CD (aa 211-565), USP30CD (aa 65-500), USP39CD (aa 222-565) and USP46ΔN (aa 8-366) are cloned into the pETNKI-LIC vector for expression in bacteria as described²³. USP1ΔN (aa 21-785 self-cleavage site glycine 671 and 672 are mutated to alanine), USP7FL (aa 1-1102), USP12FL (aa 1-355) and STREPTEV-UAF1 (6-677) are cloned into the pFastBac-HTb vector for expression in insect cells. Both USP7CD-HUBL (aa 208-1102) and USP7CD (aa 208-560) are cloned into the pGEX vector¹⁷ and USP25FL is cloned in the pET11a vector⁴⁵. Codon optimized full length USP7 and GMPS cDNA was obtained from DomainEx (Cambridge, UK). Both were amplified by PCR and subcloned (SpeI/NotI) into a pFastBac vector (Invitrogen) containing an N-terminal GST tag (BamHI/SpeI) and Precision Protease cleavage site. cDNA for USP11 and USP16 were obtained from ImaGenes (Berlin, Germany).

Protein expression and purification

As specified in figure 1, the USPs were expressed in both *E.coli* and insect cells and purified as described^{17,23}. GMPS was expressed and purified as before¹⁷. USP constructs and GMPS cloned both in bacterial and baculovirus expression vector are expressed and purified as described^{17,23}. Depending

on the type of vector, the tag was removed with either TEV or the HRV 3C protease. Bacmids were prepared following the manufacturer's guidelines. USP1, USP12 and UAF1 were produced using *Sf9* and *Sf21* insect cell expression. Infection was done using a low-MOI infection protocol⁴⁶. The cells were harvested 72 hours after a baculovirus induced growth arrest was observed. USP46 was produced in *E.coli*. USP1, 12, 46 and UAF1 were purified using Ni²⁺ sepharose (GE Healthcare) in 20 mM Hepes (pH 7.5), 150 mM NaCl, 0.1 mM PMSE, and 0.1 mM DTT followed by elution using imidazole. His-tag was removed by overnight cleavage with TEV protease whilst dialyzing to remove imidazole. Uncleaved product was removed with Ni²⁺ sepharose. Size exclusion chromatography was performed using a Superdex 200 or 75 column (GE Healthcare), equilibrated against buffer containing 10 mM Hepes [pH 7.5], 100 mM NaCl and 1 mM DTT. All proteins were concentrated to ~10 mg/ml and stored at -80°C.

UbAMC assay

Kinetics were determined as described before⁷. UAF1 and GMPS were added in a 1:1 stoichiometry. USP concentration varied between 1 and 100 nM, depending on relative activity. In order to calculate the kinetic parameters for the hydrolysis of UbAMC, curves obtained by plotting the measured enzyme initial rates (v) versus the corresponding substrate concentrations ($[S]$). These were subjected to nonlinear regression fit using the Michaelis-Menten equation $V = (V_{\max} \cdot [S]) / ([S] + K_M)$ (eqn 1), where V_{\max} is the maximal velocity at saturating substrate concentrations and K_M the Michaelis constant. The k_{cat} value was derived from the equation $k_{\text{cat}} = V_{\max} / [E_0]$ (eqn 2) where $[E_0]$ is the total enzyme concentration. Experimental data was processed using Prism 5.01 (GraphPad Software, Inc.).

Di-Ub assay

Di-Ub hydrolysis reactions were performed at 37°C in 50 mM Hepes buffer at pH 7.5, with 100 mM NaCl, 1 mM EDTA, 5 mM dithiothreitol and 0.05% (w/v) Tween-20 with constant enzyme concentration (75 nM). When indicated UAF1 was added in a 2-fold excess (150 nM) and GMPS in a 1:1 stoichiometry. Reactions were stopped by addition of SDS loading buffer and followed by SDS-PAGE analysis. For the kinetic analysis, the reaction mixture was pre-heated to 37 °C degrees before

adding USP7. Samples were run on a 12% Bis-Tris NuPage gel (duplicates on one gel), and western blots were performed with anti-Ub antibody (Santa Cruz; P4D1). The ChemiDoc system (Biorad) was used to read the chemiluminescence signal and subsequent quantification of mono-Ub was done using the quantification tools of ImageLab (Biorad) using the non-saturated di-Ub signal (corrected for conversion to mono-Ub). Experimental data was processed using Prism 5.01 (GraphPad Software, Inc.).

Solid Phase Peptide Synthesis (SPPS) of the TAMRA thiolysine peptides

SPPS was performed on a Syro II MultiSyntech Automated Peptide synthesizer using standard 9-fluorenylmethoxycarbonyl (Fmoc) based solid phase peptide chemistry at 25 μmol scale, using fourfold excess of amino acids relative to pre-loaded Fmoc amino acid Wang type resin (0.2 mmol/g, Applied Biosystems). The following protected amino acids were used during Ub peptide synthesis: Fmoc-L-Ala-OH, Fmoc-L-Arg- (Pbf)-OH, Fmoc-L-Asn (Trt)-OH, Fmoc-L-Asp (OtBu)-OH, Fmoc-L-Gln (Trt)-OH, Fmoc-L-Glu (OtBu)-OH, Fmoc-Gly-OH, Fmoc-L-His (Trt)-OH, Fmoc-L-Ile-OH, Fmoc-L-Leu-OH, Fmoc-L-Lys (Boc)-OH, Fmoc-L-Met-OH; Fmoc-L-Phe-OH; Fmoc-L-Pro-OH; Fmoc-L-Ser (tBu)-OH; Fmoc-L-Thr (tBu)-OH, Fmoc-L-Tyr (tBu)-OH, Fmoc-L-Val-OH. Fmoc-5S-(methylthioethyl)- (L)-Lys (Boc)-OH was synthesized as described previously²².

The coupling procedure starts off with single couplings in N-methylpyrrolidone (NMP) for 45 min using PyBOP (4 equiv) and DiPEA (12 equiv) in a total volume of 750 μL . Followed by the removal of Fmoc with 20% piperidine in NMP for 2 \times 2 and 1 \times 5 min. Finally the procedure ends with NMP wash steps after each coupling (3 \times) and deprotection (5 \times).

The resin was washed with diethylether and dried under high vacuum. Next, the polypeptide sequence was detached from the resin and deprotected by treatment with TFA/H₂O/Phenol/iPr₃SiH 90.5/5/2.5/2 v/v/v/v for 2.5 h. After washing the resin with 3 \times 1 mL TFA, the crude protein was precipitated with cold Et₂O/*n*-pentane 3:1 v/v. The precipitated protein was washed 3 \times with diethylether, the pellet was dissolved in a mixture of H₂O/CH₃CN/HOAc (65/25/10 v/v/v) and finally lyo-

philized. All peptides were analyzed by LC-MS and purified by RP-HPLC when necessary.

LC-MS

LC-MS measurements were performed on a Waters 2795 Separation Module (Alliance HT), equipped with a Waters 2996 Photodiode Array Detector (190-750nm), Phenomenex Kinetex C18 column (2.1 \times 50, 2.6 μm) and LCTM Orthogonal Acceleration Time of Flight Mass Spectrometer. Samples were run using two mobile phases: A = 0.1% formic acid in water and B = 0.1% formic acid in acetonitrile. Flow rate = 0.8 mL/min, runtime = 6 min, column T = 40 °C. Gradient: 0 - 0.5 min: 5% B; 0.5 - 4 min: 5% to 95% B; 4 - 5.5 min: 95% B. Data processing was performed using Waters MassLynx Mass Spectrometry Software 4.1 (deconvolution with Maxent1 function).

Ligation of Ub to the peptides followed by desulphurization

Schematic overview of reaction scheme and final yields can be found in Supplemental Figure S3. A mixture of 4-mercaptophenylacetic acid (MPAA, 100 mM) and TCEP (50 mM) in 6M Guanidinium $\cdot\text{HCl}$ (1 mL, pH 7) was added to Ub-MesNa thioester (5 mg, prepared according to the procedure described previously²²). To this the TAMRA thiolysine peptide (100 μL of a 20 mM stock solution in DMSO) was added and the whole mixture was incubated at 37 °C. After overnight incubation, all low-molecular weight material was removed using a 3 kDa cutoff spin-column (Amicon Ultra) in four centrifuge cycles. The crude material was taken up in 6M Guanidinium $\cdot\text{HCl}$, 0.1M sodium phosphate (4 mL, pH 6.5) and to this was added TCEP (187 mg) and glutathione (30 mg), after which the pH of the mixture was adjusted to pH 6.5 by addition of 1M NaOH. Next, the mixture was degassed with argon, after which radical initiator VA-044 was added. The mixture was incubated at 37 °C overnight. All constructs were purified by RP-HPLC and analyzed by LC-MS and gel electrophoresis and were obtained as purple solids.

C18 RP-HPLC

Purification by RP-HPLC was performed on a Shimadzu system equipped with a LC-20AT liquid chromatography pump, CTO-20A column oven (T = 40 °C), SPD-20A UV/VIS detector (detection simultaneously at 230 nm and 254 nm), RF-

10AXL fluorescence detector ($ex/em = 540/600$ nm) and an Atlantis Prep T3 column (10×150 mm, $5 \mu\text{m}$). Samples were run using two mobile phases: A = 0.05% trifluoroacetic acid in water and B = 0.05% trifluoroacetic acid in acetonitrile. Flow rate 10AXL fluorescence detector ($ex/em = 540/600$ nm) and an Atlantis Prep T3 column (10×150 mm, $5 \mu\text{m}$). Samples were run using two mobile phases: A = 0.05% trifluoroacetic acid in water and B = 0.05% trifluoroacetic acid in acetonitrile. Flow rate = 7.5 mL/min, runtime = 30 min. Gradient: 0 – 6 min: 5% to 10% B; 6.5 – 26 min: 25% to 47% B; 26.5 – 29.5 min: 95% B. Pure fractions were pooled and lyophilized.

Isopeptide linked Ub FP hydrolysis assay

FP assays were performed on a PerkinElmer Wallac EnVision 2100 Multilabel Reader with a 531 nm excitation filter and two 579 nm emission filters. The confocal optics were adjusted with TAMRA-KG (synthesized by SPPS as described above) and the G factor was determined using a polarization value for TAMRA-KG (25 nM) of 50 mP. The assays were performed in “non binding surface flat bottom low flange” black 384-well plates (Corning) at room temperature in a buffer containing 20 mM Tris-HCl, pH 7.5, 5 mM DTT, 100 mM NaCl, 1 mg/mL 3-[3-cholamidopropyl] dimethylammonio] propanesulfonic acid (CHAPS) and 0.5 mg/mL bovine gamma globulin (BGG). Each well had a volume of 20 μL . Buffer and enzyme were pre-dispensed and the reaction was started by the addition of substrate. Kinetic data was collected in intervals of 2.5 or 3 min. From the obtained polarization values (P) the amount of processed substrate (P_t) was calculated with to the following equation⁴⁷: $S = S_0 - S_0 \cdot ((P_t - P_{min}) / (P_{max} - P_{min}))$, where P_t is the polarization measured (in mP); P_{max} is the polarization of 100% unprocessed substrate (determined for every reagent at all used substrate concentrations); P_{min} is the polarization of 100% processed substrate (determined for every linkage at all used substrate concentrations by measuring the mP value for the corresponding deubiquitinated TAMRA-peptide, which were synthesized by SPPS according to the procedure describes above); S_0 is the amount of substrate added to the reaction. From the obtained P_t values the values for initial velocities were calculated, which were used to determine the Michaelis-Menten constants. All experimental data was processed using Ms Excel and Prism 4.03 (GraphPad

Software, Inc.).

Acknowledgements

We thank Martin A. Cohn and Alan D’Andrea for USP1, USP12, USP46 and UAF1 ccDNA, Annette Dirac and Rene Bernards for USP4 and USP8 cDNA, Elisabetta Citterio for USP21 and USP39 cDNA, Carlos Lopex-Otin for USP30 cDNA and Erik Meulmeester and Frauke Melchior for USP25 cDNA. We thank Ovaa and Sixma group members for discussion, sharing reagents and critical reading of the manuscript. This work has been supported by grants from the Dutch Cancer Society, The Netherlands Organization for Scientific Research VIDI grant, and EU-Rubicon and NWO-CW ECHO 700.59.009 and KWF-2008-4014

Author contributions

USP expression and purification was performed by M.P.A.L.V. with assistance from W.J.v.D; enzyme assays were designed and analyzed by A.C.F. and executed by M.P.A.L.V and A.C.F.; USP1, 12, 46 and UAF1 were expressed, purified and analyzed by M.C.; UbAMC was designed and synthesized by R.M.; di-Ubs were designed by F.E. and H.O. and synthesized by D.S.H.; FP reagents were designed by F.E., P.P.G. and H.O. and synthesized by P.P.G. and F.E.; FP reagent assays were performed by P.P.G.; H.O. supervised all synthesis efforts and FP experiments; T.K.S. designed and supervised USP project; Data analysis and manuscript writing by A.C.F. with M.P.A.L.V. and T.K.S..

References

1. Hochstrasser, M. Origin and function of ubiquitin-like proteins. *Nature* **458**, 422-9 (2009).
2. Pickart, C.M. Back to the future with ubiquitin. *Cell* **116**, 181-90 (2004).
3. Nijman, S.M. et al. A genomic and functional inventory of deubiquitinating enzymes. *Cell* **123**, 773-86 (2005).
4. Komander, D., Clague, M.J. & Urbe, S. Breaking the chains: structure and function of the deubiquitinases. *Nat Rev Mol Cell Biol* **10**, 550-63 (2009).
5. Zhu, X., Menard, R. & Sulea, T. High incidence of ubiquitin-like domains in human ubiquitin-specific proteases. *Proteins* **69**, 1-7 (2007).
6. Ye, Y., Scheel, H., Hofmann, K. & Komander, D. Dissection of USP catalytic domains reveals five common insertion points. *Mol Biosyst* **5**, 1797-808 (2009).
7. Luna-Vargas, M.P. et al. Ubiquitin-specific protease 4 is inhibited by its ubiquitin-like domain. *EMBO Rep* (2011).
8. Reyes-Turcu, F.E., Shanks, J.R., Komander, D. & Wilkinson, K.D. Recognition of polyubiquitin isoforms by the multiple ubiquitin binding modules of isopeptidase T. *J Biol Chem* **283**, 19581-92 (2008).
9. Borodovsky, A. et al. A novel active site-directed probe specific for deubiquitylating enzymes reveals proteasome association of USP14. *Embo J* **20**, 5187-96 (2001).
10. Komander, D. et al. The structure of the CYLD USP domain explains its specificity for Lys63-linked polyubiquitin and reveals a B box module. *Mol Cell* **29**, 451-64 (2008).
11. Avvakumov, G.V. et al. Amino-terminal dimerization, NRDP1-rhodanese interaction, and inhibited catalytic domain conformation of the ubiquitin-specific protease 8 (USP8). *J Biol Chem* **281**, 38061-70 (2006).
12. Hu, M. et al. Crystal structure of a UBP-family deubiquitinating enzyme in isolation and in complex with ubiquitin aldehyde. *Cell* **111**, 1041-54 (2002).
13. Hu, M. et al. Structure and mechanisms of the proteasome-associated deubiquitinating enzyme USP14. *Embo J* **24**, 3747-56 (2005).
14. Kohler, A., Zimmerman, E., Schneider, M., Hurt, E. & Zheng, N. Structural basis for assembly and activation of the heterotetrameric SAGA histone H2B deubiquitinase module. *Cell* **141**, 606-17 (2010).
15. Samara, N.L. et al. Structural insights into the assembly and function of the SAGA deubiquitinating module. *Science* **328**, 1025-9 (2010).
16. Sowa, M.E., Bennett, E.J., Gygi, S.P. & Harper, J.W. Defining the human deubiquitinating enzyme interaction landscape. *Cell* **138**, 389-403 (2009).
17. Faesen, A.C.e.a. *Accepted for publication on Mol. Cell* (2011).
18. Sarkari, F. et al. EBNA1-mediated recruitment of a histone H2B deubiquitylating complex to the Epstein-Barr virus latent origin of DNA replication. *PLoS Pathog* **5**, e1000624 (2009).
19. van der Knaap, J.A. et al. GMP synthetase stimulates histone H2B deubiquitylation by the epigenetic silencer USP7. *Mol Cell* **17**, 695-707 (2005).
20. Cohn, M.A., Kee, Y., Haas, W., Gygi, S.P. & D'Andrea, A.D. UAF1 is a subunit of multiple deubiquitinating enzyme complexes. *J Biol Chem* **284**, 5343-51 (2009).
21. Cohn, M.A. et al. A UAF1-containing multisubunit protein complex regulates the Fanconi anemia pathway. *Mol Cell* **28**, 786-97 (2007).
22. El Oualid, F. et al. Chemical synthesis of ubiquitin, ubiquitin-based probes, and diubiquitin. *Angew Chem Int Ed Engl* **49**, 10149-53 (2010).
23. Luna-Vargas, M.P. et al. Enabling High-Throughput Ligation-Independent Cloning and Protein Expression for the Family of Ubiquitin Specific Proteases. *J Struct Biol* (2011).
24. Dang, L.C., Melandri, F.D. & Stein, R.L. Kinetic and mechanistic studies on the hydrolysis of ubiquitin C-terminal 7-amido-4-methylcoumarin by deubiquitinating enzymes. *Biochemistry* **37**, 1868-79 (1998).
25. Fernandez-Montalvan, A. et al. Biochemical characterization of USP7 re-

- veals post-translational modification sites and structural requirements for substrate processing and subcellular localization. *Febs J* **274**, 4256-70 (2007).
26. van Leuken, R.J., Luna-Vargas, M.P., Sixma, T.K., Wolthuis, R.M. & Medema, R.H. Usp39 is essential for mitotic spindle checkpoint integrity and controls mRNA-levels of aurora B. *Cell Cycle* **7**, 2710-9 (2008).
27. Ma, J. et al. C-terminal region of USP7/HAUSP is critical for deubiquitination activity and contains a second mdm2/p53 binding site. *Arch Biochem Biophys* **503**, 207-12 (2010).
28. Pai, M.T. et al. Solution structure of the Ubp-M BUZ domain, a highly specific protein module that recognizes the C-terminal tail of free ubiquitin. *J Mol Biol* **370**, 290-302 (2007).
29. Bremm, A., Freund, S.M. & Komander, D. Lys11-linked ubiquitin chains adopt compact conformations and are preferentially hydrolyzed by the deubiquitinase Cezanne. *Nat Struct Mol Biol* **17**, 939-47 (2010).
30. Edelmann, M.J. et al. Structural basis and specificity of human otubain 1-mediated deubiquitination. *Biochem J* **418**, 379-90 (2009).
31. Wang, T. et al. Evidence for bidentate substrate binding as the basis for the K48 linkage specificity of otubain 1. *J Mol Biol* **386**, 1011-23 (2009).
32. Virdee, S., Ye, Y., Nguyen, D.P., Komander, D. & Chin, J.W. Engineered diubiquitin synthesis reveals Lys29-isopeptide specificity of an OTU deubiquitinase. *Nat Chem Biol* **6**, 750-7 (2010).
33. Song, E.J. et al. The Prp19 complex and the Usp4Sart3 deubiquitinating enzyme control reversible ubiquitination at the spliceosome. *Genes Dev* **24**, 1434-47 (2010).
34. Shanmugham, A. et al. Nonhydrolyzable ubiquitin-isopeptide isosteres as deubiquitinating enzyme probes. *J Am Chem Soc* **132**, 8834-5 (2010).
35. Tirat, A. et al. Synthesis and characterization of fluorescent ubiquitin derivatives as highly sensitive substrates for the deubiquitinating enzymes UCH-L3 and USP-2. *Anal Biochem* **343**, 244-55 (2005).
36. Jin, L., Williamson, A., Banerjee, S., Philipp, I. & Rape, M. Mechanism of ubiquitin-chain formation by the human anaphase-promoting complex. *Cell* **133**, 653-65 (2008).
37. Matsumoto, M.L. et al. K11-linked polyubiquitination in cell cycle control revealed by a K11 linkage-specific antibody. *Mol Cell* **39**, 477-84 (2010).
38. Wu, T. et al. UBE2S drives elongation of K11-linked ubiquitin chains by the anaphase-promoting complex. *Proc Natl Acad Sci U S A* **107**, 1355-60.
39. Cook, W.J., Jeffrey, L.C., Kasperek, E. & Pickart, C.M. Structure of tetraubiquitin shows how multiubiquitin chains can be formed. *J Mol Biol* **236**, 601-9 (1994).
40. Thrower, J.S., Hoffman, L., Rechsteiner, M. & Pickart, C.M. Recognition of the polyubiquitin proteolytic signal. *Embo J* **19**, 94-102 (2000).
41. Kayagaki, N. et al. DUBA: a deubiquitinase that regulates type I interferon production. *Science* **318**, 1628-32 (2007).
42. McCullough, J., Clague, M.J. & Urbe, S. AMSH is an endosome-associated ubiquitin isopeptidase. *J Cell Biol* **166**, 487-92 (2004).
43. Cooper, E.M. et al. K63-specific deubiquitination by two JAMM/MPN+ complexes: BRISC-associated Brcc36 and proteasomal Poh1. *Embo J* **28**, 621-31 (2009).
44. Kee, Y. et al. WDR20 regulates activity of the USP12 x UAF1 deubiquitinating enzyme complex. *J Biol Chem* **285**, 11252-7 (2010).
45. Meulmeester, E., Kunze, M., Hsiao, H.H., Urlaub, H. & Melchior, F. Mechanism and consequences for paralog-specific sumoylation of ubiquitin-specific protease 25. *Mol Cell* **30**, 610-9 (2008).
46. Fitzgerald, D.J. et al. Protein complex expression by using multigene baculoviral vectors. *Nat Methods* **3**, 1021-32 (2006).
47. Levine, L.M., Michener, M.L., Toth, M.V. & Holwerda, B.C. Measurement of specific protease activity utilizing fluorescence polarization. *Anal Biochem* **247**, 83-8 (1997).

Table of contents Supplementary information

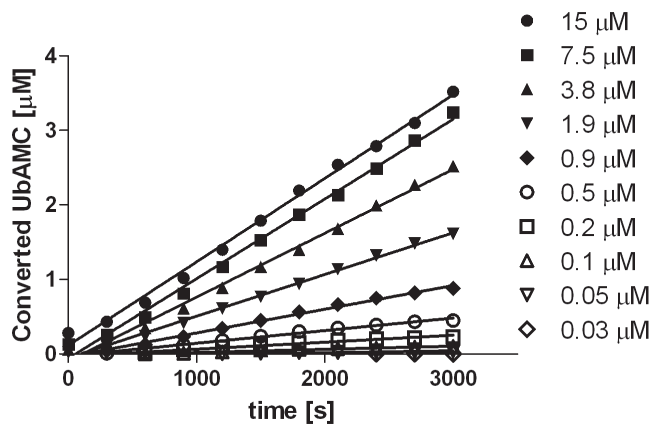
Table S1	Comparison with published UbAMC kinetics	82
Figure S1	Exemplary raw data UbAMC assay. <i>Related to Figure 2.</i>	82
Figure S2	Di-Ub assay for inactive USPs and comparison USP7CD versus USP7CD-HUBL. <i>Related to Figure 3.</i>	83
Figure S3	Synthesis, LC-MS spectra of FP-reagents, exemplary raw data and Michaelis-Menten curves of USP4 and USP7. <i>Related to Figure 4.</i>	84
Figure S4	Curves of the Michaelis-Menten analysis of the UAF1 and GMPS modulation. <i>Related to Figure 6.</i>	86

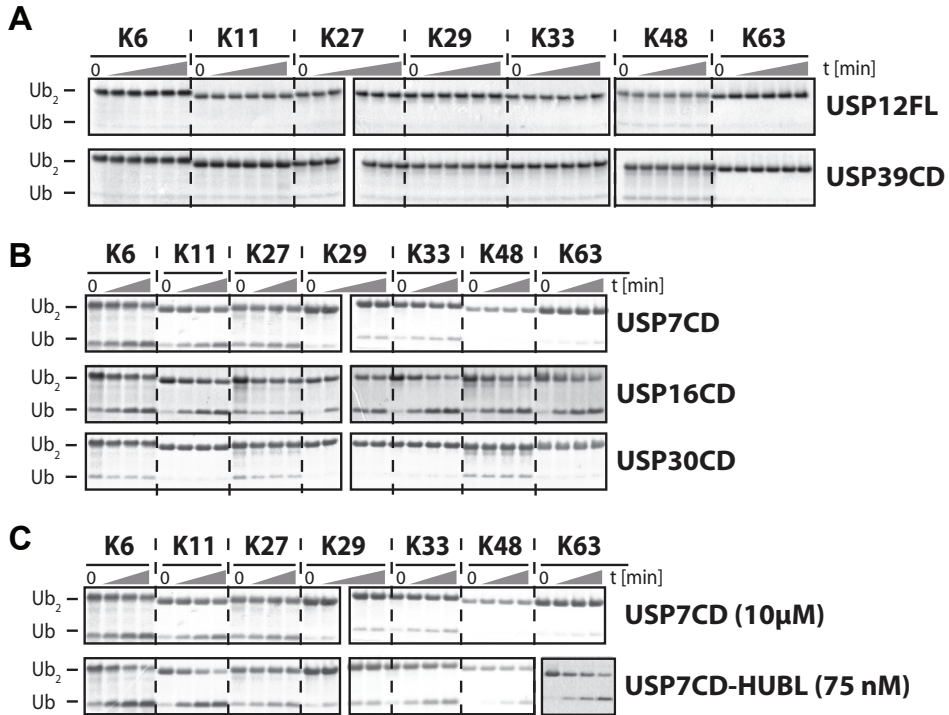
	k_{cat} [s^{-1}]	K_M [μM]	k_{cat}/K_M [$\times 10^3 M^{-1} s^{-1}$]	Reference
USP1FL	0.014	1.4	10.2	Cohn et al. (2007)
USP1FL+UAF1	0.26	0.7	371	Cohn et al. (2007)
Ubp8/SAGA	0.17	1.5	110	Samara et al. (2011)
USP2CD	0.62	2.5	250	Zhang et al. (2011)
USP2CD	0.14	0.55	252	Renatus et al. (2006)
USP7FL	3.56	17.5	203	Fernandez-Montalvan et al. (2007)
USP7CD	0.077	44.2	1.7	Fernandez-Montalvan et al. (2007)
USP7CD-HUBL	0.805	22.8	35	Fernandez-Montalvan et al. (2007)
USP8CD	2.4	10.2	235	Avvakumov et al. (2006)
USP21CD	0.041	0.26	158	Ye et al. (2011)
USP25FL	0.12	5	24	Meulmeester et al. (2008)

Supplemental Table S1. Related to Figure 1. Comparison with published UbAMC kinetics.

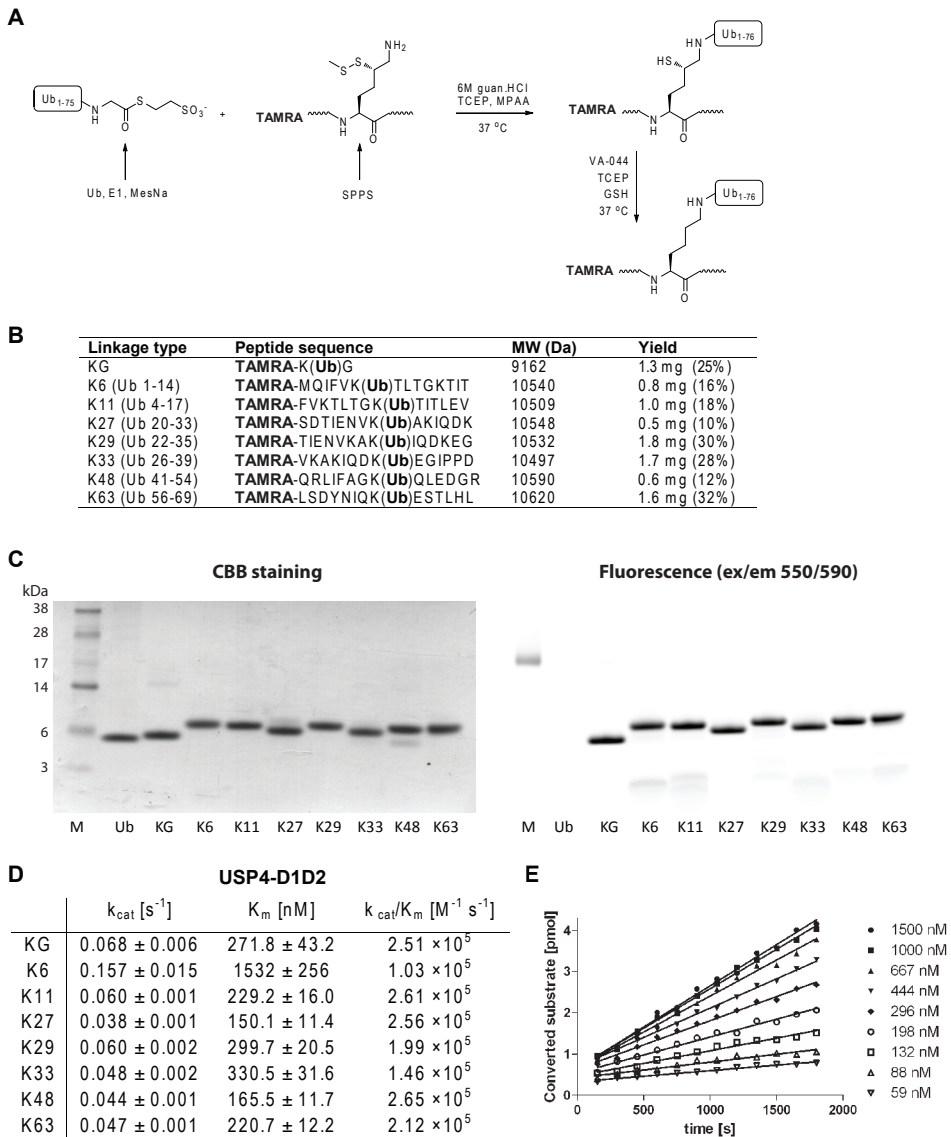
4

Supplemental Figure S1. Related to Figure 2. Exemplary raw data of UbAMC hydrolysis by USP7CD-HUBL. Measurements were done using a five minute interval. The signal was stable for at least one hour.





Supplemental Figure S2. Related to Figure 3. Di-Ub assay for inactive USPs and comparison USP7CD versus USP7CD-HUBL. A and B Di-Ub assay for USP12FL, USP39CD, USP46FL, USP7CD, USP16CD and USP30CD. Time-course using all di-Ub topoisomers (5 μM) (Linear, K6, K11, K27, K29, K33, K48 and K63) for USPs (75 nM). Samples from each time-point (0, 5, 10, 30, 60, 180 min) (A) and (0, 10, 30, 60 min) (B) were analyzed on coomassie stained SDS-PAGE gels. **C** Di-Ub assay USP7CD versus USP7CD-HUBL. Time-course using all di-Ub topoisomers (5 μM) (Linear, K6, K11, K27, K29, K33, K48 and K63) for USP7 constructs (10 μM and 75 nM). Samples from each time-point (0, 10, 30, 60 min) were analyzed on coomassie stained SDS-PAGE gels.



Supplemental Figure S3. Related to Figure 4. Synthesis, LC-MS of FP reagents, exemplary raw data and Michaelis-Menten curves of USP4 and USP7. A. Ligation of Ub to the peptides. **B.** Peptide sequence, molecular weight and typical yield of the reaction. **C.** Coomassie staining and fluorescence scan of SDS electrophoresis analysis of the FP-reagent. **D.** Kinetic parameters of USP4-D1D2 using the FP-reagents. **E.** Exemplary data of hydrolysis of FP reagents.

Figure and legend continue on next page

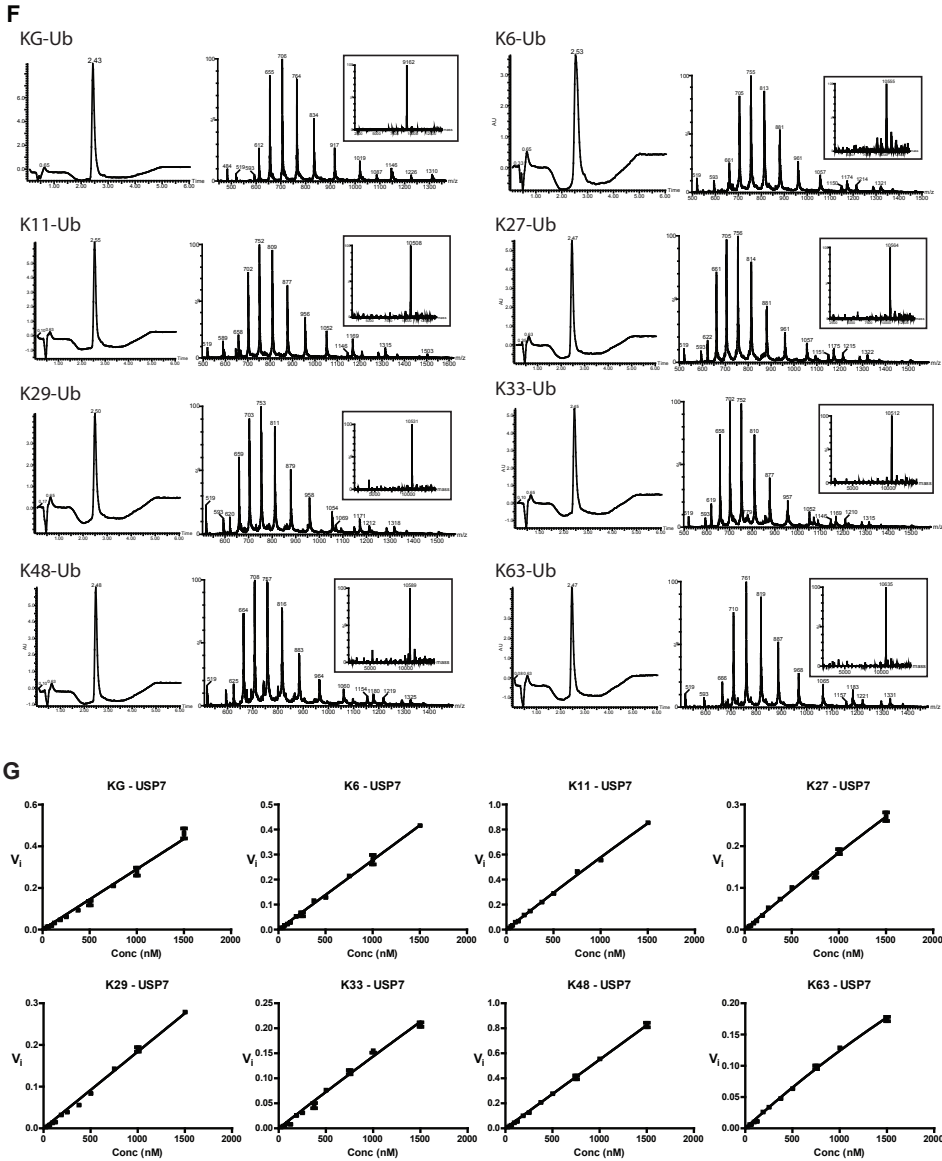


Figure and legend continued from previous page.

Supplemental Figure S3. Related to Figure 4. Synthesis, LC-MS of FP reagents, exemplary raw data and Michaelis-Menten curves of USP4 and USP7. F. LC-MS spectra of the FP-reagents. G. Michaelis-Menten analysis of USP7 hydrolysis of the FP reagents. Data could not be fitted with an exponential Michaelis-Menten curve.

Figure and legend continue on next page

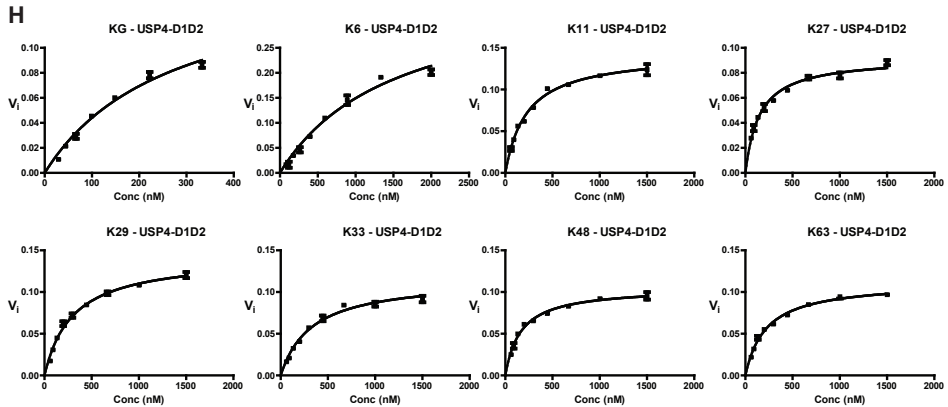
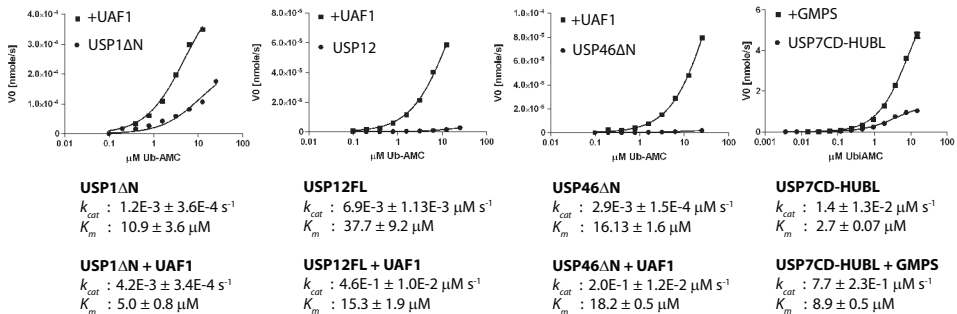


Figure and legend continued from previous page.

Supplemental Figure S3. Related to Figure 4. Synthesis, LC-MS of FP reagents, exemplary raw data and Michaelis-Menten curves of USP4 and USP7. H. Michaelis-Menten analysis of USP4 hydrolysis of the FP reagents. Kinetic parameters are in (D).



Supplemental Figure S4. Related to Figure 6. Curves of the Michaelis-Menten analysis of the UAF1 and GMPS modulation. The Michaelis-Menten curves for the different USPs obtained by determining the initial rates (V_0) at 2-fold serial dilutions of UbAMC.

Ubiquitin-specific protease 4 is inhibited by its ubiquitin-like domain

Mark P.A. Luna-Vargas¹, Alex C. Faesen¹, Willem J. van Dijk¹, Michael Rape², Alexander Fish¹ & Titia K. Sixma^{1*}

EMBO rep. 2011 ;12(4):365-372

¹Division of Biochemistry and Center for Biomedical Genetics, The Netherlands Cancer Institute, Amsterdam, The Netherlands, and

²Department of Molecular and Cell Biology, University of California at Berkeley, Berkeley, California, USA

* Correspondence: t.sixma@nki.nl (T.K.S.)

5

Abstract

USP4 is a member of the ubiquitin-specific protease (USP) family of deubiquitinating enzymes that has a role in spliceosome regulation. Here, we show that the crystal structure of the minimal catalytic domain of USP4 has the conserved USP-like fold with its typical ubiquitin-binding site. A ubiquitin-like (Ubl) domain inserted into the catalytic domain has autoregulatory function. This Ubl domain can bind to the catalytic domain and compete with the ubiquitin substrate, partly inhibiting USP4 activity against different substrates. Interestingly, other USPs, such as USP39, could relieve this inhibition.

Introduction

Post-translational modification by the small, highly conserved ubiquitin (Ub) protein has an essential role in the regulation of many cellular processes in eukaryotes^{1,2}. In this process, the carboxy-terminus of Ub forms an isopeptide with lysines on the target proteins, or on Ub itself, to form poly-Ub chains. The activity of the conjugating enzymes E1–E2–E3 is actively balanced through hydrolysis by deubiquitinating enzymes (DUBs)^{2–6}. Deregulation of the ubiquitination pathway can lead to cancer and neurodegenerative diseases^{7,8}. More than 100 putative DUBs are known so far, belonging to five subfamilies of isopeptidases. The Ub-specific protease (USP) family is the largest, with more than 60 members in the human genome^{5,6,9}. USPs share a papain-like catalytic domain and crystal structures show a conserved catalytic core that undergoes conformational changes on Ub binding^{10–15}. USPs are variable in size with modular domain architecture including, for example, TRAF-like, DUSP or Znf domains^{5,6}. Sequence analysis predicted the presence of Ub-like (Ubl) domains in 17 different USPs¹⁶. Integrated Ubl domains are stretches of 45–80 amino acids that share the b-grasp fold of Ub, but often have poor sequence conservation among subfamilies^{17,18}. The Ubl domains in the USP family are located amino-terminally, within or C-terminally to the catalytic domain. Structural studies of the N-terminal Ubl domain of USP14 confirmed the Ubl-fold (Protein Data Bank (PDB): 1WGG) and showed involvement in proteasome binding that promotes the DUB activity of USP14¹². Similar to USP14, USP4 has a Ubl domain N-terminal of its catalytic domain, but it has an additional Ubl domain embedded in the catalytic domain. USP4 was previously known as ubiquitous nuclear protein (UNP)¹⁹. Identified as a proto-oncogene related to Tre 2/Tre 17 (USP6), USP4 shows a consistently elevated gene expression level in small cell tumours and lung adenocarcinomas, suggesting that it may have a possible causative role in neo-

plasia²⁰. Besides possible roles in Wnt signalling²¹ and recruitment to the A2A receptor²², USP4 is recruited to the spliceosome by complex formation with Sart3²³. Here, it preferentially deubiquitinates K63-linked chains on the U4 component Prp3. Another component of the spliceosome complex is the catalytically inactive USP39^{23,24}, which controls the messenger RNA levels of Aurora B²⁵. Here, we report on the crystal structure of the catalytic domain of USP4 without the internal Ubl domain, and show how this Ubl domain acts as an autoregulatory domain that partially inhibits catalytic activity by competitive inhibition.

Results

Identification of USP4-D1D2

To gain insight into the structure and function of USP4, we expressed and purified the USP4 catalytic domain (amino acids 296–954, Fig 1A) in *Escherichia coli*. To improve the chances for crystallization, we used limited proteolysis. After treatment with thermolysin, two fragments—domain 1 (D1) and 2 (D2)—were obtained, which copurified on size exclusion chromatography and together retained DUB activity (supplementary Fig S1A,B online). We identified the composition of D1 and D2 using mass spectrometry and N-terminal sequencing (supplementary Fig S1C online) and compared them against a multi-sequence alignment of USP family members. This showed that the protease treatment removed an insertion between Leu 481 and Leu 766 (supplementary Fig S2 online), yielding a minimal catalytic domain consisting of an enzymatically active complex of two fragments: USP4–D1D2.

Structure of the USP4–D1D2 catalytic domain

We crystallized and determined the USP4–D1D2 structure by molecular replacement using the

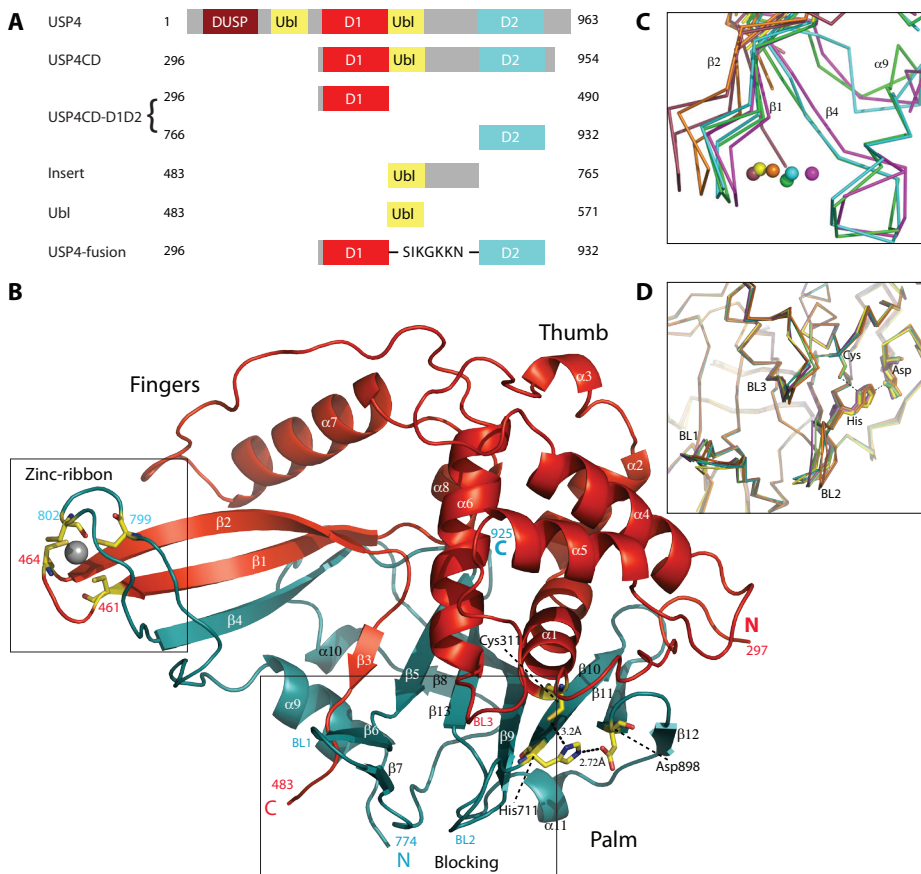


Figure 1. The catalytic domain of USP4–D1D2. **A**) Domain architecture of USP4 and fragments expressed. **B**) Crystal structure of USP4–D1D2 catalytic domain in cartoon representation, with secondary structure elements labeled. D1 and D2 are coloured as in (A). Catalytic triad and the cysteines (yellow) coordinating zinc (grey sphere) are shown in stick representation. **C and D**) Superposition of six non-crystallographic symmetry-related copies in the asymmetrical unit showing flexibility in (C) the zinc-finger ribbon and (D) blocking loops, BL1–3. BL, blocking loop; Ub, ubiquitin; Ubl, ubiquitin-like; USP, ubiquitin-specific protease.

USP8 catalytic domain (PDB: 2GFO) as the search molecule, and refined it to 2.4Å resolution with an R/R_{free} of 0.178/0.21 and good geometry (Fig 1B; supplementary Table S1 online). There are six molecules of USP4–D1D2 per asymmetrical unit, with a pairwise root-meansquare deviation of approximately 0.7Å over 344 residues using the PISA. Similar to crystal structures of other USPs, the catalytic domain of USP4–D1D2 resembles an extended right hand comprising three domains: Fingers, Thumb and Palm (Fig 1B; supplementary Fig S3 online). The D1 fragment contains the Thumb domain and part of the Fingers domain with the Cys box (amino acids 303–320) and QQD box (amino acids 390–403) of the active site, whereas the D2

fragment completes the active site with the His box (amino acids 864–885, 894–903, 915–922) and makes the remaining part of the Fingers and the Palm⁹ (supplementary Fig S2 online). Like other USP structures^{10,12–15}, except USP7¹¹, the catalytic triad is in a catalytically competent configuration, wherein His 711-ND1 is 3.2Å away from Cys 311-SG and His 711-ND2 is hydrogen bonding with Asp 898-OD1 (2.7Å; Fig 1B).

The zinc-finger ribbon observed in USP2 and USP8 is present in USP4 (Fig 1B,C). The Zn^{2+} ion brings together the D1 and D2 domains, tetrahedrally coordinated by cysteines on anti-parallel β -strands β 1 and β 2 in D1,

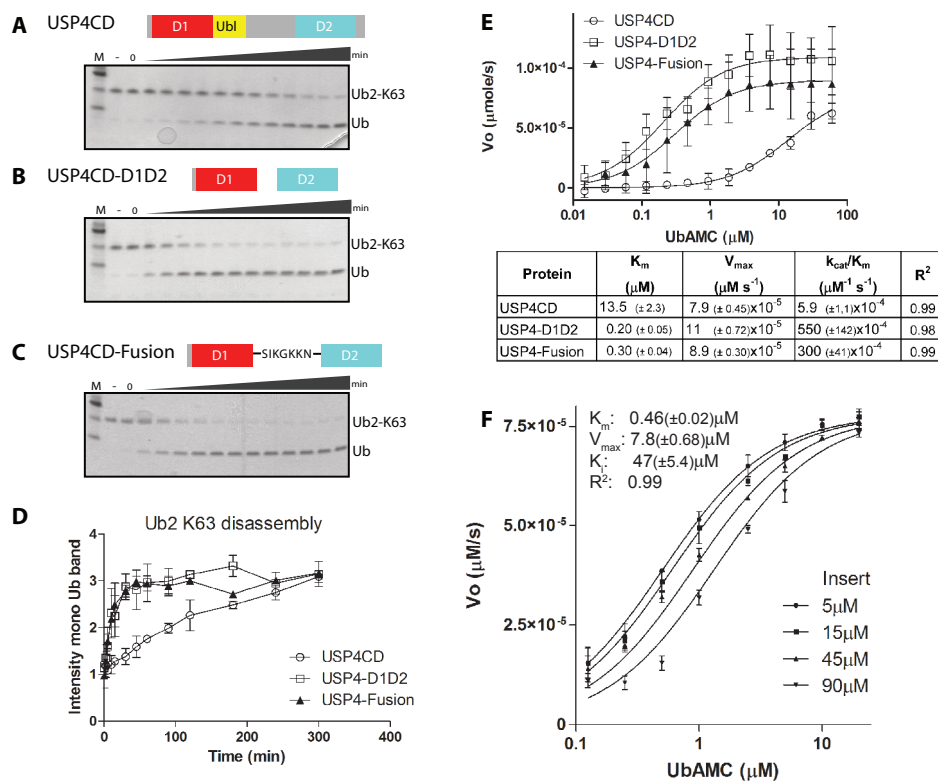


Figure 2. Insert inhibits the DUB activity of USP4CD. (A–C) The full-length USP4 catalytic domain (A) is much less active than (B) USP4–D1D2 or (C) USP4 fusion in deubiquitinating K63 di-Ub (Coomassie-stained SDS–PAGE gels). (D) Quantification of mono-Ub in K63 di-Ub cleavage assays. The intensity of the mono-Ub band is plotted against time. (E) The inhibitory effect of the insert is observed in a Ub-AMC assay. On comparing K_{cat}/K_m between USP4CD and D1D2, we observed a 90 times lower enzyme efficiency for the insert containing USP4CD. (F) Inhibition of USP4–D1D2 *in trans* in Ub-AMC assays at different Ubl-insert concentrations (5, 15, 45 and 90 μM) can be jointly fit as a competitive inhibitor. SDS–PAGE, SDS–polyacrylamide gel electrophoresis; Ub, ubiquitin; Ub-AMC, ubiquitin-7-amido-4-methylcoumarin; Ubl, ubiquitin-like; USP, ubiquitin-specific protease.

and b4 in D2. This zinc-finger ribbon in the Fingers domain seems to be in the contracted ‘closed-hand’ configuration seen in USP8 that blocks access of Ub to its binding site¹⁰. A similar role was assigned to the two Ub-binding surface loops (BL1 and BL2) in USP14¹² that block the active site, but relocate on Ub binding. In USP4, both loops (Fig 1D)—as well as a third blocking loop (BL3) that hinders access of the C-terminal tail of Ub to the binding pocket—are observed. Superposition of the six non-crystallographic symmetry-related molecules of USP4–D1D2 shows that both the zinc-finger ribbon and the three blocking loops show flexibility (maximal $C\alpha$ displacement 4Å; Fig 1C,D), which is in agreement

with their role in activation^{10,12}.

The insert inhibits deubiquitinating activity

We compared the catalytic activity of the USP4 catalytic domain with and without the large insert, by using *in vitro* deubiquitinating assays. In these assays we followed the hydrolysis of K63- and K48-linked di-Ub into mono-Ub (Fig 2A,B; supplementary Fig S4A,B online). We observed that K63 di-Ub is more efficiently degraded than K48, in agreement with the role of USP4 in splicing²³. Interestingly, quantification (Fig 2D; supplementary Fig S4D online) shows that USP4–D1D2 without insert is more efficient at degrading both di-Ubs than the

complete catalytic domain. When D1 and D2 are fused through a short linker, as found in USP7 (supplementary Fig S2 online), their activity is similar to that of USP4–D1D2, showing that the cause of the activation is the lack of insert and not the chain break (Fig 2C; supplementary Fig S4C online).

In Ub-7-amido-4-methylcoumarin (Ub-AMC) assays the intact USP4 catalytic domain is also less active than USP4–D1D2 or the fusion protein. As only AMC is cleaved off, the inhibition is not dependent on the protein target. When analysed by Michaelis–Menten kinetic analysis (Fig 2E) the V_{\max} values were similar, but the K_M for the

intact catalytic domain (13.5 μM) was weaker than that for USP4–D1D2 (0.20 μM), leading to approximately 90-fold lower catalytic efficiency overall (k_{cat}/K_M) for USP4CD than for USP4–D1D2.

As the insert seems to inhibit the DUB activity of USP4, we tested whether it could do so *in trans*. We expressed and purified the insert (amino acids 483–765) and added it in increasing amounts to USP4–D1D2 in the Ub-AMC assay (supplementary Fig S5A online). We observed that the insert slows deubiquitination by USP4–D1D2. To investigate whether this reduction in DUB activity is due to molecular crowding, we repeated

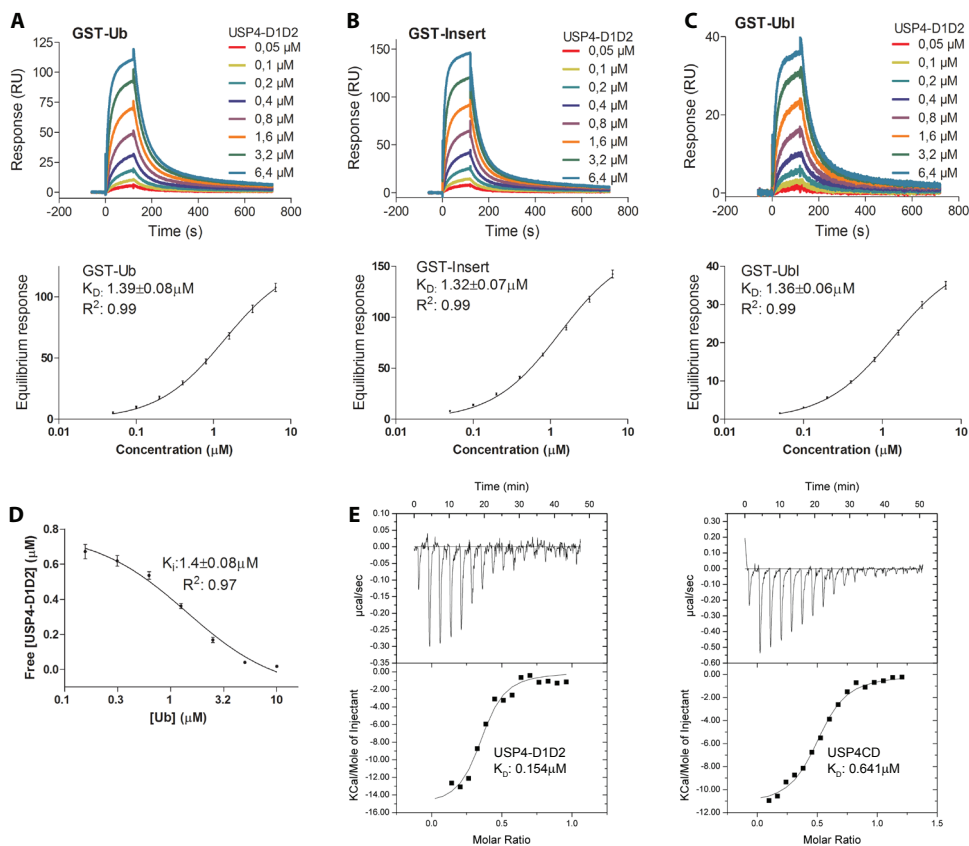


Figure 3. Ubiquitin competes with the insert or Ubl-domain for binding to USP4–D1D2. (A–C) Interaction of Ub and the insert fragments with USP4–D1D2 was studied by SPR experiments. Top: (A) GST-tagged Ub, (B) GST-insert and (C) GST-Ubl domain were immobilized on anti-GST antibodies coupled to a CM5 Biacore chip and USP4–D1D2 was flowed over the chip at different concentrations. Bottom: Langmuir binding curves. **D**) Competition experiment with immobilized GST insert on USP4–D1D2 with varying concentrations of Ub. A one-site competition binding model was fitted ($K_i = 1.4 \mu\text{M}$). **E**) The interaction of Ub with USP4–D1D2 (left) and with full-length USP4CD (right) were studied by ITC analyses. Thermodynamic values for USP4–D1D2 ($\Delta H = -14.3 \text{ kcal/mol}$ and $\Delta S = -16.9 \text{ cal/mol/deg}$), for USP4CD ($\Delta H = -11.4 \text{ kcal/mol}$ and $\Delta S = -10.0 \text{ cal/mol/deg}$). GST, glutathione S-transferase; ITC, isothermal titration calorimetry; Ub, ubiquitin; Ubl, ubiquitin-like; USP, ubiquitin-specific protease.

the *in trans* inhibition assay with USP4–D1D2 in the presence of either SUMO or BSA (supplementary Fig S6 online). Neither of these reduced DUB activity, confirming that the insert is intrinsically able to inhibit the catalytic activity of USP4.

Competitive inhibition of the USP4 insert

We tested whether USP4–D1D2 would directly interact with the insert. In a surface plasmon resonance (SPR; Fig 3B) experiment, we observed binding of USP4–D1D2 to the insert, with a K_d of 1.32 μM after equilibrium fitting. This affinity closely resembled the affinity of USP4–D1D2 for Ub itself (K_d of 1.39 μM ; Fig 3A).

Therefore, we tested whether the insert could compete with Ub for binding to USP4–D1D2, and would therefore bind to the same binding site. In an SPR competition experiment we flowed USP4–D1D2 over a glutathione S-transferase (GST)-tagged insert in the presence of increasing amounts of Ub (Fig 3D). We observed decreasing binding of USP4–D1D2 to the GST-insert as the Ub concentration increased. The data could be fitted with a one-site competition binding model with a K_i of 1.4 μM , showing that the USP4 insert competes with Ub for binding to USP4–D1D2. Interestingly, the K_d of intact USP4CD for Ub is

only fourfold less, compared to USP4–D1D2 in an isothermal titration calorimetry (ITC) experiment (Fig 3E). Although the exact K_d s are slightly tighter in the ITC experiment, qualitative analysis of SPR experiments agrees with this assessment. Non-specific binding at high concentrations precluded detailed fitting of these data (supplementary Fig S7 online), but the curves show that binding of Ub to USP4CD has a slower off-rate than that of Ub to USP4–D1D2, and together with the K_d value also suggests that it has a slower on-rate. As the K_M is dependent on K_d and the binding rate, the combination of slow kinetics and slightly lower affinity explains the differences in K_M values. Apparently, the insert prevents rapid binding as well as rapid release of the Ub substrate, allowing competitive binding. Finally we analysed whether the enzymatic activity is competitively inhibited by the addition of the insert *in trans*. We tested the enzymatic activity with varying inhibitor concentrations against a range of substrate concentrations (Fig 2F), and fitted the data against different inhibition models²⁶. We found that the data were best explained by competitive inhibition with $K_i = 47 \mu\text{M}$. Although this value is lower than expected on the basis of the binding data alone, it explains why the USP4CD is not completely inhibited in the continuous presence of the insert. It seems that

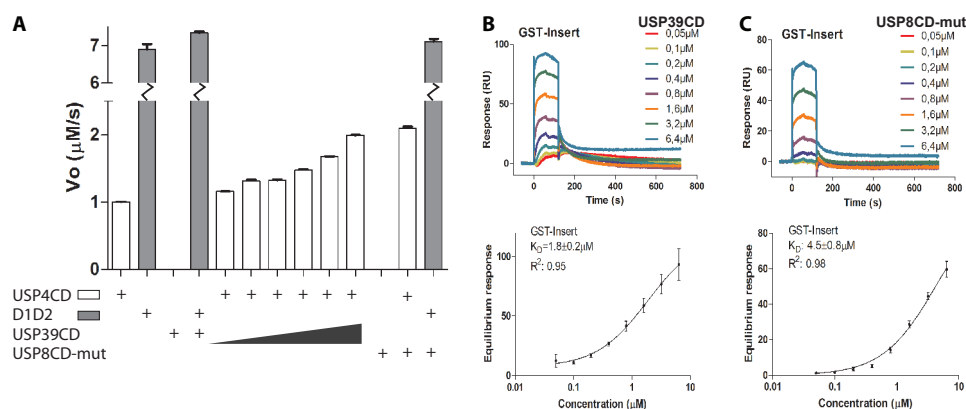


Figure 4. USP39CD binds to the Ubl domain and increases the deubiquitinating-enzyme activity of USP4CD. **A**) Other USPs activate the DUB activity of USP4CD *in trans* in a Ub-AMC assay (USP39CD: 10, 20, 50, 100, 500 and 1,000 nM; USP8CD-mut: 1,000 nM). **B**) USP39 and **C**) USP8-mut bind to Ubl insert, in an SPR assay analogous to Fig 2B. DUB, deubiquitinating enzyme; GST, glutathione-S-transferase; mut, mutant; Ub, ubiquitin; Ub-AMC, ubiquitin-7-amido-4-methylcoumarin; Ubl, ubiquitin-like; USP, ubiquitin-specific protease.

additional conformational changes take place. One possibility is that the enzyme reaches a state after turnover that has lower affinity for the insert, and is therefore not as effectively inhibited.

The Ubl domain is sufficient for inhibition

The presence of a Ubl domain within the insert was predicted (supplementary Fig S2 online)¹⁶. To test whether the Ubl domain is sufficient for binding to the USP4 catalytic domain, we performed the SPR experiment with the purified Ubl domain (amino acids 483–571, Fig 1A) and found a K_d of 1.36 μM towards USP4–D1D2, which is similar to that for the complete insert (Fig 3C). This suggests that the Ubl domain is the functional part of the insert.

To test whether the Ubl domain can inhibit the DUB activity of USP4, we repeated the *in trans* inhibition assay with USP4–D1D2 in the presence of increasing amounts of the Ubl domain (supplementary Fig S6 online) and found that it provides inhibition equal to the insert. We therefore conclude that the Ubl domain is sufficient to

inhibit the DUB activity of USP4, through competitive inhibition of Ub binding.

Regulation by other USP enzymes

As the Ubl domain seems to bind in the substrate Ub-binding site of USP4, we wondered whether other USP enzymes could also bind to the Ubl domain. We tested whether our Ubl domain containing insert could bind to the catalytic domain of USP39 and USP8, and found similarly high affinities as for USP4CD (Fig 4B,C).

Then, we analysed whether these DUBs could modulate USP4CD activity. We repeated the *in trans* Ub-AMC assay with USP4CD in the presence of the intrinsically inactive USP39CD or an inactive variant of the USP8 catalytic domain, USP8CD-mut (Fig 4A). For both USPs we observe a modest activation of USP4CD that was dependent on the presence of the Ubl-containing insert, as it does not increase the DUB activity of USP4–D1D2 in this manner.

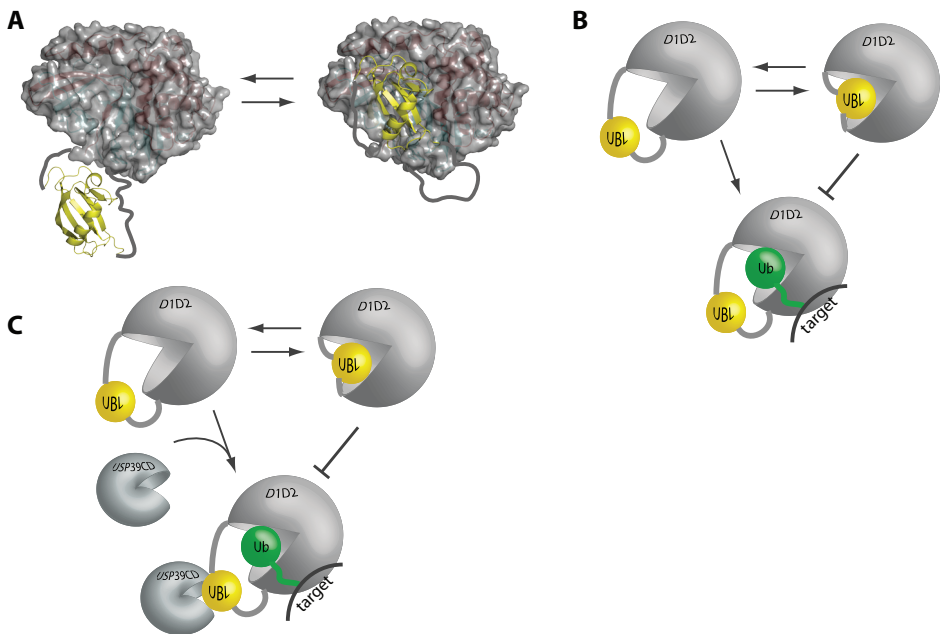


Figure 5. Model for Ubl domain inhibition on USP4. **A)** Structural model in which interaction of the Ubl domain with USP4CD inhibits the binding of Ub. **B)** Schematic model of the auto-inhibitory role of the Ubl domain in USP4. **C)** Other USP enzymes, such as USP39, may relieve the inhibition by binding to the Ubl domain. Ub, ubiquitin; Ubl, ubiquitin-like; USP, ubiquitin-specific protease.

Apparently, other USP enzymes can regulate USP4 activity by competing for binding to the Ubl domain. This effect could be larger when the USPs have further interactions. As USP39 forms a stable complex with USP4 in cells^{23,24}, it is a prime candidate for an activating role *in vivo*.

Discussion

We show that the predicted Ubl domain within a large insert embedded in the USP4 catalytic domain partially inhibits DUB activity by competing with Ub for binding. Superposition of the crystal structure of USP4-D1D2 and any Ubl domain on USP7 in complex with Ub-aldehyde (PDB: 1NBF), respectively, shows that the Ubl domain would fit like a Ub molecule into the hand of USP4-D1D2 (Fig 5A), only requiring movements in the blocking loops and the zinc-finger ribbon. Hence, we propose a model in which the Ubl domain partly inhibits DUB activity through competitive inhibition by binding into the hand of USP4 and thus preventing Ub substrate binding (Fig 5B).

This function of an integrated Ubl domain is relatively new. The Ubl domains in proteasomal shuttle factors Rad23 and Dsk2, as well as in Parkin and USP14, function in recruitment of ubiquitinated proteins to the proteasome^{12,27}. Other Ubl domains regulate the enzymatic activities of immune-response inducible kinases such as IKK β (a subunit of I κ B kinase complex)²⁸, or as PB1 (Phox and Bem1) domains, have a role in the regulation of signal transduction in proteins such as P62, MEK5 and protein kinase C^{29,30}. However, all these Ubl-domain families have low sequence similarities, indicating that their functions are probably distinct between subfamilies.

The activity of USPs is regulated through an inactive conformation of the catalytic triad, as in USP7, or through a series of blocking loops or a blocking zinc-finger ribbon. USP4 seems to combine the blocking loops and zinc-finger ribbon with a further regulation through the Ubl domain.

Whether Ubl domains provide a common regulation mechanism for the DUB activity of USPs is an interesting question for future research. A second Ubl domain is found within USP4, at its N-terminus. A recent crystal structure (PDB: 3JYU, amino acids 139–226) shows that this Ubl domain interacts extensively with the adjacent DUSP (do-

main in USP) domain (amino acids 27–125). This region of the protein is primarily important for interaction with Sart3²³ and hence might not have this function.

However, USP4 is not the only DUB with a Ubl fold within its catalytic domain. Sequence analysis by Zhu and co-workers identified an integrated Ubl fold within the catalytic domain of USPs 6, 11, 15, 19, 31, 32 and 43, embedded in a larger insert, like in USP4¹⁶. In particular, USP11 and USP15 are closely related to USP4. This subgroup of USPs probably also regulates DUB activity through its Ubl domain.

The way in which Ubl-domain inhibition itself is regulated is an exciting question. One could imagine that further posttranslational modification by, for example, phosphorylation or acetylation would enable the release of the full activity of the DUB enzyme. In addition, we have shown that binding partners such as USP39, can activate USP4 function by binding to the Ubl domain (Fig 5C). Although the activation is modest (Fig 4A), this could be increased by further interactions, as observed in the spliceosome complex.

Whatever the mechanisms that are identified to regulate USP4 activation, it is clear that this type of internal regulation by a Ubl domain allows the creation of an extremely fast response element to external signals.

Material and Methods

Plasmids and cloning

cDNA for human USP4 and USP8 was a gift from Hidde Ploegh and cDNA for USP39 was a gift from R. Medema. USP4CD (aa 296-954) and the D1 fragment (aa 296-490) of human USP4, USP39CD (aa 219-565) and USP8CD (aa 771-1118) were cloned using ligation independent cloning into pET-46 Ek/LIC vector (Novagen). The D2 fragment (aa 766-932) of USP4 was cloned into the pET-NKI b/3C (Luna-Vargas, in preparation). The fused USP4-D1D2 was created by inserting aa 353-359 of USP7 (SIKGKNN) between residues Leu479 and Leu777. The USP4 insert (aa 483-765), Ubl domain (aa 483-571) and Ub were cloned into pGEX-6P-1 (GE Healthcare). The USP8CD mutant was generated by site-directed mutagenesis of the catalytic cysteine (C786A).

Protein preparation

Purification of E2-25K³¹, Ubc13/Mms2³² was as described. GST-tagged proteins were overexpressed in *Escherichia coli* strain Rosetta2(DE3)-T1R using IPTG (200 μM) induction overnight at 15°C. Cells were lysed by microfluidizer into buffer A (50mM Hepes pH7.5, 150mM NaCl, 5mM β-mercaptoethanol, 1mM PMSF). The fusion protein was purified using glutathione sepharose resin, eluted, followed by removal of the GST-tag with 3C protease and size-exclusion using HiLoad 16/60 Superdex 200 (GE Healthcare). Peak fractions were concentrated to 10mg/ml in 25mM Hepes (pH7.5), 200mM NaCl and 5mM β-mercaptoethanol. D1 and D2 co-expression, other USP4 variants, USP39CD and USP8CD-mut were overexpressed as above, with 200 μM ZnCl₂ during induction and lysed in buffer A supplemented with 1mM ZnCl₂ and 10mM Imidazole. These His-tagged proteins were purified by a Co²⁺-affinity (Talon resin) step. Upon Imidazole elution the His-tag was removed by TEV cleavage at 4°C overnight during dialysis in buffer B (25mM Hepes pH7.5, 150mM NaCl, 5mM β-mercaptoethanol). This was followed by POROS Q affinity chromatography and size-exclusion using HiLoad 16/60 Superdex 200 (GE Healthcare), where the protein eluted as a monomer. The peak fractions were concentrated to 5mg/ml in buffer B.

Limited Proteolysis and protein identification

Purified USP4CD (9mg/ml) was incubated with Thermolysin (0.8units) for 1.5hr at room temperature and subjected to size exclusion chromatography using Superdex75 16/60. Fractions containing USP4-D1 and -D2 were subjected to LC-MS analysis. LC-MS measurements were performed on a system equipped with a Waters 2795 Separation Module (Alliance HT), Waters 2996 Photodiode Array Detector (190-750nm), Waters Alltime C18 (2.1x100mm, 3 μm), Waters Symmetry300_{TM} C4 (2.1x100mm, 3.5 μm) and LCT_{TM} Orthogonal Acceleration Time of Flight Mass Spectrometer. Data processing was performed using Waters MassLynx Mass Spectrometry Software 4.1 (deconvolution with Maxent 1 function). N-terminal sequencing of USP4-D1 and -D2 were performed by AltaBioscience in Birmingham, England.

Crystallization and structure determination of the USP4-D1D2

Crystals were grown overnight in sitting-drops mixing 200nl USP4-D1D2 (~3.5mg/ml) with 200 nl 100mM Bis-Tris propane [pH8.5], 25mM Na₂SO₄ and 18% PEG3350 (w/v) at 19°C. Crystals were cryoprotected in mother liquor with 25% ethylene glycol. The crystals belong to the space group P2₁2₁2₁ with six molecules per asymmetric unit (supplementary Table S1). Diffraction data were collected at the ESRF (Grenoble, France) beamline ID14-2 and processed with MOSFLM³³ and SCALA³⁴. The structure was solved by molecular replacement with PHASER³⁵ using USP8CD (PDB:2GFO) as search model. Iterative rebuilding and refinement were done with Coot³⁶ and PHENIX³⁷ and BUSTER³⁸. The structure was validated with MOLPROBITY³⁹ and WHAT-CHECK⁴⁰ and structure figures were generated using PYMOL⁴¹. Cysteine residue 311 in all chains have been chemically modified by β-mercaptoethanol.

Ub-AMC assay

UbAMC assays were done in 50mM Hepes [pH7.5], 100mM NaCl, 5mM DTT, 0.05% Tween-20 and 1mM EDTA and reaction progress was monitored with a Fluostar Optima plate-reader (BMG Tech) by the increase in fluorescence emission at 460nm (λ_{ex} = 355nm) generated by Ub-AMC cleavage. Quantitative activity (triplicate) and *in trans* inhibition (duplicate) assays or USP modulation assays (triplicate) were performed using Ub-AMC with 10nM enzyme in 30 μl reaction volume in 384-well plates and preincubated for 15 min at 21°C, for inhibition assays with Ubl insert and with other DUBs for modulation assays. Initial velocities against Ub-AMC concentration were computed to derive steady-state kinetic parameters using GraphPad Prism5 (GraphPad Software Inc.). Non-linear fitting of four inhibition models was compared in GraphPad.

Di-ubiquitin assay

Di-Ub assays were performed in similar buffer as in UbAMC assays at 37°C in 75 μl reaction volume. Aliquots (5 μl) were stopped by addition of 4x SDS-sample loading buffer and subjected to SDS-PAGE analysis on a 4-12% coomassie stained gel (Invitrogen). K48 and K63 di-Ub substrates were produced and purified as described⁴². 75nM enzyme was

incubated with 3 μM di-Ub, subjected to SDS-polyacrylamide gel electrophoresis and image analysis, and quantitation was performed in duplicate with TINA 2.09 (Raytest Co.).

Surface plasmon resonance

SPR was performed on a Biacore T-100, with GST-Ub, GST-insert and GST-Ubl domain immobilized on anti-GST antibodies coupled to a CM5 chip. Data (duplicate) were processed using BiaE-valuation (GE Healthcare) and GraphPad Prism5. Quantitative binding analysis was done in duplicate at 25°C on a Biacore T-100 instrument (GE Healthcare). GST fused Ub, insert and Ubl domain were immobilized on α -GST antibodies lysine-coupled to a CM5 chip. USPs were injected in varying concentrations over the sensor chip at 30 $\mu\text{l}/\text{min}$ with a 120s association phase followed by a 10min dissociation phase. For the binding inhibition assay Ub was added in varying concentrations to USP4-D1D2. Standard double referencing data subtraction methods were used before and equilibrium curve fitting with BiaEvaluation (GE Healthcare) and GraphPad software (GraphPad Software Inc).

Isothermal Titration Calorimetry

ITC experiments were performed with the VP-ITC Micro Calorimeter (MicroCal, Inc.) at 25°C. Stock solutions of USP4CD, USP4-D1D2 and Ub were prepared by dialysis of the purified proteins against a buffer containing 25mM Hepes pH8.0, 150mM NaCl and 5mM β -mercaptoethanol at 4°C and were degassed before use. The sample cell (1.8ml) contained USP4-D1D2 (10 μM) or USP4CD (20 μM) which was titrated with 100 μM Ub or 200 μM Ub respectively using 16 injections. The injections after saturation were used to determine the background signal. Corrected data were analyzed using software supplied by the ITC manufacturer to calculate the dissociation constant K_d and fitted with a one to one binding model.

Accession number

Atomic coordinates and structure factors have been deposited to the Protein Data Bank with accession number: **2Y6E**

Supplementary information is available at EMBO reports online (<http://www.emboreports.org>).

Acknowledgements

We thank J. Lebbink for mass spectrometry, European Synchrotron Radiation Facility beamline scientists for assistance during X-ray data collection, A. Perrakis and P. Rucktooa for help with crystallographic analysis, R.G. Hibbert for help with SPR data analysis, and lab members for discussion and sharing of reagents. This study was supported by the European Union Network of Excellence project RUBICON and Dutch Cancer Society Project KWF 2008-4014.

Conflict of interest

The authors declare that they have no conflict of interest.

References

1. Hochstrasser, M. Origin and function of ubiquitin-like proteins. *Nature* **458**, 422-9 (2009).
2. Pickart, C.M. Back to the future with ubiquitin. *Cell* **116**, 181-90 (2004).
3. Amerik, A.Y. & Hochstrasser, M. Mechanism and function of deubiquitinating enzymes. *Biochim Biophys Acta* **1695**, 189-207 (2004).
4. Deshaies, R.J. & Joazeiro, C.A. RING domain E3 ubiquitin ligases. *Annu Rev Biochem* **78**, 399-434 (2009).
5. Komander, D., Clague, M.J. & Urbe, S. Breaking the chains: structure and function of the deubiquitinases. *Nat Rev Mol Cell Biol* **10**, 550-63 (2009).
6. Nijman, S.M. et al. A genomic and functional inventory of deubiquitinating enzymes. *Cell* **123**, 773-86 (2005).
7. Hoeller, D. & Dikic, I. Targeting the ubiquitin system in cancer therapy. *Nature* **458**, 438-44 (2009).
8. Lopez-Otin, C. & Hunter, T. The regulatory crosstalk between kinases and proteases in cancer. *Nat Rev Cancer* **10**, 278-92 (2010).
9. Quesada, V. et al. Cloning and enzymatic analysis of 22 novel human ubiquitin-specific proteases. *Biochem Biophys Res Commun* **314**, 54-62 (2004).
10. Avvakumov, G.V. et al. Amino-terminal dimerization, NRDP1-rhodanese interaction, and inhibited catalytic domain conformation of the ubiquitin-specific protease 8 (USP8). *J Biol Chem* **281**, 38061-70 (2006).
11. Hu, M. et al. Crystal structure of a UBP-family deubiquitinating enzyme in isolation and in complex with ubiquitin aldehyde. *Cell* **111**, 1041-54 (2002).
12. Hu, M. et al. Structure and mechanisms of the proteasome-associated deubiquitinating enzyme USP14. *EMBO J* **24**, 3747-56 (2005).
13. Kohler, A., Zimmerman, E., Schneider, M., Hurt, E. & Zheng, N. Structural basis for assembly and activation of the heterotetrameric SAGA histone H2B deubiquitinase module. *Cell* **141**, 606-17 (2010).
14. Renatus, M. et al. Structural basis of ubiquitin recognition by the deubiquitinating protease USP2. *Structure* **14**, 1293-302 (2006).
15. Samara, N.L. et al. Structural insights into the assembly and function of the SAGA deubiquitinating module. *Science* **328**, 1025-9 (2010).
16. Zhu, X., Menard, R. & Sulea, T. High incidence of ubiquitin-like domains in human ubiquitin-specific proteases. *Proteins* **69**, 1-7 (2007).
17. Burroughs, A.M., Balaji, S., Iyer, L.M. & Aravind, L. Small but versatile: the extraordinary functional and structural diversity of the beta-grasp fold. *Biol Direct* **2**, 18 (2007).
18. Kiel, C. & Serrano, L. The ubiquitin domain superfold: structure-based sequence alignments and characterization of binding epitopes. *J Mol Biol* **355**, 821-44 (2006).
19. Gupta, K., Copeland, N.G., Gilbert, D.J., Jenkins, N.A. & Gray, D.A. Unp, a mouse gene related to the tre oncogene. *Oncogene* **8**, 2307-10 (1993).
20. Gray, D.A. et al. Elevated expression of Unph, a proto-oncogene at 3p21.3, in human lung tumors. *Oncogene* **10**, 2179-83 (1995).
21. Zhao, B., Schlesiger, C., Masucci, M.G. & Lindsten, K. The ubiquitin specific protease 4 (USP4) is a new player in the Wnt signalling pathway. *J Cell Mol Med* **13**, 1886-95 (2009).
22. Milojevic, T. et al. The ubiquitin-specific protease Usp4 regulates the cell surface level of the A2A receptor. *Mol Pharmacol* **69**, 1083-94 (2006).
23. Song, E.J. et al. The Prp19 complex and the Usp4Sart3 deubiquitinating enzyme control reversible ubiquitination at the spliceosome. *Genes Dev* **24**, 1434-47 (2010).
24. Sowa, M.E., Bennett, E.J., Gygi, S.P. & Harper, J.W. Defining the human deubiquitinating enzyme interaction landscape. *Cell* **138**, 389-403 (2009).
25. van Leuken, R.J., Luna-Vargas, M.P., Sixma, T.K., Wolthuis, R.M. & Medema, R.H. Usp39 is essential

- for mitotic spindle checkpoint integrity and controls mRNA-levels of aurora B. *Cell Cycle* **7**, 2710-9 (2008).
26. Copeland, R.A. *Enzymes: A practical introduction to structure, mechanism and data analysis.*, (Wiley, 2000).
27. Sakata, E. et al. Parkin binds the Rpn10 subunit of 26S proteasomes through its ubiquitin-like domain. *EMBO Rep* **4**, 301-6 (2003).
28. May, M.J., Larsen, S.E., Shim, J.H., Madge, L.A. & Ghosh, S. A novel ubiquitin-like domain in I κ B kinase beta is required for functional activity of the kinase. *J Biol Chem* **279**, 45528-39 (2004).
29. Sumimoto, H., Kamakura, S. & Ito, T. Structure and function of the PB1 domain, a protein interaction module conserved in animals, fungi, amoebas, and plants. *Sci STKE* **2007**, re6 (2007).
30. Terasawa, H. et al. Structure and ligand recognition of the PB1 domain: a novel protein module binding to the PC motif. *EMBO J* **20**, 3947-56 (2001).
31. Pichler, A. et al. SUMO modification of the ubiquitin-conjugating enzyme E2-25K. *Nat Struct Mol Biol* **12**, 264-9 (2005).
32. Marteiijn, J.A. et al. The ubiquitin ligase Triad1 inhibits myelopoiesis through UbcH7 and Ubc13 interacting domains. *Leukemia* **23**, 1480-9 (2009).
33. Leslie, A.G. The integration of macromolecular diffraction data. *Acta Crystallogr D Biol Crystallogr* **62**, 48-57 (2006).
34. Evans, P. Scaling and assessment of data quality. *Acta Crystallogr D Biol Crystallogr* **62**, 72-82 (2006).
35. McCoy, A.J. et al. Phaser crystallographic software. *J Appl Crystallogr* **40**, 658-674 (2007).
36. Emsley, P. & Cowtan, K. Coot: model-building tools for molecular graphics. *Acta Crystallogr D Biol Crystallogr* **60**, 2126-32 (2004).
37. Terwilliger, T.C. et al. Iterative model building, structure refinement and density modification with the PHENIX AutoBuild wizard. *Acta Crystallogr D Biol Crystallogr* **64**, 61-9 (2008).
38. Blanc, E. et al. Refinement of severely incomplete structures with maximum likelihood in BUSTER-TNT. *Acta Crystallogr D Biol Crystallogr* **60**, 2210-21 (2004).
39. Davis, I.W. et al. MolProbity: all-atom contacts and structure validation for proteins and nucleic acids. *Nucleic Acids Res* **35**, W375-83 (2007).
40. Hooft, R.W., Vriend, G., Sander, C. & Abola, E.E. Errors in protein structures. *Nature* **381**, 272 (1996).
41. Delano, W.L. The PyMol molecular graphics system. (Delano Scientific, San Carlos, CA, USA, 2002).
42. Pickart, C.M. & Raasi, S. Controlled synthesis of polyubiquitin chains. *Methods Enzymol* **399**, 21-36 (2005).

Table of contents Supplementary information

Table S1	Data collection and refinement statistics.	103
Figure S1	Identification of USP4-D1D2.	104
Figure S2	Structure based multiple sequence alignment.	104
Figure S3	Overview and superposition of USP catalytic domain structures with USP4-D1D2.	106
Figure S4	Deubiquitinating assay with K48 di-Ub as substrate.	107
Figure S5	In trans inhibition of USP4-D1D2 DUB activity.	107
Figure S6	The molecular crowding of high concentrations of SUMO or BSA (100 μ M) does not have an effect on USP4-D1D2 DUB activity.	108
Figure S7	Kinetic comparison of USP4-D1D2 and USP4CD binding to Ub, Ubl and insert on SPR.	108

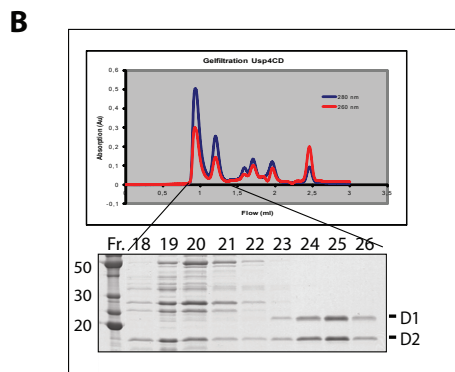
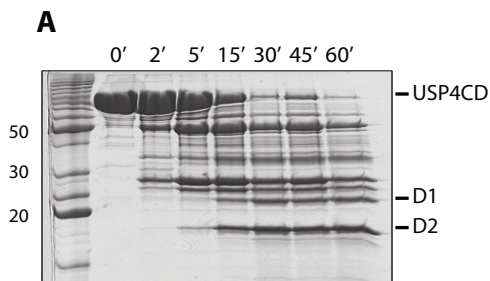
Table SI Data collection and refinement statistics.

Data collection statistics	Native
Wavelength (Å)	0.993
Space group	P2 ₁ 2 ₁ 2 ₁
Unit cell (Å)	110.5, 151.0, 178.7
Molecules per asymmetric unit	6
Resolution (Å) ^a	47.0 - 2.4 (2.53 - 2.4)
R _{merge} (%)	8.8 (66.1)
<I/σ(I)>	11.0 (1.1)
Completeness (%)	94.9 (74.0)
Redundancy	3.4 (2.4)
Refinement	
R _{work} /R _{free} (%)	17.5/21.3
Number of reflections	111078
Number of protein atoms	15775
Number of zinc ions	6
Number of waters	867
RMSD from ideal geometry	
Bond lengths (Å)	0.009
Bond angles (°)	1.01
Ramachandran statistic ^b (preferred/allowed/outliers)	1849 / 66 / 2

^a Numbers in parentheses are for the highest-resolution shell

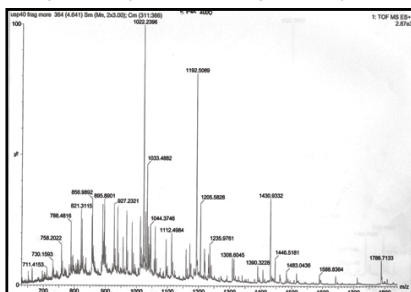
^b Calculated using Molprobit

Supplemental Figures



C

Calc. mass: *Theor. mass:*
D1) 19687,46 Da D1) 19685,54 Da
D2) 22230,30 Da D2) 22227,46 Da



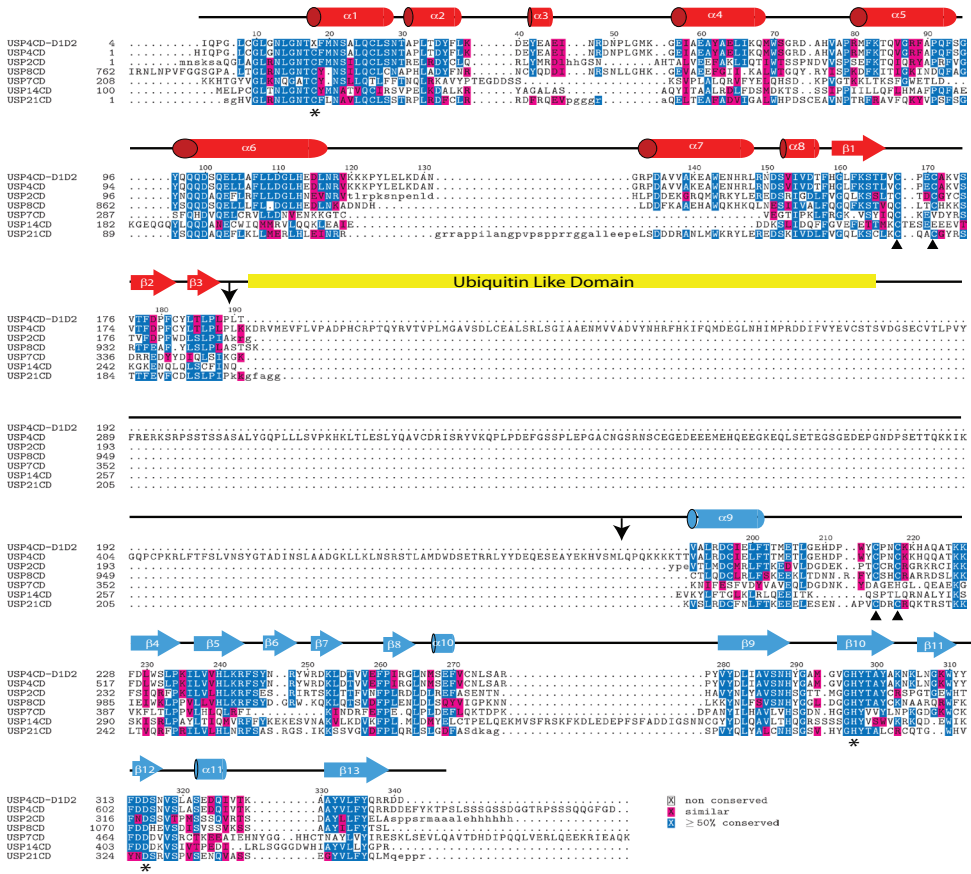
N-terminal sequencing:

D1) Gly - Met - His - Ile - Gln

D2) Leu - Gln - Pro - Gln - Lys

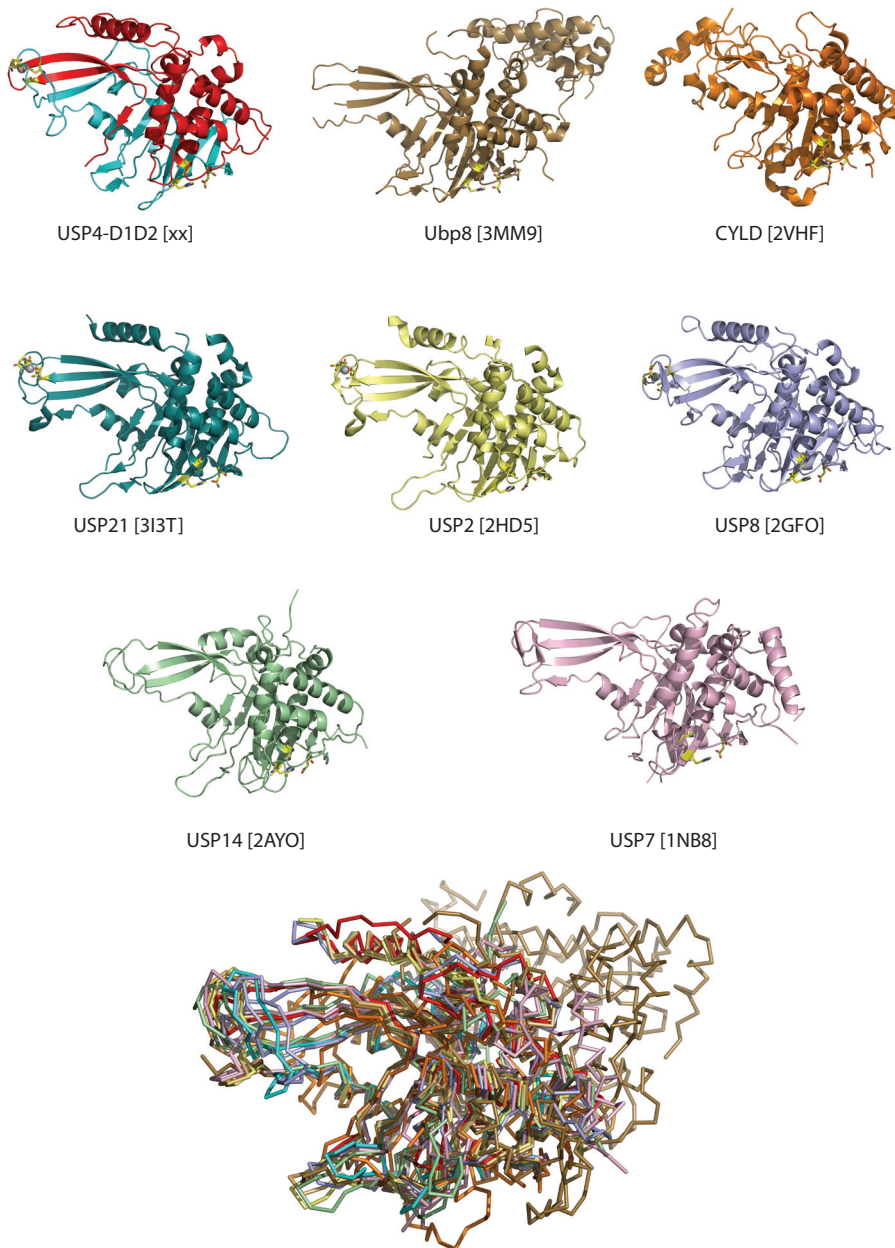
Supplemental Figure S1

Identification of USP4-D1D2. **A)** Limited proteolysis analysis of thermolysin cleavage on USP4CD at 37°C. Samples at different time-points were taken and analyzed on a SDS-PAGE gel. **B)** Proteolytic sample of USP4CD was subjected to a size exclusion chromatography and fraction samples were analyzed on a SDS-PAGE gel. **C)** Mass Spectrometry analysis and N-terminal sequencing determined the identity of the two fragments, D1 and D2.



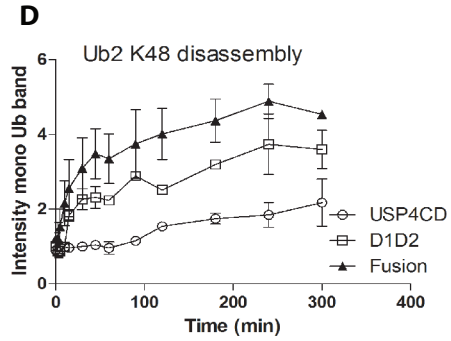
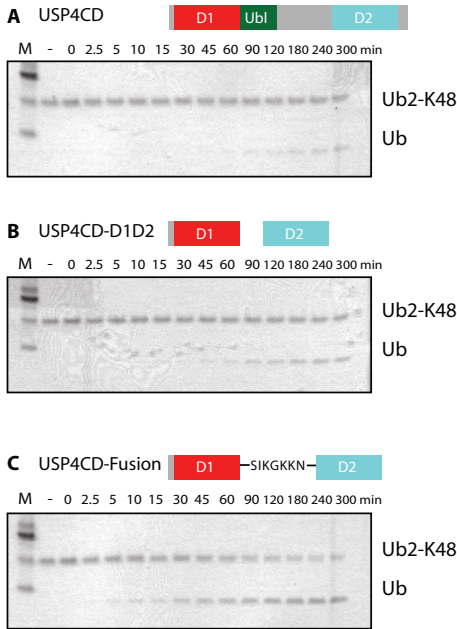
Supplemental Figure S2

Structure based multiple sequence alignment. Secondary structure elements are colored and labeled according to structure of USP4-D1D2 in Figure 1. The internal Ubl is depicted as a yellow bar and the two black arrows indicate where the protease thermolysin cleaved in the catalytic domain of USP4. The catalytic triad residues are indicated with an asterisk. The four black triangles indicate the positions of the Cys residues coordinating the zinc ion.



Supplemental Figure S3

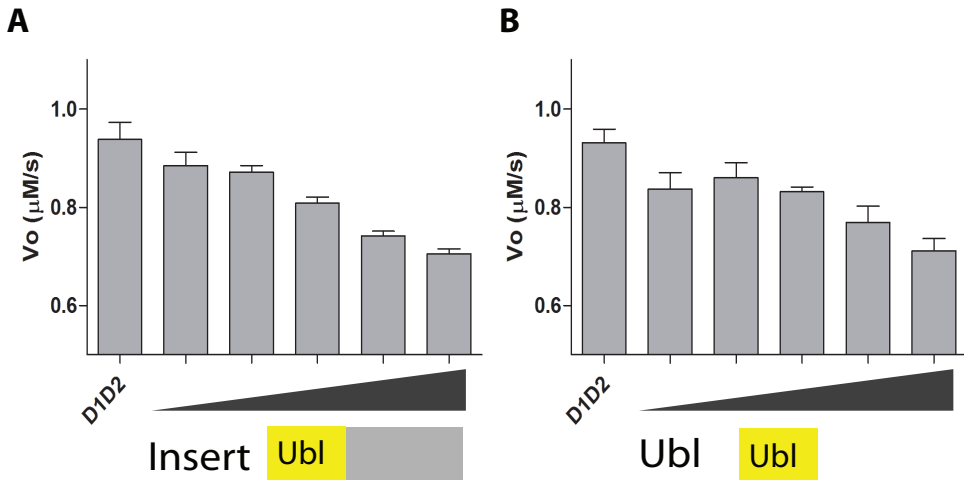
Overview and superposition of USP catalytic domain structures with USP4-D1D2. Comparison between catalytic domains depicted in cartoon representation of USP4-D1D2 (red-cyan), Ubp8 (brown, PDB: 3MM9), CYLD (orange, PDB: 2VHF), USP21 (marine blue, PDB: 3I3T), USP2 (yellow, PDB: 2HD5), USP8 (purple, PDB: 2GFO), USP14 (green, PDB: 2AYO) and USP7 (light pink, PDB: 1NB8). The structures depicted in ribbon representation were superposed in Coot (RMSD of 2.1Å over 323 residues).



Supplemental Figure S4

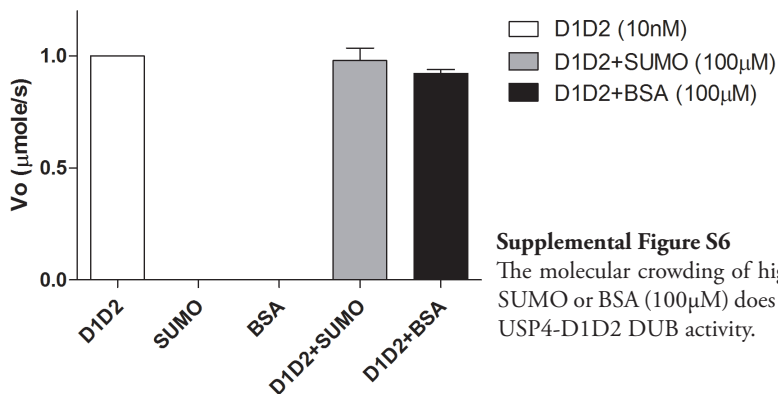
Deubiquitinating assay with K48 di-Ub as substrate. A-C) The full-length USP4 catalytic domain (A) is much less active than USP4-D1D2 (B) or USP4-fusion (C) in a deubiquitinating assay using K48 di-Ub as substrate on coomassie-stained SDS-PAGE gels. D) Quantification of mono-Ub in K48 di-Ub cleavage assays. The intensity of the mono-Ub band is plotted against time

5

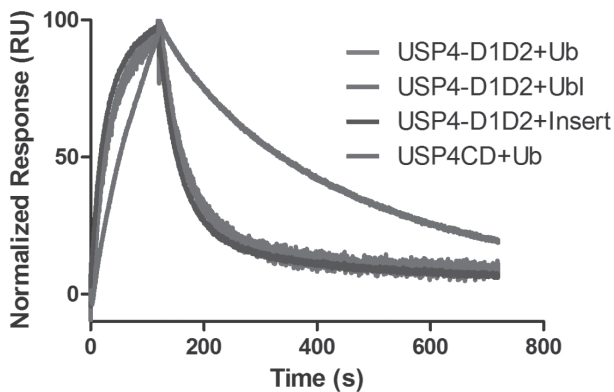


Supplemental Figure S5

In trans inhibition of USP4-D1D2 DUB activity. A) The inhibitory effect of the insert is observed in a Ub-AMC assay with increasing amounts of insert (5, 10, 25, 50 and 75 μM). B) The Ubl domain (5, 10, 25, 50 and 100 μM) is sufficient to show this *in trans* inhibition.



5



General Discussion

6



General Discussion

The USP family: small and multifunctional

More and more functional roles of USPs in important biological cellular processes are being discovered. Also the role they play in tumorigenesis is recognized in the ubiquitin field. Therefore members of the large USP family are being actively pursued as drug targets.

In **chapter 2** a genomic and functional overview is given on the large family of deubiquitinating enzymes encoded in the human genome. The analysis of the ENSEMBL human genome database revealed 95 putative DUBs of which 79 are expressed in cells and display Ub/Ubl protease activity. Compared to the number of E3 ubiquitin ligases, the DUBs are remarkably outnumbered. One possible explanation is that not all DUBs have been identified yet or their associated cofactors that may determine specificity. Another explanation is that a DUB may have different targets. For instance USP7 seems to be able to deubiquitinate several different targets such as p53, Mdm2, PTEN, FOXO4 and H2B¹⁻⁵. As already mentioned in **chapter 1**, USP4 also has different targets e.g. the U4 spliceosome component Prp3, TAK1 and more recently the E3 Ub ligase ARF-BP1⁶⁻⁸. More USPs seem to have more than one target, like USP1 (targets FANCD2 and PCNA)^{9,10}, USP2 (fatty acid synthase and Mdm2)^{11,12}, and CYLD (targets NEMO, TRAF-2 and TRAF-6)¹³⁻¹⁵. Another explanation for the excess of E3 Ub ligases could be that only a fraction of the targets that are ubiquitinated are regulated by specific USPs. It is possible that only proteins that demand extremely tight regulation, such as p53 and H2A/B, require additional regulation by deubiquitination. Indeed p53 and H2A/B seem to have more than one USP for their deubiquitination, USP2, USP7, USP10 and USP3, USP16, USP21, USP22 respectively. Undoubtedly, future studies will uncover more about the functional roles of members of the USP family and why the E3 Ub ligases outnumber the DUBs.

High-throughput equals low-output

In order to understand and explain the molecular and biochemical function of USPs one should turn to structural molecular biology. Once the three-dimensional structure of a USP is determined it could

help decipher basic principles of protein structure and assembly, mechanisms of biochemical reactions and details of macromolecular interactions. As stated in **chapter 1** only the crystal structures of the catalytic domain of several USP members and more recently of USP4 (**chapter 5**) have been solved. Despite the low sequence similarity the overall structure of the catalytic domain is highly conserved. The structures also reveal that the catalytic activity of USPs is regulated by substrate- or scaffold-induced conformational changes. It will be very interesting to determine full-length USPs and see how their additional domains interact with the catalytic domain. In the process of determining the three-dimensional protein structures it is important to produce a large number of soluble recombinant protein variants. In **chapter 3** a set of protein expression vectors for ligation-independent cloning is described and their use for protein expression in *E.coli* on 35 different members of the USP family. Out of 145 different expression constructs, 38 soluble recombinant proteins for 21 different USPs were obtained. Looking more carefully, the level of protein solubility amongst the 21 USPs differ substantially. An explanation for this solubility difference could be the use of high-throughput methods. The protein expression and solubility screening was done in 96-well blocks and working with small volumes one can easily make a mistake in the different steps such as cell lysis, affinity binding and elution of recombinant protein. The use of robotics in automating these different steps can help substantially in identifying the correct construct that gives high protein expression and solubility.

Most of the constructs that give soluble protein for the 21 different USPs are either representing the catalytic domain only or with variations at the N- and C-terminal ends of the catalytic domain. The expression of the full-length protein of only two USPs (USP16 (823aa) and USP46 (366aa)) was possible in *E.coli*. Interestingly, the USP12 construct which has high sequence similarity with USP46 did not give soluble protein in the *E.coli* expression system. However expressing the USP12 construct in the *Sf9* insect cell expression resulted in a high yield of soluble full-length protein (**chapter 4**). It looks like the *Sf9* insect cell expression system might be a more

suitable system for expressing the full-length USP protein. Indeed when testing the pFastBac- NKI-LIC vector in *Sf9* insect cells, the construct for full-length USP7 gave high yield of soluble protein.

Another way of improving the expression and solubility of the USPs is the use of synthetic genes containing optimized codons. In *E.coli* the protein expression is maximized by using codons corresponding to tRNAs that retain amino acid charging during starvation¹⁶. The expression and solubility of USP7 in *E.coli* for instance has been greatly improved by using synthetic genes (**chapter 4**).

Although the development and the use of high-throughput methods did not achieve the desired results in getting a large number of USP constructs giving soluble protein in large amounts, the use of these high-throughput methods are now well established and the ligation-independent cloning using the pET-NKI vectors is currently the standard method in our lab. Furthermore, the number of USPs that we finally could obtain was used for the characterization in **chapter 4**.

USPs look similar, but behave differently

Even though many studies show the vital role of a number of USPs in important cellular pathways and the implication in tumorigenesis, not much is known about the proteases themselves in terms of enzyme kinetics and preference for ubiquitin-chain type. We have tried to address these topics by characterizing a set of twelve USPs using synthetic tools including all seven di-ubiquitin topoisomers (**chapter 4**).

The analysis of the enzyme kinetics showed that there are large differences in DUB activity amongst the twelve USPs. Based on their K_M and k_{cat} values, these USPs can be grouped in three classes: the inactive, the intermediate and the very active group. Future studies will show whether these three classes still hold true after characterizing the enzyme kinetics for the rest of the USP family. It seems that the USP family doesn't show any real preference for a certain ubiquitin-chain type, but rather show a modest differential activity towards the seven di-ubiquitin topoisomers which was variable between USPs.

Many USPs have additional domains and internal insertions within the catalytic domain and some USPs are known to have external modulators

that regulate the DUB activity. As shown for USP7 and USP16, both show increased DUB activity in the presence of their additional domains (the HUBL and ZnF-UBP domain, respectively). The ZnF-UBP domain of USP16 enhances the DUB activity by increasing the k_{cat} . This activation of DUB activity has been previously shown for USP5 as demonstrated by Reyes-Turcu et al.¹⁷. They show that binding of free Ub to the ZnF-UBP domain enhances the USP5 DUB activity *in vitro*. Besides USP16 and USP5, several other USPs (USP3, USP44, USP45 and USP49) have a similar ZnF-UBP domain. It is possible that enhancement of USP activity following free ubiquitin binding would be a general regulatory mechanism¹⁸. The activity of USP7 is modulated by its HUBL domain which affects both the K_M and k_{cat} . Despite a clear difference in DUB activity, no change in ubiquitin-chain type preference was seen between the catalytic domain and full-length of USP7 and USP16. Interestingly, our data show that the preference of USP7 for di-ubiquitin topoisomers can be attributed to the binding affinity (K_M) for the substrate.

A similar enhancement of DUB activity by increasing the k_{cat} is seen for USP1, USP12 and USP46 in presence with their external modulator, the WD40-repeat containing UAF1. Also for USP7 the k_{cat} is increased by adding its external modulator GMPS. Similar to the HUBL and ZnF-UBP domain, both external modulators do not seem to affect the preference for ubiquitin-chain type.

Because of the important cellular roles of several USPs, their DUB activity must be tightly regulated. Several studies have revealed that kinases play an important role in USP control and a number of USPs, such as USP7, USP16 and USP44, are activated by phosphorylation¹⁹⁻²². It seems that the DUB activity of USPs is further regulated by intramolecular modulating domains (HUBL and ZnF-UBP) and by intermolecular modulators (GMPS and UAF1). The identification of new intra- and intermolecular modulators for other USPs will be interesting and challenging for future studies and will unveil whether they also can affect the preference for ubiquitin-chain type.

New role for the Ubl domain

The knowledge about functions for the Ubl domains in USP family members is limited. Only one example has been described which is the Ubl

domain located at the N-terminus of the catalytic domain of USP14. It functions as an anchor for recruitment to the proteasome where USP14 is activated²³. Very recently Faesen and co-workers show the crystal structure of five Ubl domains located C-terminal of the catalytic domain of USP7²⁴. Here the first three Ubl domains seem to be required as a docking station for the intermolecular modulator GMPS, while the last two Ubl domains apparently are responsible for activating USP7. This activation is achieved by interacting with the Cys-loop and position the catalytic triad in a catalytic competent configuration. Finally in **chapter 5**, a new role for the Ubl domain in USPs is described. The Ubl domain of USP4 located within the catalytic domain plays a role as the internal inhibitor of the DUB activity of USP4. The Ubl domain inhibits USP4 activity by binding to the catalytic domain with similar affinity as for ubiquitin and thereby preventing ubiquitin substrate binding.

It seems that the Ubl domain in USPs can have different functions: recruiting, activating and inhibiting DUB activity. These functions might be a common feature in USPs as similar Ubl domains have been identified in a large number of USPs²⁵. Interestingly, the Ubl domains which recruits, activates and inhibits are each located differently with respect to the catalytic domain. The recruiting Ubl domain of USP14, the activating Ubl domain of HAUSP and the inhibiting Ubl domain of USP4 are located respectively N-terminal, C-terminal and internal of the catalytic domain. Whether the location of the Ubl domain in respect of the catalytic domain plays an important role in Ubl function is an interesting question.

Interestingly, the inhibitory role of the Ubl domain within the USP4 catalytic domain can be blocked by USP39 through binding to the Ubl domain, thus activating USP4 function. The interaction between USPs opens up a new door for USP regulation. Looking at the domain architecture of the USP family containing ubiquitin binding domains and Ubl domains, it is very likely that other USPs can interact with each other and possibly alter USP function. Indeed recently, Maertens et al show the interaction between USP7 and USP11 and how they regulate the ubiquitination status of several components of the Polycomb repressive complex 1^{26,27}. How they interact remains unclear, but as USP11 looks very similar in domain architecture as USP4 with Ubl domains,

it is possible that USP7 binds to USP11 through one of its Ubl domains. Or USP11 binds to one of the HUBL domains of USP7 and thereby altering each others function. Future research into Ubl domains should be conducted to investigate whether the Ubl domains predicted in other USPs have similar or might display new functions.

Concluding remarks

In the last decade the importance of DUBs as a key regulatory step in ubiquitin-dependent pathways and as an important factor in tumorigenesis, have been increasingly recognized. Although many exciting studies on DUBs are ongoing, there is still a long way to go before we fully characterize this intriguing protease family. The largest subfamily of DUBs, the USP family, has been the focus of this thesis. We have seen that USPs, even in small number compared to the E3 ubiquitin ligases, are multifunctional in that they have more than one target. We have also seen that a subset of USPs displays a large variation in DUB activity with no real preference for a ubiquitin-chain type. Furthermore, the USP activity not only is regulated on the level of phosphorylation, but it also involves inter- and intramolecular modulators. Finally, a new inhibitory role for the integrated Ubl domain in the catalytic domain of USP4 has been described. Hopefully, the experiments and data shown in this thesis will contribute to the further understanding of the USP family.

References

1. Li, M., Brooks, C.L., Kon, N. & Gu, W. A dynamic role of HAUSP in the p53-Mdm2 pathway. *Mol Cell* **13**, 879-86 (2004).
2. Li, M. et al. Deubiquitination of p53 by HAUSP is an important pathway for p53 stabilization. *Nature* **416**, 648-53 (2002).
3. Song, M.S. et al. The deubiquitinylation and localization of PTEN are regulated by a HAUSP-PML network. *Nature* **455**, 813-7 (2008).
4. van der Horst, A. et al. FOXO4 transcriptional activity is regulated by monoubiquitination and USP7/HAUSP. *Nat Cell Biol* **8**, 1064-73 (2006).
5. van der Knaap, J.A. et al. GMP synthetase stimulates histone H2B deubiquitylation by the epigenetic silencer USP7. *Mol Cell* **17**, 695-707 (2005).
6. Fan, Y.H., Yu Y., Mao R.F., Tan X.J., Xu G.F., Zhang H., Lu X.B., Fu S.B., Yang J. USP4 targets TAK1 to down-regulate TNF α -induced NF- κ B activation. *Cell Death Differ.* (2011).
7. Song, E.J. et al. The Prp19 complex and the Usp4Sart3 deubiquitinating enzyme control reversible ubiquitination at the spliceosome. *Genes Dev* **24**, 1434-47 (2010).
8. Zhang, X., Berger, F.G., Yang, J. & Lu, X. USP4 inhibits p53 through deubiquitinating and stabilizing ARF-BP1. *EMBO J* **30**, 2177-89 (2011).
9. Huang, T.T. et al. Regulation of monoubiquitinated PCNA by DUB autocleavage. *Nat Cell Biol* **8**, 339-47 (2006).
10. Nijman, S.M. et al. The deubiquitinating enzyme USP1 regulates the Fanconi anemia pathway. *Mol Cell* **17**, 331-9 (2005).
11. Graner, E. et al. The isopeptidase USP2a regulates the stability of fatty acid synthase in prostate cancer. *Cancer Cell* **5**, 253-61 (2004).
12. Stevenson, L.F. et al. The deubiquitinating enzyme USP2a regulates the p53 pathway by targeting Mdm2. *EMBO J* **26**, 976-86 (2007).
13. Brummelkamp, T.R., Nijman, S.M., Dirac, A.M. & Bernards, R. Loss of the cylindromatosis tumour suppressor inhibits apoptosis by activating NF- κ B. *Nature* **424**, 797-801 (2003).
14. Kovalenko, A. et al. The tumour suppressor CYLD negatively regulates NF- κ B signalling by deubiquitination. *Nature* **424**, 801-5 (2003).
15. Trompouki, E. et al. CYLD is a deubiquitinating enzyme that negatively regulates NF- κ B activation by TNFR family members. *Nature* **424**, 793-6 (2003).
16. Welch, M. et al. Design parameters to control synthetic gene expression in *Escherichia coli*. *PLoS One* **4**, e7002 (2009).
17. Reyes-Turcu, F.E. et al. The ubiquitin binding domain ZnF UBP recognizes the C-terminal diglycine motif of unanchored ubiquitin. *Cell* **124**, 1197-208 (2006).
18. Bonnet, J., Romier, C., Tora, L. & Devys, D. Zinc-finger UBPs: regulators of deubiquitylation. *Trends Biochem Sci* **33**, 369-75 (2008).
19. Fernandez-Montalvan, A. et al. Biochemical characterization of USP7 reveals post-translational modification sites and structural requirements for substrate processing and subcellular localization. *FEBS J* **274**, 4256-70 (2007).
20. Joo, H.Y. et al. Regulation of cell cycle progression and gene expression by H2A deubiquitination. *Nature* **449**, 1068-72 (2007).
21. Lopez-Otin, C. & Hunter, T. The regulatory crosstalk between kinases and proteases in cancer. *Nat Rev Cancer* **10**, 278-92 (2010).
22. Stegmeier, F. et al. Anaphase initiation is regulated by antagonistic ubiquitination and deubiquitination activities. *Nature* **446**, 876-81 (2007).
23. Hu, M. et al. Structure and mechanisms of the proteasome-associated deubiquitinating enzyme USP14. *EMBO J* **24**, 3747-56 (2005).
24. Faesen, A.C. et al. Mechanism of USP7/HAUSP activation by its C-terminal ubiquitin-like domain (HUBL) and allosteric regulation by GMP-synthetase. *Mol Cell* (2011).
25. Zhu, X., Menard, R. & Sulea, T. High incidence of ubiquitin-like do-

- mains in human ubiquitin-specific proteases. *Proteins* **69**, 1-7 (2007).
26. Maertens, G.N., El Messaoudi-Aubert, S., Elderkin, S., Hiom, K. & Peters, G. Ubiquitin-specific proteases 7 and 11 modulate Polycomb regulation of the INK4a tumour suppressor. *EMBO J* **29**, 2553-65 (2010).
27. Sowa, M.E., Bennett, E.J., Gygi, S.P. & Harper, J.W. Defining the human deubiquitinating enzyme interaction landscape. *Cell* **138**, 389-403 (2009).

Addendum

Summary
Samenvatting
List of abbreviations
Curriculum Vitae
PhD portfolio
List of publications
Acknowledgements

A

SUMMARY

Since the discovery of ubiquitin (Ub), it is increasingly apparent that Ub mediated events are critical in cell proliferation. In the last several decades much attention is placed on the ubiquitination pathway and recently the role of deubiquitinating enzymes (DUBs) in the reverse pathway is being recognized as important regulators of these processes. There is also a growing recognition of DUBs that are mutated in human cancers making them interesting drug targets. To better understand these DUBs, this thesis focuses on the structural and functional aspects of the largest subclass of DUBs, the ubiquitin-specific protease (USP) family.

Chapter 2 gives a genomic and functional overview of the DUB family and describes the five different subclasses. Describing examples of the cellular roles of USPs in different pathways with known protein substrates, it shows that even though the USP family is relatively small, the USP family member is multifunctional by having more than one substrate. It also shows how some important substrates such as p53 and H2A/B requires additional regulation by having more than one USP for their deubiquitination.

In order to better understand the molecular and biochemical roles of USPs, soluble protein is required for both crystallographic and biochemical studies. To obtain soluble protein, one must produce and screen a large number of DNA constructs. In **chapter 3** the development and the use of the pET-NKI-LIC vectors as high-throughput methods to obtain DNA constructs, which results in high protein expression and improves protein solubility, is described. Ligation-independent cloning (LIC) using the pET-NKI-LIC vectors is currently the standard method in our lab and the implementation of LIC for a large number of USPs, resulted in a number of soluble USP proteins.

Chapter 4 shows the enzymatic characterization of the obtained soluble USPs using synthetic substrates including all seven lysine-linked di-ubiquitins. The analysis shows that the USPs behave differently in terms of

DUB activity and that based on their kinetic behaviour they can be grouped into three classes: the inactive, the intermediate and the very active group. Furthermore, we provide the first comprehensive analysis comparing the Ub chain preference and show that USPs display a modest activity towards the seven di-ubiquitin topoisomers which was variable amongst the USPs and that this Ub chain-type preference in the case for USP7 can be attributed to the binding affinity (K_M) for its substrate. Finally, the existence of intermolecular modulating domains (HUBL and ZnF-UBP) and intramolecular modulators (GMPS and UAF1) help regulate the DUB activity of USPs by mainly increasing the catalytic turnover (k_{cat}).

In **chapter 5** the three-dimensional crystal structure of minimal catalytic domain USP4-D1D2 is shown and a new role for the Ubl domain embedded within the catalytic domain of USP4 is described. The crystal structure of the USP4 catalytic domain has the conserved USP-like fold with its typical Ub binding site. Our findings show that the integrated Ubl domain acts as an intermolecular modulating domain that inhibits the DUB activity of USP4. This inhibitory function of the integrated Ubl domain is induced by binding to the catalytic domain of USP4 with similar affinity as for Ub and thereby preventing Ub substrate binding. Interestingly, a binding partner of USP4, USP39 is able to bind to the same Ubl domain and relieve the inhibition.

Together the work presented in this thesis illustrates how complex and diverse the function and the regulation are of this relative small USP family. Hopefully this work gives interesting leads for future studies and helps contribute into the understanding of the intriguing DUB family, the USPs.

A

SAMENVATTING

Sinds de ontdekking van ubiquitine (Ub), wordt het steeds duidelijker dat Ub gemedeerde gebeurtenissen belangrijk zijn in de cel proliferatie. In de laatste decennia is er veel aandacht besteed aan de ubiquitinerings route en onlangs is de rol van deubiquitineringsenzymen (DUBs) in de omgekeerde route erkend als belangrijke toezichthouders van deze processen. Er is ook een toenemende erkenning van DUBs die gemuteerd zijn in menselijke kankers, waardoor ze interessant zijn als drug targets. Om deze DUBs beter te begrijpen, concentreert dit proefschrift zich op de structurele and functionele aspecten van de grootste subgroep van DUBs, de ubiquitine-specifieke protease (USP) familie.

Hoofdstuk 2 geeft een genomisch en functioneel overzicht van de DUB familie en beschrijft de vijf verschillende subgroepen. Door voorbeelden te beschrijven van cellulaire rollen van USPs in de verschillende routes met bekende eiwit substraten, laat hoofdstuk 2 zien dat de USP familie leden, ondank het kleine aantal, multifunctioneel zijn door meer dan één substraat te hebben. Verder wordt ook beschreven dat sommige belangrijke substraten zoals p53 en H2A/B extra regulatie vereisen door meer dan één USP voor hun deubiquitinerings te hebben.

Om beter inzicht te krijgen in de moleculaire en biochemische rollen van USPs, is oplosbaar eiwit nodig voor zowel de kristallografische en biochemische studies. Om oplosbaar eiwit te verkrijgen, moet men een groot aantal DNA constructen produceren en screenen. In **hoofdstuk 3** worden de ontwikkeling en het gebruik van de pET-NKI-LIC vectoren beschreven. Deze vectoren worden gebruikt als hoge-doorstroom methodes om DNA constructen te verkrijgen die kunnen leiden tot hoger eiwit expressie en betere eiwit oplosbaarheid. Ligatie-onafhankelijke klonering (LIC) door middel van de pET-NKI-LIC vectoren is tegenwoordig de standaard methode in ons lab en de implementatie van LIC op een groot aantal USPs resulteerde in een aantal oplosbare USP eiwitten.

Hoofdstuk 4 laat de enzymatische

karacterisatie van de verkregen oplosbare USPs zien door gebruik te maken van de synthetische substraten inclusief alle zeven lysine-gekoppelde di-ubiquitines. De analyse laat zien dat de USPs zich anders gedragen in termen van DUB activiteit en dat gebaseerd op hun kinetisch gedrag ze in drie groepen verdeeld kunnen worden: de inactieve, de gemiddelde en de zeer actieve groep. Bovendien geven we de eerste uitgebreide analyse waarin de voorkeur voor een Ub keten wordt vergeleken. We laten ook zien dat de USPs een gemiddelde activiteit vertonen tegenover de zeven di-ubiquitine topoisomeren. De activiteit is variabel tussen de USPs en de Ub keten-type voorkeur in het geval van USP7 is toe te schrijven aan de bindingsaffiniteit (K_M) voor zijn substraat. Tenslotte laat hoofdstuk 4 zien dat het bestaan van intermoleculaire modulerende domeinen (HUBL en ZnF-UBP) en intramoleculaire modulators (GMPS en UAF1) in USPs meehelpt aan de regulatie van de DUB activiteit door voornamelijk de katalytische omzetting (k_{cat}) toe te laten nemen.

In **hoofdstuk 5** wordt de driedimensionale kristal structuur van het minimale katalytische domein USP4-D1D2 getoond en wordt een nieuwe rol voor het Ubl domein dat geïntegreerd is in het katalytische domein van USP4, beschreven. De kristal structuur van het USP4 katalytisch domein heeft het geconserveerde UPS-lijkende vouwing met zijn typische Ub bindingsplaats. Onze bevindingen laten zien dat het geïntegreerd Ubl domein als een intermoleculaire modulerende domein functioneert door de DUB activiteit van USP4 te inhiberen. Deze inhiberende functie van het geïntegreerde Ubl domein wordt tot stand gebracht door in het katalytische domein van USP4 te binden met eenzelfde affiniteit als voor Ub en hierdoor wordt Ub substraat binding voorkomen. Verder is het interessant dat USP39, een bindingspartner van USP4, aan hetzelfde Ubl domein kan binden en hiermee de inhibitie van het Ubl domein opheft.

Tezamen illustreert het werk gepresenteerd in dit proefschrift, hoe complex en divers de functie en de regulatie van deze re-

latieve kleine USP familie zijn. Hopelijk geeft dit werk interessante aanknopingspunten voor toekomstige onderzoeken en draagt het bij in het begrijpen van deze intrigerende DUB familie, de USPs.

**A**

A



LIST OF ABBREVIATIONS

DNA	deoxyribonucleic acid
Ub	ubiquitin
Ubl	ubiquitin-like
Da	Dalton
E1	ubiquitin activating enzyme
E2	ubiquitin conjugating enzyme
E3	ubiquitin ligase
UBA1	ubiquitin-like modifier activating enzyme 1
MgATP	magnesium adenosine triphosphate
RING	Really Interesting New Gene
HECT	Homologous with E6-associated protein C-Terminus
URM1	ubiquitin related modifier 1
ATG12	autophagy related protein
Nedd8	neural precursor cell expressed, developmentally down-regulated 8
SUMO	small ubiquitin-like modifier
FAT10	ubiquitin like protein
ISG15	interferon-stimulated ubiquitin like protein
LC3	ubiquitin like protein
Cys	cysteine
Ser	serine
Thr	threonine
UBD	ubiquitin-binding domain
ZnF-UBP	zinc finger ubiquitin-specific protease
UIM	ubiquitin-interacting motif
UBA	ubiquitin-associated
UCH	ubiquitin C-terminal hydrolase
USP	ubiquitin-specific protease
OTU	ovarian tumor
JAMM	JAB1/MPN/MOV34
PCNA	proliferating cell nuclear antigen
K	lysine
ERAD	endoplasmic-reticulum-associated-degradation
UFD	ubiquitin fusion degradation
BRCA1	breast cancer 1
BARD1	BRCA1-associated RING domain protein 1
Ufd2	ubiquitin chain elongation enzyme
LUBAC	linear ubiquitin chain assembly complex
NF- κ B	nuclear factor kappa-light-chain-enhancer of activated B cells
Ile	isoleucine
Kd	dissociation constant
TRAF	TNF receptor associated factor
RAP80	receptor associated protein
NEMO	NF- κ B essential modulator
ABIN	A20-binding inhibitor of NF- κ B
UBAN	ubiquitin-binding in ABIN and NEMO
IKK	I κ B kinase
TNF- α	tumor necrosis factor- α
SAGA	Spt-Ada-Gcn5 acetyltransferase
Akt	kinase

I κ B	inhibitor of NF- κ B
TNF- α	tumor necrosis factor α
IL-1	interleukin 1
IKK	I κ B kinase
SCF	Skp, cullin, F-box containing
RIP	ribosome inactivating protein
HR	homologous recombination
UBE2T	ubiquitin conjugating enzyme
HERC2	HECT domain and RCC1-like domain containing protein 2
RNF8	Ring finger protein 8
RNF168	Ring finger protein 168
RIDDLE	radiosensitivity, immunodeficiency, dysmorphic features and learning difficulties
Ubc13	ubiquitin conjugating enzyme 13
53BP1	p53 binding protein 1
UPS	Ubiquitin-proteasome system
CYLD	cylindromatosis (turban tumor syndrome)
Wnt	wingless int
TGF β	transforming growth factor beta
BCL-2	B-cell lymphoma 2
MCL1	myeloid cell leukemia 1
Mdm2	murine double mutant 2
COP1	caspase recruitment domain-containing protein 1
Pirh2	p53-induced ring-h2 domain
ARF-BP1	alternate reading frame-binding protein 1
HAUSP	herpesvirus associated ubiquitin-specific protease
PTEN	phosphatase and tensin homolog
Asp	aspartate
Asn	asparagines
DUSP	domain in USPs
Rad23	UV excision repair protein 23
Dsk2	ubl/ub associated containing protein
SG	structural genomics
RIKEN	Rikagaku Kenkyusho (institute of physical and chemical research)
PSI	protein structure initiative
SGC	structural genomics consortium
SPINE	structural proteomics in Europe
NMR	nuclear magnetic resonance

A

CURRICULUM VITAE

Mark Luna-Vargas was born on the 17th of March, 1979 in Amsterdam. In 1997 he finished his high-school and received his VWO-gymnasium diploma at the Katholieke College Amsterdam. In the same year he started his studies at the Chemistry faculty of the University of Amsterdam. After receiving his Master's degree in Biochemistry in 2003, he started working as a technician in the group of Prof. Dr. Titia Sixma. During the period 2004-2011 he worked on this thesis under the supervision of Prof. Dr. Titia Sixma at the Netherlands Cancer Institute.

In January 2012 he will move to New York where he will join the group of Prof. Dr. Ming-Ming Zhou at Mount Sinai School of Medicine. There he will conduct research into the molecular interactions and regulation of histone-directed chromatin biology in the cell nucleus.

A

PHD PORTFOLIO

SUMMARY OF PHD TRAINING AND TEACHING

Name PhD student: Mark Patrick Alexander Luna-Vargas
 Erasmus Department: Genetics
 Research School: Onderzoeksschool Oncologie Amsterdam
 PhD period: 2004-2011
 Promotor/Supervisor: Prof. dr. Titia K. Sixma

1. PhD training

General courses

Radiation course	2004
Scientific writing and presenting in English	2009

Specific courses

Functional Genomics, NKI, Amsterdam, The Netherlands	2005
Protein Structure and Function, NKI, Amsterdam, The Netherlands	2006
Basics of Crystallography, NKI, Amsterdam, The Netherlands	2007&2009
Bio Crystallography Practical Course, ITQB, Oeiras, Portugal	2008

Seminars & Workshops

Bioinformatics, IGBMC, Strassbourg, France	2005
Seminar Staff -Meeting, NKI, Amsterdam, The Netherlands	2010

(Inter)national conferences

2004	SPINE congress, London, England (<i>oral presentation</i>)
2004-2009	Annual meeting Dutch studygroups of NWO, Lunteren, The Netherlands (<i>poster presentation</i>)
2005-2006	OOA PhD student retreat, Texel, The Netherlands
2005&2007	The Ubiquitin Family conference, Cold Spring Harbor, NY, USA (<i>poster presentation</i>)
2006-2011	Rubicon Network of Excellence, ubiquitin conference, Florence, Rome (Italy), Barcelona (Spain) (<i>poster presentation</i>) and Malta (<i>oral presentation</i>)

2. Teaching

2007-2008	Supervising master's thesis research project of Master student
-----------	--

A

LIST OF PUBLICATIONS

Faesen AC*, **Luna-Vargas MPA***, Geurink PP, Clerici M, Merckx R, Van Dijk WJ, Hameed DS, El Oualid F, Ovaa H, Sixma TK. The differential modulation of USP activity by internal regulatory domains, interactors and seven ubiquitin-chain types. *Submitted*

* These authors contributed equally to this work

Luna-Vargas MPA, Faesen AC, Van Dijk WJ, Rape M, Fish A, Sixma TK. Ubiquitin-specific protease 4 is inhibited by its ubiquitin-like domain. *EMBO rep.* 2011; **12**(4):365-372

Luna-Vargas MPA, Christodoulou E, Alfieri A, Van Dijk WJ, Stadnik M, Hibbert RG, Sahtoe DD, Clerici M, De Marco V, Littler D, Celie PHN, Sixma TK, Perrakis A. Enabling high-throughput ligation-independent cloning and protein expression for the family of ubiquitin specific proteases. *J Struct Biol* 2011; **175**(2):113-9

Shanmugham A, Fish A, **Luna-Vargas MPA**, Faesen AC, El Oualid F, Sixma TK, Ovaa H. Design and use of hydrolytically stable ubiquitin-isopeptide isosteres. *J Am Chem Soc.* 2010; **132**(26):8834-5

Van Leuken RJ, **Luna-Vargas MPA**, Sixma TK, Wolthuis RM, Medema RH. USP39 is essential for mitotic spindle checkpoint integrity and controls mRNA-levels of AuroraB. *Cell Cycle* 2008; **17**:2710-9

Alzari PM, Berglund H, Berrow NS, Blagova E, Busso D, Cambillau C, Campanacci V, Christodoulou E, Eiler S, Fogg MJ, Folkers G, Geerlof A, Hart D, Haouz A, Herman MD, Macieira S, Nordlund P, Perrakis A, Quevillon-Cheruel S, Tarandeu F, Van Tilbeurgh H, Unger T, **Luna-Vargas MPA**, Velarde M, Willmanns M, Owens RJ. Implementation of semi-automated cloning and prokaryotic expression screening: the impact of SPINE. *Acta Crystallogr D Biol Crystallogr.* 2006; **62**(pt10):1103-13

Nijman SM, **Luna-Vargas MPA**, Velds A, Brummelkamp TR, Dirac AM, Sixma TK, Bernards R. A genomic and functional inventory of deubiquitinating enzymes. *Cell* 2005; **123**(5):773-86
Review

Sewalt RG, Lachner M, **Luna-Vargas MPA**, Hamer KM, Den Blaauwen JL, Hendrix T, Melcher M, Schweizer D, Jenuwein T, Otte AP. Selective interactions between vertebrate polycomb homologs and the SUV39H1 histones lysine methyltransferase suggest that histone H3-K9 methylation contributes to chromosomal targeting of Polycomb group proteins. *Mol Cell Biol.* 2002; **22**(15):5539-53

A

ACKNOWLEDGEMENTS

Finally, I've made it. The last chapter of my thesis: the acknowledgements. It has been a (very) long journey/adventure/struggle, but one that I would not have enjoyed/endured/experienced without the help/guidance/support from certain people I would like to thank.

First of all my biggest thanks for *Titia*, who first hired me as a technician and after one year gave me the opportunity to start a PhD in her group. Throughout my PhD I have seen the small crystallography group from H2 grow into a big and flourishing department under your guidance and supervision. I admire your endless enthusiasm and your vast knowledge and your attention for details. I have learned a lot from you and I know it has not been easy for both of us, but thank you for your listening ear and support! I wish and your family all the best for the future!

Pim, the 'engine' of the department, sitting next to you starting in H2 and ending in B8 has been a never-dull-moment experience I will never forget! I will miss our laughs and talks. Thanks for being there and helping me prepping all those damned difficult USPs.

Dancing with *Alex*. I never thought we would have teamed up to tackle the USP project, but I'm glad we did. I admire how focused you can be and how you manage everything with the dancing, the science and having a family. I wish you all the best in Germany!!

Tassos, you and your group I have also seen evolve throughout the years. Thanks for all your help with the crystallography. From being a temperamental and thundering Greek god to a more relaxed and diplomatic group-leader, I enjoyed our discussions about (Greek) football and your passion for food. Maybe one day we will meet again in the Arena where Ajax and Panathinaikos will play each other again in the Champions League. Of course this time Ajax will win ;)

I always tell people around me that working in the lab is like playing in the 'speeltoern'. Not only the environment contributed to that feeling but of course the people I had the pleasure of working and

discussing with. *Herrie*, the Muts-factory, one day I will come and visit you in Hungary and see your magnificent 'castle'. *Patrick*, I think you and I are the last ones remaining (except for Pim and Herrie) from Titia's 'klasje 2004'. I wish you all the best with the protein facility, it is in good hands! *Fra*, sempre con un grande sorriso, will never forget your 'ajuuto!' and 'Gateaux Pimonde' on Reunion Island. Hang on, don't give up, you're almost there!! And next time we meet, your Dutch will be as perfetto as my Italian ;) *Alex* aka *Sasha*, thanks for all your help with the infamous Biacore! I will miss our talks about boxing and judo. Maybe one day your sons will be the new Dutch judoka champions ;) *Rick*, thanks for all the discussions about analyzing biacore data and enzyme kinetics. Wish you all the best for the future! *Kash*, everyone in the lab says your default mode is being grumpy, but luckily I haven't experienced that 'Mode' much ;) Thanks for being there when I needed to talk about science and life and I'm glad you will be standing next to me as my paranimf. You better not turn into default ;p *Judith*, your finishing-my-phd-in-four-years plan did not turn up what you were hoping for, but I am sure you will finish it way faster than I did. At least nothing explodes anymore in the lab and everything is Judith-proof :P *Mariano*, mio amico italiano, I was hoping I could have practiced my Italian with you more often, but I guess I have to come and visit you and your new group in Napoli one day and discuss about women in the Italian way ;) *Flora*, when are we going hiking again? We should organize a reunion-hike on Reunion Island! *Danny*, is ADO going to repeat season '10-'11 again someday? Really hope you will get your BAP1/ASX-structure ;) *Marcell(in)o*, I will miss our discussions about USPs, our travels and the different restaurant we have been to :D I have a feeling our paths will cross again soon. Good luck with continuing the USP project! *Michael*, the last member to join the Sixma lab. Wish you all the best! Biertje? To all the other people in the lab: Eli, John, Robbie, Leonie, Krista, Jens, Magda, Caroline, Christop(hino) –take care next time! I won't be there to drag you to your hotelroom ;) – and finally Tati –my 'little sister' always taking care of things in the lab and helping everyone out. Will miss the fun and teasing in the lab ;) : it was great having you as my colleagues and thank you for all your help and advice.

Of course being in the lab for so long, I have met

and worked with many other people who left the lab: Valerie, Puck, Joyce, Gretel, Sari, Ganesh, Victor, Chris, Annet, Andrea, Azusa, Vangelis & Valeria, Kostas, Serge, Oli, Mark H., Koen, Angelina, Mobien, Suzan, Diederick, Cristiane, Wijnand, Dene, Eirini (gyftaki) and Bernat: thank you all!! I enjoyed working with you.

Special thanks to the Ovaa-lab: Huib, Farid, Paul, Remco, Reggy and Dharjath. Thank you all for the chemical tools/reagents. After a slow start, we all can finally benefit from each other's skills.

Sa wakas, nay, tay at Maribel! Pagkatapos ng matagal ng paghihintay, ito na natapos ko na! Hindi ko alam kung paano sisimulan ang pasasalamat. Walang tamang salita para malarawan ko ang inyong walang sawang suporta. Kahit na halos "abracadabra" ang tingin nyo sa librong ito, ang inyong pananaw ay naging malaking tulong upang matapos ko ang librong ito. Maraming salamat sa inyong suporta, pagmamalaki, interes, pagmamahal, tulong at lagi kayong nandyan para sa akin!!

A

Dear Ale, even though I will be going to the other side of the ocean, you will always be with me. Mmmmbeeeeee!!!

I've made it!
Mark

